Multidisciplinary Approach to Address Water Scarcity in Informal Settlements in Lima, Peru: Fog Water Collection, The Fog Resource and the Health Context

Shara I. Feld

A dissertation

submitted in partial fulfillment of the

requirements for the degree of

Doctor of Philosophy

University of Washington

2014

Reading Committee:

Susan Bolton, Chair

Benjamin Spencer

Joachim Voss

Program Authorized to Offer Degree:

Civil and Environmental Engineering

1

www.manaraa.com

University of Washington

Abstract

Multidisciplinary Approach to Address Water Scarcity in Informal Settlements in Lima, Peru: Fog Water Collection, The Fog Resource and the Health Context

Shara Ilana Feld

Chair of the Supervisory Committee:
Professor Susan M. Bolton
School of Environmental and Forest Sciences

Many arid regions of the world have very limited and shrinking water availability, which puts vulnerable populations such as informal settlement (slum) dwellers at risk for having the least access to clean drinking water. This is particularly a concern in coastal Peru, where many informal settlements already experience water scarcity that will be exacerbated by both shrinking water supply and a continuously growing population. In Lima, the capital city, rapid growth of the population has resulted in large informal settlements forming up the hillsides surrounding the city. Given the projected growth of Lima, the public water supply has already been found to be inadequate to supply the current water needs of Lima.

In order to address this complex problem of inadequate water resources in the informal settlements in Lima, Peru, this dissertation focused on relevant technological, social and environmental factors. The first study demonstrated the improved

effectiveness of a nonwoven three-dimensional turf mesh in a passive fog collection system that captures the abundant wind-blown fog that surrounds the city. The material increased yields over traditional fog collection materials by 50% to 150% in field testing.

The second focus was on the impact on health and social factors that could be affected by improved water access, as well as have an influence on the ability to develop and sustain any water resource system. Therefore, the second study evaluated demographic, physical and mental health, and social relationship factors of individuals in the community that would be benefit from the fog water collection. We found nearly half of the participants in the community were overweight or obese, yet the prevalence of non-communicable disease was low, and the mental health and social relationship surveys did not indicate significant impacts for the well-being of the community, which may positively contribute to the likelihood of a fog collection system's success.

Finally, the fog resource can be assessed by the coastal low cloud conditions. Knowledge about the availability and predictability of these conditions along coastal Peru was explored as the third component of this dissertation. Reduced quantities of stratus clouds were observed with increased temperatures in the El Niño 3.4 region, the El Niño 1+2 region and along coastal Peru. While annually greater quantities of stratocumulus clouds were generally observed with increased El Niño 3.4 temperatures, we observed a negative correlation between seasonal stratocumulus in many coastal Peruvian stations and SST in the El Niño index regions and along coastal Peru. With projected increases in equatorial sea surface temperatures, and warming coastal Peruvian currents, we could see reductions in low cloud cover.

4

In conclusion, by testing efficiency improvements to a method to acquire atmospheric water, exploring individual and social conditions within the type of community where this system could be used, and evaluating conditions that would affect the availability of water throughout the year, this dissertation has contributed to our understanding of many aspects of the problem of water resources in this under-served community. Furthermore, this series of studies has provided direction to the development of community-based water solutions in Lima, Peru.

Table of contents

List of Figures

List of Tables

Acknowledgements

A very special thanks to my dissertation committee, from whom I have learned so much: Susan, Ben, Joachim, Luanne and Cynthia. Thanks to the Peru team – Coco, Leann, Rekha, Francisca, Brooke, Gayna – you were instrumental. And thanks to the students in the Landscape Architecture courses who worked on the P3 project. And finally, many thanks to the community of Eliseo Collazos, in particular Marcia and Joel.

A final thanks to the friends and family who have either provided a read-through of paper drafts, or a needed culinary/adventure break.

Chapter 1 Introduction

Water is an essential resource for human health, well-being, and survival. However, many regions of the world have very limited and shrinking water resources. Furthermore, the most vulnerable populations are often at greatest risk for having the least water access. Reasons for this situation are complex, involving technological, social and environmental factors (UNDP, 2006). The search for potential interventions must take into account all these complex factors to arrive at solutions that will be effective and sustainable.

The studies in this report recognize the need to address the multifaceted nature of the limited water resource problem in urban informal settlements and the search for potential solutions by exploring: 1) technological improvements to harvest fog water to provide water resources independent of the public utility to water scarce regions, 2) social and health factors related to the use of these technologies, and 3) environmental factors that influence the availability of the water resources. Specifically, these studies investigate 1) an improved method to capture water through a fog water collection system, 2) physical health, mental well-being, and community social factors that could be related to a project's development and maintenance, and 3) climatological patterns that influence the sustainability of the fog water resource in Lima, Peru.

1.1 Background:

The water scarcity problem

Global water scarcity: A large proportion of the world's population has limited access to water resources (UN Water, 2007). More than 1.2 billion people, or 20% of the world's population, live in regions with water scarcity, defined as areas that lack water sufficient to meet population demand (CA, 2007). By the year 2050, due to increasing population and environmental pressures, this number is expected to reach 4.8 billion, or 52% of the world's population (UN Water, 2005). Water scarcity must be addressed proactively before the reduction of this precious resource leads to greater conflicts and significant disruption of societies.

Population growth patterns contribute to global water scarcity: Compounding the problem of global water scarcity is population growth in water-poor regions that outpaces the development of a municipal infrastructure. The year 2007 marked the first time in human history that the majority of the world's population lived in urban areas (Sclar, Garau, & Carolini, 2007). According to United Nations projections, by 2030 the world's urban population will increase by more than 2 billion (United Nations, 2003). In the developing world, a large proportion of this urban growth will be in informal urban settlements (slums). Nearly one billion people live in informal settlements currently, with that number expected to reach three billion by 2050 (UN Habitat, 2003). Limited water infrastructure is a typical problem for these areas (Sheuya, 2008; UN Habitat, 2003; UNDP, 2006), leading to concerns about safe drinking water, sanitation, and ability to

maintain green space. As global water scarcity increases, these impoverished communities will become even more vulnerable to inequities related to water distribution.

Peru water scarcity: Many communities in the costal regions of Peru are characterized by both water scarcity and rapid population growth. Water resources in Peru are unevenly distributed, and while around 70% of the population lives in the Pacific basin, only 2% of the water resources are found in this area (Multisectoral Technical Commission, 2004). Lima, Peru, a city with 8.8 million citizens, receives only 10-15mm of rain a year. The city's main water supply comes from an alluvial aquifer and three glacially-fed rivers, the Rimac, Chillon and Lurin Rivers. Recent forecasting models estimate that the Andean glaciers below 5500 meters which feed the three rivers will disappear within the next decade (Painter, 2007), dramatically reducing Lima's water supply.

Furthermore, while Lima's water supply is shrinking, the city grows. Lima is the largest city in Peru, with a population of 8.8 million as of 2013 (The World Factbook 2013-14, 2013). Increased urban migration led to the population's rapid growth since 1950, when it had fewer than 400,000 residents (United Nations, 2001). Lima's population has expanded in the form of informal settlements up the hills surrounding the city. A third of the population lives in these informal settlements (Riofrío, 2003). However, the public water system, SEDEPAL, acknowledges that supplying water for the projected growth of Lima is not possible with the current water reserves (Lubovich,

2007). The environmental pressures from a small water supply combined with the

difficulty of municipal infrastructure keeping pace with the rate of development will

greatly strain the water supply system in Peru's capital city Lima. Lima urgently needs to

develop new sustainable water sources, and one such source could be the abundant

costal fog that covers Lima from roughly May through November every year.

1.2 Use of fog water as a potential solution

Harvesting fog water provides one possibility for a water resource that is readily

available in Lima and cities with similar climates. In Lima's case, fog water could

supplement the water supply for human consumption or agriculture in the urban informal

settlements. Passive fog collectors can be constructed to intercept wind-blown fog,

capturing the water resource as it intercepts the hills. Projects to collect water for

human uses from wind-blown fog date back to the 1960s in South America and Africa

(Klemm et al., 2012).

Standard fog collectors consist of a hydrophobic mesh tensioned in a frame,

oriented with maximum exposure to the wind (Klemm et al., 2012). Newer models for

fog collection have been considered, including novel shapes to collect fog from multiple

wind directions (Valiente et al., 2011), increasing the surface area of mesh used within a

given footprint (Heerden et al., 2010; Lummerich & Tiedemann, 2011) or using new

materials (Chhatre et al., 2009; Sarsour et al., 2010).

Important considerations concerning the feasibility of improved fog water collection systems:

Schemenauer et al. (2005) emphasize not only technical feasibility of the fog collection system, but also how appropriate the technology is for the community. An effective system in low resource environments will be low cost and easy to install. Systems with a more complex form will require more involved installations and maintenance. Installation is a simpler prospect when using materials that are locally available. Novel materials have been evaluated to a limited extent. While these tests are promising, the testing of the materials has either been inadequate, or the materials are difficult to acquire in arid and impoverished areas where they would be used. Further, any materials with higher cost than traditional Raschel mesh must show an increase in fog collection efficiency, which is best demonstrated with side by side tests. Chapter 2 describes a study where a material is evaluated for potential to increase fog collection over standard fog collectors.

Chapter 3 addresses the social factors in these communities where we propose supplementing the water resources with fog collection. Better water access can be used for consumption, sanitation, and local agricultural opportunities, potentially improving health, reducing household expenditures and empowering individuals and communities through gained skills and economic opportunity within informal settlements. In turn, a stronger foundation in the physical, social and psychological health of the community can improve reception to and ability to maintain a water resource project. For a more complete health assessment, recent literature

recommends that urban health assessments include poverty, social and physical environment, and health service components (Harpham, 2009; Vlahov et al., 2007). However, little attention has been paid to these variables. One exception to this was the "Young Lives" study of young adults from Peru and three other countries. However, this study, which was designed to assess progress to the United Nations Millennium Development Goals (Cueto et al., 2011; Escobal, 2012) looked at only a limited number of variables to assess multi-factor contributions to, and consequences of, childhood poverty. National surveys (INEI, 2012; IHME, 2013) assessing demographic and physical health risks in Lima, Peru provide an incomplete picture of health in the informal settlements. Measurements of mental health and social capital variables were either not taken, or referred to only diagnosed mental illness. Further, even where physical health and demographics measures were taken, existing metrics did not consistently separate residents of informal settlements from regions of higher socioeconomic status.

Finally, in addition to a fog collection structure that captures sufficient fog volumes, fog collection projects require adequate local fog resources (Klemm et al., 2012; Schemenauer et al., 2005). While Lima, Peru is known to have fog cover for roughly six months of the year, this duration is variable and predictors are poorly characterized. Understanding relations between low cloud cover and predictable climate indices would provide an initial assessment of the viability of fog collection in the region and demonstrate methods for analyzing fog cover duration for other regions. One climate index that influences atmospheric moisture and transport is the El Niño –

19

southern oscillation, which describes the variation in sea surface temperatures and air pressure. To some extent, the onset and spatial patterns of El Niño events can be predicted (Chen & Cane, 2008; Chen et al., 2004). Previous work showed that fog and low cloud frequencies in the East Pacific Ocean are linked to sea surface temperatures (Park & Leovy, 2004; Eichler & Londoño, 2013). Therefore, given the promise of fog water as a distributed water resource, it would be useful to be able to characterize the onshore annual duration and frequency of fog cover given larger scale climatic conditions. Chapter 4 addresses a gap in knowledge about the influence of predictive climatic conditions on low cloud cover in coastal Peru, particularly regarding annual duration, and characterizing which region of the sea surface best predicts fog frequency.

In conclusion, water resource solutions must recognize that multiple factors affect and are affected by their implementation. There is both a need and an opportunity to improve 1) the efficiency of systems that can be used for distributed water resource collection from fog, 2) the baseline data on social factors, including health and well-being, that can inform understanding the factors that can affect the success of these projects in informal settlements, and 3) the understanding of the potential and prediction of the fog resource potential.

1.3 Research Site

This work is based in the community of Eliseo Collazos (latitude: -11.877° and longitude: -77.082°) within the Alto Zapallal (sometimes referred to as Lomas de

20

Zapallal) neighborhood in the Puente Piedra district of North Lima [Figure 1.1]. Alto Zapallal was settled in the early 1990s and since that time the population has grown to approximately 27,000 with immigration from throughout Lima and Peru. Eliseo Collazos is one of the more recent communities with the first few houses showing up in 2007. Most of the informal urban settlers came to Lima in the hopes of finding better economic opportunity, education opportunity, and refuge from civil unrest and terrorism in their original communities (Riofrío, 2003).

Residents of the Eliseo Collazos have purchased their lots, yet are in the process of gaining full tenure. Residents live in one or two room houses constructed out of a variety of materials, including pre-fabricated wooden siding, metal and plastic roofing, or cement. Homes have electricity but are not served by running water or sanitation. Water is acquired from a central hose and stored in household barrels. Each house has its own latrine. The environment is dusty with very little rainfall, but frequent fog in most mornings from May through November.

This community is particularly well suited for this research for two reasons: (a) project personnel have established trust and made contacts within the community through repeat visits and (b) a series of participatory workshops in 2011 revealed that community priorities included addressing water shortages, water contamination and lack of vegetation and green space. Work here can provide examples to be used in similar communities in Lima and worldwide.

Fig. 1.1. Location of Lima, Peru and a view of Eliseo Collazos.

1.4 Purpose Statement

Recognizing the interconnectedness of technological, social, and environmental factors in developing effective solutions to growing water scarcity and increased pressure on water resources, this research seeks to 1) improve the efficacy of a method to capture fog water, 2) provide data on individual physical health and mental well-being, as well as community social factors, that could potentially affect, and be affected by, the success of this system and similar projects in informal settlements, and 3) characterize climatological patterns over time in Lima that could influence the availability of a fog water resource

22

1.5 Research Questions

1. Can fog water collection volumes be increased by using turf reinforcement mats (TRMs), a low-cost, widely available, technologically-simple, non-woven, three-dimensional material?

2. What is the physical health and well-being status (including social capital, stress, empathy, threatening experiences and quality of life) of community members in Eliseo Collazos who participate in the implementation of a community garden project and would be served by fog water collection?

3. Over a period of 30 years based on existing meteorological and ocean surface temperature data, what is the climatological normal duration of fog cover in Lima, Peru, and is there a correlation with El Niño cycles?

Each of the next three chapters will address one of these research questions and there will be a final synthesis chapter at the end of the dissertation.

Chapter 2 Improved Fog Collection Using Turf Reinforcement Mats

2.1 Abstract

Impoverished communities are particularly vulnerable to increasing water scarcity. The development of low-cost technologies that improve access to unconventional water sources, such as the freshwater contained in fog, is one way to address water scarcity. Passive fog collectors, sited to maximize exposure to orographic and advection fog, are typically constructed using 35% Raschel mesh stretched within a structural frame.   To assess improvements to this technology, the fog collection potential of non-woven turf reinforcement mats, Enkamat® 7010 and Enkamat® 7220, were tested in a laboratory fog tunnel and at a field site in Lima, Peru. Increases of 26% and 33% over traditional Raschel mesh were observed in fog tunnel tests. Collection volume increases of 50-150% over traditional Raschel mesh were observed during field tests. Differences in performance during field site tests were likely dependent on orientation to prevailing winds. Performance differences between the laboratory and field tests demonstrate the importance of validating laboratory studies on site. This work suggests that non-woven turf reinforcement mat has the potential to improve water access in arid yet foggy areas.

2.2 Introduction

Access to water is one of the defining social and environmental issues of modern times. More than 1.2 billion people, or 20% of the world's population, live in regions with water scarcity (CA, 2007). By the year 2050, this number is expected to reach 4.8 billion, or 52% of the world's population (UN Water, 2005). Adding to this problem, global fresh water resources are unevenly distributed geographically (FAO, 2007) which frequently results in higher costs and lower access in impoverished communities (UNDP, 2006).

As global water scarcity increases, the poor will continue to be particularly vulnerable. One way to address this inequity is to continue to develop low-cost technologies that improve access to unconventional water sources, such as the freshwater contained in fog. Fog water collection is technologically simple and can be accomplished using passive fog collectors that intercept orographic or advection fog (Cereceda et al., 2002). Traditional collectors measure 4 m x 10 m and consist of 2 layers of 35% Raschel tensioned between two vertical poles (Klemm et al., 2012). They are oriented perpendicular to the predominant wind direction. As fog-laden wind passes through a collector, droplets of water accumulate on the mesh and drip into a gutter below.

Fog water collection is best suited to regions where dense fog is present throughout much of the year and to sites where topography intercepts the cloud belt and is exposed to consistent prevailing winds (additional siting considerations are found in Schemenauer & Cereceda, 1994a). This technology is particularly valuable in arid regions of the world where the fog is one of few replenished water resources. Arid

25

regions that have potential for fog collection include the western coast of South America, the western coast of Africa, the Middle East, southern Europe and parts of Asia (Klemm et al., 2012).

Several novel designs have been proposed to increase fog water collection efficiency. Omni-directional collectors that intercept fog-laden wind from multiple directions provide hourly collection rates comparable to traditional fog collectors during periods when their orientation is perpendicular to wind direction (Valiente et al., 2011). However, they show increased collection rates when wind direction varies. Three-dimensional collectors provide greater surface area for the accumulation of fog droplets, without significantly decreasing permeability to fog-laden winds. For example, a design called the "Eiffel" showed increased fog collection rates utilizing two panels of mesh set 0.3 meters apart, with ten vertical mesh stripes (Lummerich & Tiedemann, 2011). A similar system joined nine fog collection panels together in the form of four equilateral triangles (Heerden et al., 2010). Although these more complex designs have shown functionality, it is important to note that structure accounts for a significant portion of fog collector cost. Designs with more complex structures can cost more to build and be more difficult to maintain.

Work is also being done to evaluate novel fog collection materials. Biologically-inspired, three-dimensional, deep drawn/thermoforming meshes show promise for increased water capture. Initial tests show increased yields in laboratory and field testing (Sarsour et al., 2010). Coatings have been developed that allow for tunable mesh wettability. These coatings can be designed for a broad range of wetted and non-

wetted states to increase efficacy of fog capture for a given distribution of fog droplet sizes (Chhatre et al., 2009). Such specially designed three dimensional meshes and coatings are not widely or commercially available and may be much more expensive than the traditional meshes.

This study examines whether turf reinforcement mats (TRMs), a relatively low-cost, widely available, technologically-simple non-woven, three-dimensional material, increases fog water collection volumes over the recommended 35% Raschel mesh and commonly used 50% Raschel mesh.

2.3 Methods
2.3.1 Materials evaluated

This study compares the collection rates of two types of Enkamat® brand TRM made of fused PA6 polymer monofilaments (Enkamat® 7220 and Enkamat® 7010) to the standard 35% Raschel mesh made with polypropylene threads recommended in Schemenauer & Cereceda (1994a) as well as the 50% Raschel mesh [Figure 2.1] which is currently widely used in Peru. Enkamat® TRM is UV-resistant, non-toxic and distributed worldwide. Other materials were evaluated during laboratory testing. However, Enkamat® TRM outperformed of these materials. Enkamat® 7220 is a 18 mm thick mesh with an three dimensional open structure on one side and a flat open structure on the other side. Enkamat® 7010 is a 10 mm thick mesh with three dimensional open structures on both sides.
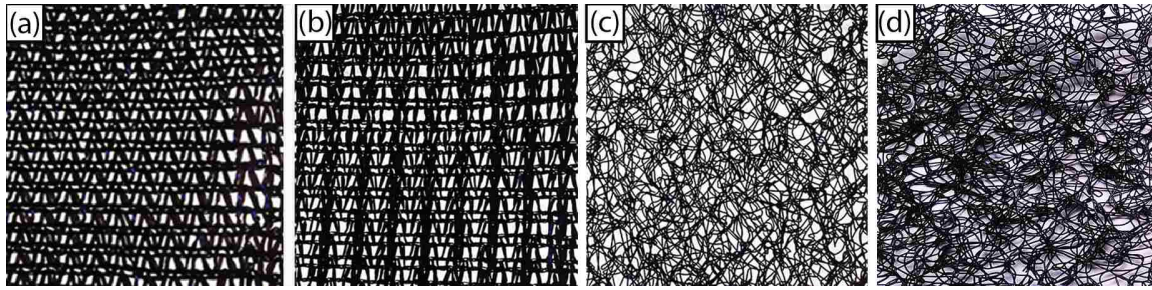
Fig. 2.1. Materials tested. (a) Double 35% Raschel mesh. (b) Double 50% Raschel Mesh. (c) Double layer of Enkamat® 7010. (d) Single layer of Enkamat® 7220.

2.3.2 Laboratory Testing

Laboratory testing was conducted in a modified plastic hoop-house or 'fog tunnel' designed to simulate wind-blown fog [Figure 2.2]. The fog tunnel was 9.1 m long, 3.0 m wide and 2.75 m tall at the highest point. A 320 cmm exhaust fan was installed at one end of the fog tunnel and an air inlet/door was constructed at the other. A fog nozzle manifold with eight high-pressure Meefog™ fog nozzles was installed 5.0 m from the exhaust fan.
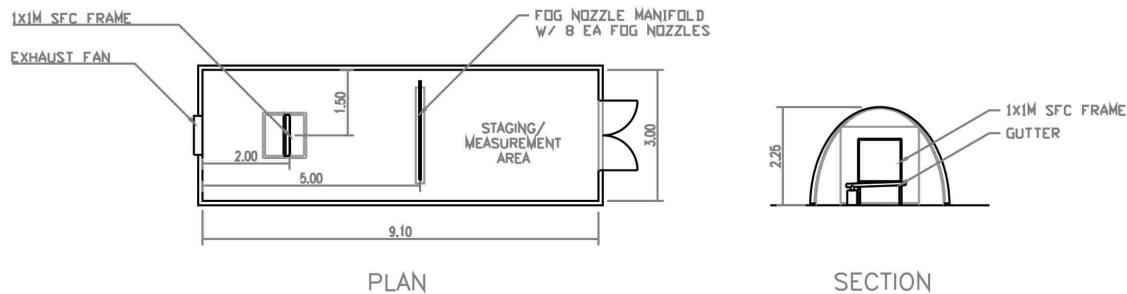
Figure 2.2. Fog tunnel schematic

The fog collector design used in lab tests followed Schemenauer & Cereceda (1994a) standard fog collector (SFC) specifications, with modifications for laboratory testing. Several SFC frames were constructed to provide a common unit of comparison

28

during fog collection experiments. One frame held 2 layers of 35% Raschel mesh to match SFC specifications (Schemenauer et al., 2005). Another frame held two layers of 50% Raschel mesh to reflect material used in Lima. Enkamat® 7220 was tested as a single layer with the three dimensional open side towards the fog nozzles; Enkamat® 7010 was tested as a double layer. A 1.0 m wide by 1.5 m tall PVC stand that held one SFC frame at a time was positioned 2.0 m upwind of the exhaust fan and 3.0 m downwind of the fog nozzle manifold, and centered between the fog tunnel's side walls. SFC frames were elevated 0.5 m above the ground, instead of the recommended 2.0 m, so they would fit inside the tunnel. The PVC stand also held a 1.25 m long, 10.2 cm wide gutter to collect water from the SFC frame.

Individual frames were installed in the fog tunnel and the exhaust fan was set to high which produced wind speeds of ~1 m s^{-1} as measured at the SFC frame location, with no SFC frame in the tunnel. The fog nozzle manifold received water from a pressure washer maintained at 7584 kPa creating a stream of fog droplets with a mean diameter of 13 microns at that water pressure (Chaker, 2007) The wind pulled fog through the mesh, where it collected, dripped into the gutter, and flowed into a collection container for measurement. To account for variation in the time to saturation of different materials, the test consisted of two periods: an initial 45 minute period starting from dry mesh to completely saturate materials, immediately followed by a 45 minute fog collection period. Reported results on fog collection yields are from the second 45 minute period. Six baseline collection value tests were conducted with 35% Raschel

29

mesh and four with 50% Raschel mesh. Four tests were conducted with Enkamat®

7010 and five with Enkamat® 7220.

A Datametrics Model 800 VTP anemometer was used to evaluate airflow through

and around fog collectors inside the fog tunnel. Wind speed was measured directly in

front of, behind, and on either side of several prototypes. Outdoor meteorological data

were acquired from a weather station located 150 meters from the fog tunnel to evaluate

the influence of climatic conditions on collection. Temperature and relative humidity

were measured with Vaisala 45C instruments, wind direction and wind speed with RM

Young instruments, and radiation with an Apogee sensor.

2.3.3 Field Testing

The field test site was located along a ridgeline rising from the north end of the

Eliseo Collazos neighborhood in the Lomas de Zapallal (LDZ) community, an informal

settlement (slum) in the Puente Piedra district of northern Lima, Peru, latitude: -11.877°

and longitude: -77.082° [Figure 2.3].
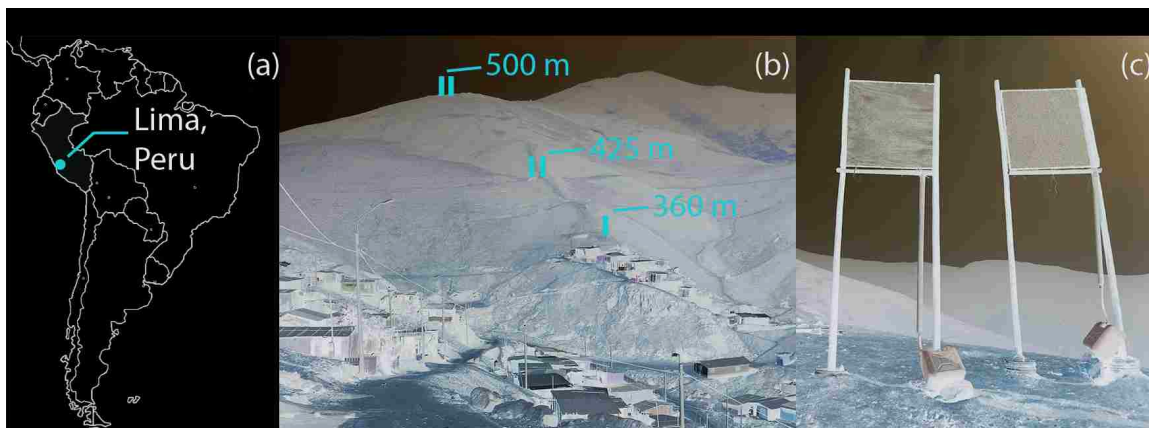
Fig. 2.3. Site Location. (a) Lima, Peru. (b) Nets are located above Eliseo Collazos, at
360 m, 425 m and 500 m. (c) Test SFC nets at the 425m site.

30

The combination of cool waters from the Humboldt Current that flows along the Chilean and Peruvian coastlines and the stabilizing influence of the Pacific anticyclone produce a low layer of stratus clouds for 6-9 months out of the year (Heileman et al., 2009; Proyecto Regional Manejo Integrado del Gran Ecosistema de la Corriente de Humboldt, 2002). These clouds are typically present between May and December with interannual variability in quantity and duration. Fog collection is possible where the hills surrounding Lima intercept these clouds.

The Eliseo Collazos neighborhood was selected as a test site based on social and climatic considerations. In 2011, a series of participatory workshops revealed that community priorities included addressing water shortages, water contamination and lack of vegetation and green space. The community was receptive to a fog collection project and participated in the installation of SFCs and fog collection monitoring.

Five SFCs consisting of 35% Raschel mesh were installed in September, 2012 at three elevations. One SFC was installed at 360 m, paired SFCs were installed at 425 m and 500 m [Table 2.1]. SFCs were installed perpendicular to what was perceived as the dominant wind direction. The SFCs at 425 m and 500 m were installed with a slight variation in orientation to assess whether this resulted in differences in collection volume.

All materials for the fog collection system were purchased at local hardware stores to allow for ease of replication and repair by the community with the exception of the 35% Raschel mesh, which was purchased directly from the distributor in Lima. In 2013, the configuration of one of the SFCs at both the 500 m and 425 m level were altered slightly such that the pair had the same aspect to facilitate side by side

31

comparisons between the different materials [Table 2.2]. The SFC at 360 m was not

reoriented and one net of each pair at 425m and 500m was kept in the same orientation

to allow comparison of fog collection volumes between the years. The paired SFCs at

425 m and 500 m were located 1 m apart. SFC materials and the different test periods

are shown in Table 2. In 2012, data were collected to the nearest 250 ml, in 2013 to the

nearest 1 ml. Daily measurements were normalized to fog volume collected per 24

hours. Days with less than 100 ml collection volume were excluded from the analysis.

Table 2.1. Fog collector elevation, aspect and material in 2012.

Elevation	Aspect	Material
500 m	239° and 184° True	Both 35% Raschel
425 m	220° and 180° True	Both 35% Raschel
360 m	205° True	35% Raschel

Table 2.2. Fog collector elevation, aspect and material for the three test periods in 2013.

Elevation	Aspect	August 6-22	August 22 – Sept 7	Sept. 7-22
500 m	Both 184° True	Enkamat® 7010, 35% Raschel	Enkamat® 7220, 35% Raschel	Both 35% Raschel
425 m	Both 220° True	Enkamat® 7220, 35% Raschel	Enkamat® 7010, 35% Raschel	Both 35% Raschel
360 m	205° True	35% Raschel	35% Raschel	35% Raschel

Site meteorological conditions in 2013 were determined with a Davis Vantage

Pro 2 meteorological station installed near the lowest SFC at an elevation of 360

meters. This station recorded air temperature, relative humidity and barometric

pressure 3 m above the ground and wind direction and wind speed 3.6 m above ground.

The station was oriented to face the same direction (205°) as the SFC at the lowest

elevation. The station averaged and archived data hourly. To determine daily-average weather conditions that corresponded to fog-collection time periods, the meteorological data were averaged from noon on the preceding day to noon on the date of fog measurement.

Wind direction and variability at the 425 m and 500 m sites were determined with an oil drip wind vane installed from 9/13/13 through 9/21/13. This system consisted of a 1 L plastic bottle with a small needle hole in its base suspended 1.6 meters above the ground. The bottle was filled with cooking oil that slowly dripped over the course of 24 hours. The oil drips were carried by the wind a short distance as they fell, creating an oil pattern on the ground that illustrated the predominant wind direction and variation. Every day, a compass and measuring tapes oriented in the cardinal directions were laid over the oil pattern, and the site was photographed from the south, north and west. Photographs were analyzed, an angle was drawn around the dominant range of splatter and the center of this angle was recorded as the dominant wind direction [Figure 2.4].
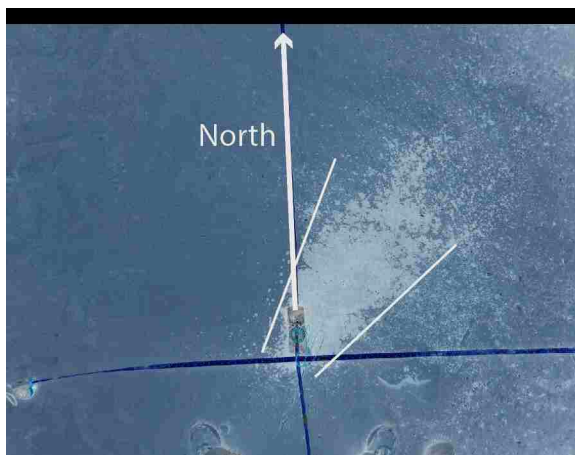
Fig. 2.4. Example output from an oil drip wind vane. Shown is the marked range of observed wind directions.

Large-scale meteorological conditions were acquired from the Moderate Resolution Imaging Spectroradiometer (Modis) instrument on the Aqua and Terra satellites. With 36 spectral bands at wavelengths from 0.4µm to 14.4µm and a trajectory covering the entire earth surface every 1-2 days, the instrument produces information on global processes on land, in the ocean and atmosphere. Effective cloud particle radius was acquired from the MOD08_D3 level 3 data set for 8/2/13 – 9/21/13 [http://ladsweb.nascom.nasa.gov/ Accessed 10/15/13].

2.4 Results and Discussion

2.4.1 Laboratory Testing Results

In the fog tunnel tests, Enkamat® 7010 and Enkamat® 7220 collected greater average volumes of water per square meter than either 35% Raschel mesh or 50% Raschel mesh (p<.05) [Table 2.3]. Compared to 35% Raschel mesh, Enkamat® 7010 increased collection yields by 33% and Enkamat® 7220 increased collection yields by 26%. Fog tunnel tests also indicated that 50% Raschel mesh was less effective than 35% Raschel mesh as a fog collection material.

Table 2.3. Fog collection volumes in the fog tunnel and percent difference from SFC 35% Raschel mesh.

Material	No. tests	Min $L\ m^{-2}\ hr^{-1}$	Max $L\ m^{-2}\ hr^{-1}$	Avg $L\ m^{-2}\ hr^{-1}$	vs SFC 35%	vs SFC 50%
SFC (35% Raschel)	6	1040	1293	1180	-	18%
SFC (50% Raschel)	4	935	1150	1000	-15%	-
Enkamat® 7010	4	1280	1895	1575	33%	58%
Enkamat® 7220	5	1215	1855	1485	26%	49%

34

To identify potential influences on collection rates in the fog tunnel due to outdoor conditions, a Spearman correlation was run between meteorological metrics and collection volume. The factors that most strongly affected collected volumes were the outdoor relative humidity ($p = 0.08$) and irradiance ($p = 0.08$). Tests conducted on days with $< 50\%$ humidity were excluded from analysis so that evaluated tests took place only on cloudy, humid days. In-tunnel observers noted that very low levels of fog were produced by the fog nozzles when the sky was not cloudy.

Higher wind speeds (average 0.17 m/s vs 0.055 m/s) were recorded directly in front of the SFC frames with the Enkamat® materials than the SFC frames with 35% Raschel mesh. Wind speeds measured behind all of the SFC frames were approximately equivalent. Holding other variables constant, it is presumed that the passage of fog-laden wind through an SFC at higher wind speeds results in increased fog collection volumes.

2.4.2. Lima Test Results

Fog volumes collected in 2012 from the SFCs with 35% Raschel mesh indicated the Eliseo Collazos site's potential for fog collection. SFCs with 35% Raschel mesh at the same elevation and facing the same orientation in 2012 and 2013, showed lower fog collection volumes in 2013 than in 2012 ($p<.05$) [Figure 2.5], indicative of a less foggy season in 2013. Furthermore, observed plant growth on the hills appeared later and in lower quantities in 2013 than in 2012. During both 2012 and 2013, larger volumes of

water were collected on the SFCs at higher elevations on the hill [Figure 2.5], as these SFCs were most often within the fog belt.
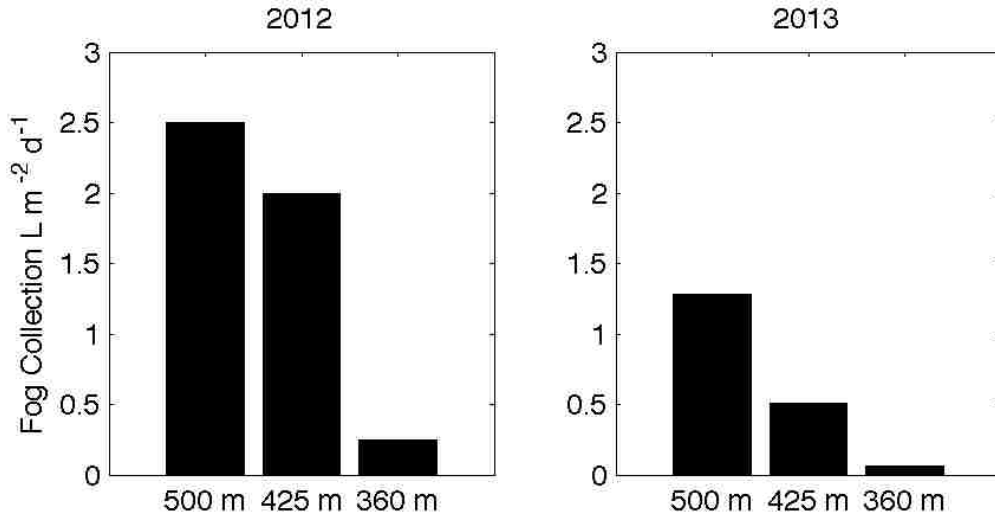
Fig. 2.5. Median fog collection volumes (L m^{-2} d^{-1}) from 35% Raschel mesh at the three test sites during 2012 and 2013.

During 2012, we assessed whether there was a significant difference in collection volume for the two angles at which SFCs were installed at 425 m and at 500 m. With 52 days of data from each SFC, there was no significant difference in average collection volume related to SFC orientation.

We evaluated ambient weather and moisture conditions during the three test periods in 2013 for differences that could affect results. A greater number of sunny days were observed as the study progressed, with temperatures warming over the course of the study period (daily mean temperatures of 13.7° C during the first test period, 14.5° C during the second test period and 15.6° C during the final test period). However, mean relative humidity was consistently high during the three test periods, with test period averages of 90% - 93%. The volume of fog collected on the SFCs with

36

Raschel mesh was similar for the first two test periods (in which the Enkamat® mesh was evaluated), with the average fog collection volume from the 35% Raschel mesh at the 500 meter site of 2.050 L day^{-1} m^{-2} during the first test period and 1.810 L day^{-1} m^{-2} during the second test period. On average, conditions with lower fog collection volumes (when an average of 0.920 L was collected per 24 hours) occurred during the third test period, when 35% Raschel mesh was installed on both frames. Weather conditions were similar during Enkamat® testing periods and there is not a significant time period effect between trials at both sites.

2.4.3 Field Testing Performance

The Enkamat® TRM materials collected median volumes of 2.2 to 2.8 L m^{-2} d^{-1} compared to a median collection volume of 1.3 L m^{-2} d^{-1} from the 35% Raschel at the 500 m site. At the 425 m site the Enkamat® TRM materials collected median volumes of 1.5 L m^{-2} d^{-1} compared to a median collection volume of 0.5 L m^{-2} d^{-1} from the 35% Raschel [Figure 2.6]. While the volumes collected are not large, these are measurements from the end of the fog season, and thus represent conservative amounts of overall collection volumes.
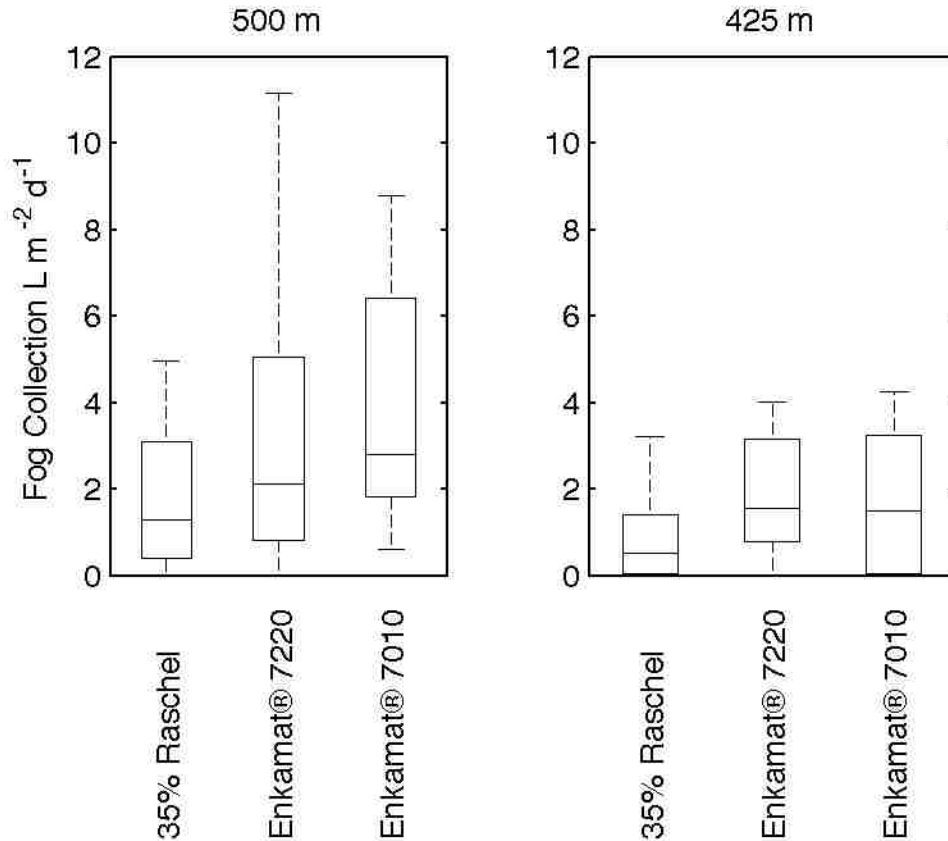
Fig. 2.6. SFC collection volumes during 2013 at the 500 m site and 425 m site from 35% Raschel mesh and two TRM materials. The box traces the 25th to 75th percentile, with the median shown. Range bars extend to +/- 2σ.

A one-sample t-test conducted on the log of the ratio of fog volume collection from Enkamat® to 35% Raschel mesh at the 500 m and 425 m sites indicates that the Enkamat® 7010 and 7220 meshes performed significantly better than the 35% Raschel mesh ($p < 0.001$) [Table 2.4]. There was no significant difference in the mean 24-hour collection volumes when 35% Raschel mesh was installed on both frames at the 500 m and 425 m sites. This indicates that the observed difference was not due to the frame on which the Enkamat® was installed.

Table 2.4. One-sample t-test results comparing the log ratio of Enkamat® 7010 and Enkamat® 7220 mesh to 35% Raschel. Confidence intervals have been converted from log ratio to the ratio.

Ratio	P Value	95% Confidence Interval	
		Lower Limit	Upper Limit
Enkamat® 7220, 35% Raschel (500 m site)	<0.001	1.29	1.77
Enkamat® 7220, 35% Raschel (425 m site)	<0.001	2.31	2.95
Enkamat® 7010, 35% Raschel (500 m site)	<0.001	1.48	1.89
Enkamat® 7010, 35% Raschel (425 m site)	<0.001	2.41	3.52
35% Raschel both frames (500 m site)	0.92	0.89	1.13
35% Raschel both frames (425 m site)	0.31	0.64	1.18

There is a positive linear correlation between collection volumes from the 35% Raschel mesh and the Enkamat® materials. Enkamat® materials increased collection volumes between 50% and 150% above the amount collected by 35% Raschel mesh [Figure 2.7 and Table 2.5]. The best fit linear regression with a zero intercept is justified given that (a) no fog collection from the 35% Raschel mesh indicates negligible fog presence and (b) a linear regression with non-zero intercept results in nonsignificant ($p>0.05$) intercept values.
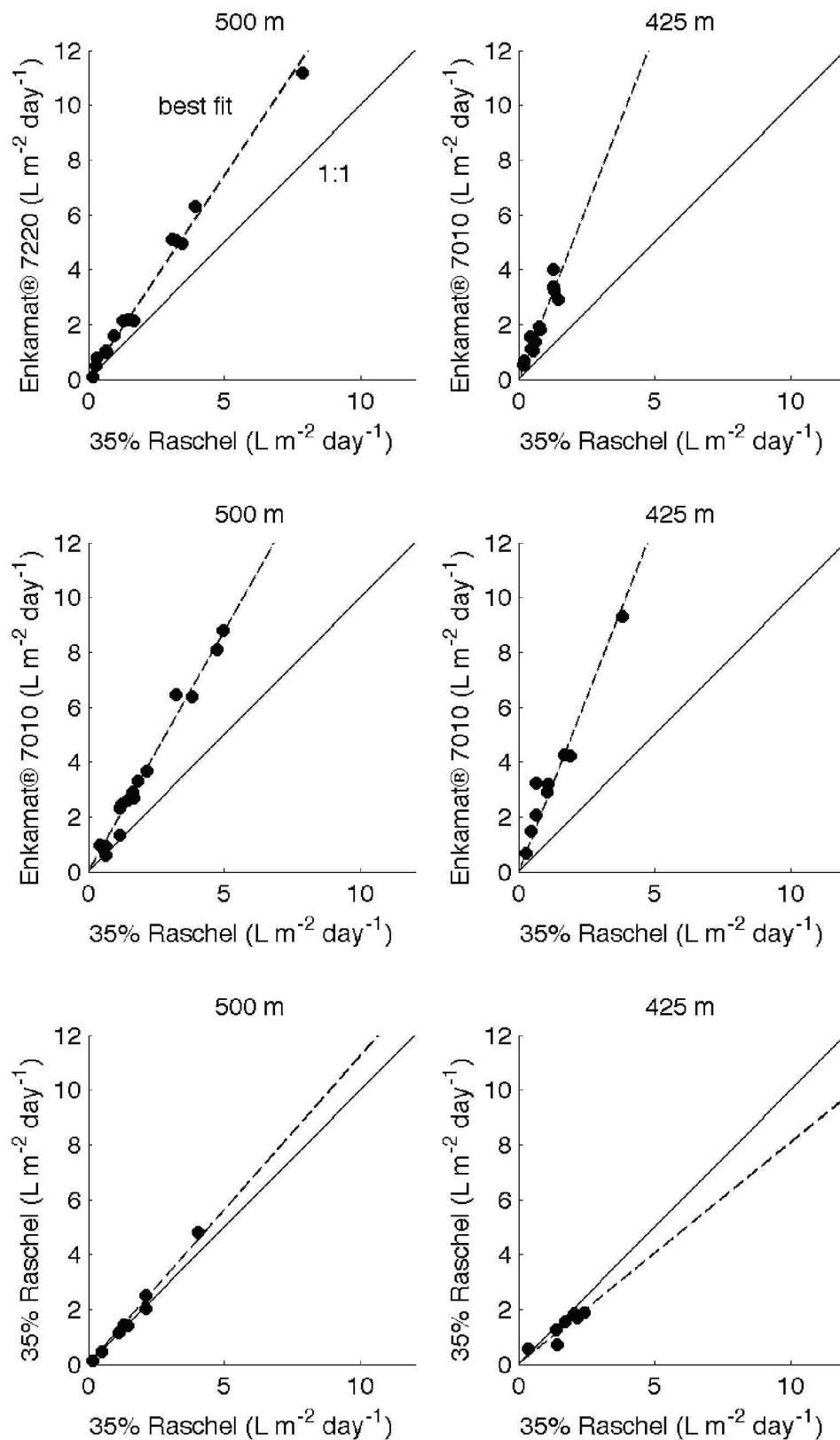
Figure 2.7. Scatter plots of daily collection volumes of 35% Raschel and comparison
material with a 1:1 line (-) and best fit line (--).

Table 2.5. Slope and R^2 Value for best fit line with a zero intercept between 24-hour collection volumes of 35% Raschel and comparison material (Enkamat® 7010 or Enkamat® 7220).

Comparison	Slope	95% Confidence Interval	R^2
Enkamat® 7220, 35% Raschel (500 m site)	1.49	1.42-1.55	0.99
Enkamat® 7220, 35% Raschel (425 m site)	2.52	2.23-2.76	0.91
Enkamat® 7010, 35% Raschel (500 m site)	1.76	1.68-1.84	0.98
Enkamat® 7010, 35% Raschel (425 m site)	2.53	2.22-2.84	0.94

2.4.4 Differences in Results Between Field Test Sites

Enkamat® TRM enhanced fog collection volumes to different extents depending on the test site [Figure 2.8]. While median fog collection volumes from both Enkamat® 7010 and 7220 were 50-75% greater than 35% Raschel mesh at the 500 m site, they were approximately 150% greater than 35% Raschel mesh collection volumes at the 425 m site. The difference between collection volumes from the same material at the two test sites was statistically significant ($p<0.001$) as evaluated by a two-sample t-test between the log ratio of Enkamat® TRM to the 35% Raschel mesh at the 500 m site and the 425 m site. While measurements with each material at the two sites were collected during different time periods, the previously noted similarity in weather conditions indicates that this is a valid comparison. Furthermore, we can conclude that the performance of Enkamat® TRM is not due to the test frame on which it was installed at either the 500 m site or the 425 m site, as there was no significant difference between fog collection volumes from the paired SFCs when 35% Raschel mesh was installed on both frames at either site [Figure 2.8].

41
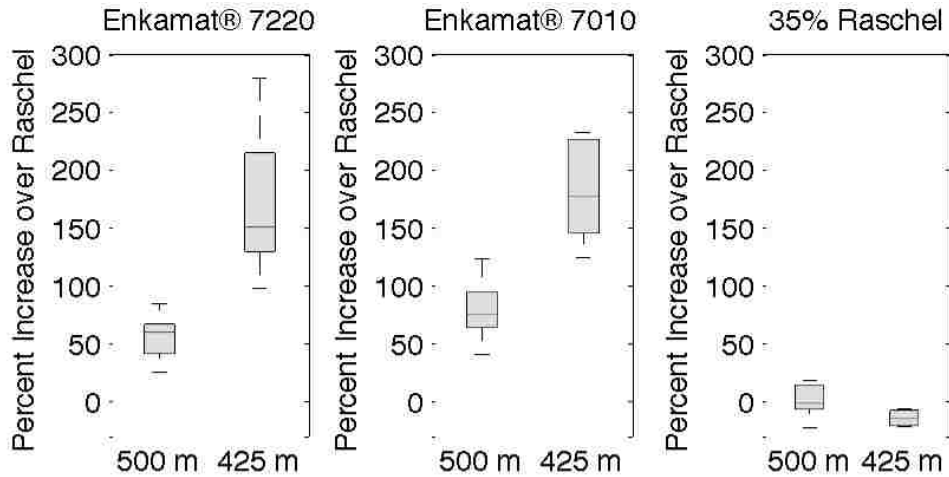
Figure 2.8: The difference in fog collection yield over the 35% Raschel mesh (given as a percent increase), as a function of material evaluated and test site. The box traces the 25th to 75th percentile, with the median shown. Range bars extend to +/- 2σ.

We assess the characteristics of the 425 m and 500 m sites to determine why Enkamat® TRM yields are higher relative to 35% Raschel mesh yields at the 425 m site. We consider two possibilities for the performance differences between these sites: site topography and aspect of the SFCs relative to prevailing winds.

Site topography can affect the variability in direction of fog-laden winds. The 425 m site is located on a flat section of an open ridgeline, with gentle slopes upwind and to the sides of the collectors. The 500 m site is located on a steep slope just below a hill top. Numerous boulders are located 2 meters away from the collectors. While the boulders may affect the wind flow and speed as it encounters the collectors, the boulders are distributed such that we expect equal impacts. We evaluated the range of observed wind directions from the oil vane wind drips installed at the 500 m and 425 m sites from 9/14/13 to 9/21/13. The average range observed was 44° between 202° True and 246° True. There was no statistically significant difference ($p > 0.05$) between the range of wind directions at the two sites.

www.manaraa.com

The SFCs at the 425 m and 500 m test sites have different orientations which may have influenced their fog collection rates. To consider the role of aspect on SFC performance, we first assess the prevailing wind directions as measured at the meteorological station during foggy days in 2013 (days with > 1 L m^{-2} day^{-1} water collected at the 500 m SFC), and distinguish these days from days without fog. During foggy conditions, daily-averaged wind direction is from the southwest (221° True) with no significant difference from overnight wind direction. During drier conditions, the daily-averaged wind direction is from the south (194° True). Overnight-averaged wind direction (from 6 pm to 6 am, the time period of generally greater fog quantities) is even more southerly in these conditions, 170° True. These relationships remained consistent for the duration of the 2013 study period; there was no significant (p>0.05) difference between the daily-averaged wind direction in the three test periods.

We confirm that wind direction measured at the meteorological station reflects the wind direction at the 500 m and 425 m sites using the observed wind directions from the oil drip wind vanes installed at these sites from 9/14/13 to 9/21/13. There was no statistically significant difference (p >.05) between the median wind direction measured at the 425 m site and the 500 m site. Furthermore, wind direction at upper sites was not significantly different from wind direction measured at the meteorological station. Thus we can evaluate the impact of the difference in orientation of the fog collectors at the 425 m and 500 m sites relative to the wind direction measured at the meteorological station.

43

Given the prevailing wind direction at the test sites, we can assess how SFC aspect may be affecting the finding that Enkamat® TRM had better performance compared to the Raschel at the 425 m site than the 500 m site. The SFCs at the two test sites have different orientations. The SFCs at the 500 m site are oriented to face 184° True while the SFCs at the 425 m site face 220° True. Thus the nets have different aspects to the prevailing fog-laden wind on days with higher fog levels. On days with more fog, the SFCs at 425 m are oriented directly into the wind while the SFCs at 500 m are oriented 37° from the wind direction.

Enkamat® TRM materials do not increase fog collection volumes relative to 35% Raschel mesh at the 500m site as much as at the 425 m site. This may be due to the SFCs non-perpendicular orientation to the prevailing wind direction at the 500 m site. This orientation may increase the material's opacity to wind-flow through the collector. Photographs taken on a light table (Figure 2.1) indicate that Enkamat® TRM has an opacity of 50%, when oriented directly into the wind. This is comparable to the measured opacity for a double layered Raschel mesh of 65%. When the Enkamat® is angled at 37° to the wind as at the 500 meter site, opacity increases by 20% (measured on a light table), while the opacity of double layered Raschel mesh only increased by 8%. Thus fog-laden wind had a longer travel path through the angled Enkamat® TRM at the 500 meter site. This likely resulted in interaction with more fibers, and may have decreased permeability. Rivera (2011) uses an aerodynamic model to demonstrate an optimum shade coefficient for fog capture. As more fibers are encountered in the travel path, wind speed through the collector slows sufficiently that the majority of the fog

44

passes around the collector and avoids capture, affecting the thicker TRM to a greater extent than the Raschel mesh.

2.4.5 Differences in the Field vs. Laboratory Results

Collection efficiency for Enkamat® TRM as compared to 35% Raschel mesh differed between laboratory and field testing. Higher wind speeds could account for these performance differences. Higher wind speeds result in greater fog collection efficiency (R.S. Schemenauer & Joe, 1989). We measured higher frontal velocities for the Enkamat® TRM compared to the Raschel mesh in lab testing, indicating greater rates of wind-flow through Enkamat® materials; an effect that may have been enhanced in the field site.

Larger and more varied fog droplet sizes could also account for Enkamat® TRM performance differences between the lab and field tests. While the fog nozzles produce fog droplets with a mean diameter of ~13 microns at our operating pressure, the mean cloud effective liquid radius (i.e. cloud liquid water droplet radius) as evaluated from Modis data, was 11.7 microns with a diameter of 23.4 microns. Enkamat® TRM may be more effective at capturing larger fog droplets, resulting in improved performance as mean fog droplet size increases. Further, the combination of fog drop size and wind speed may be an important factor. Schemenauer & Joe (1989) show that the size of fog drops influences the impact that wind speed has on collection efficiency, with larger radii corresponding to a larger increase in efficiency at higher wind speeds.

2.4.6 Better collection efficiency of TRM

Three dimensional, nonwoven TRM performed better than flat Raschel mesh. TRM is composed of cylindrical fibers instead of the flat rectangular fibers in traditional fog collection materials. Schemenauer & Joe (1989) demonstrated that theoretical fog collection efficiency decreases as the ribbon width of the fog collector mesh increases. Reduced resistance to airflow through the mesh increases the amount of fog-laden wind that is transported through and intercepted by mesh fibers. Rivera (2011) demonstrated that resistance to airflow can be reduced, and thus fog collection efficiency can be improved, by decreasing the ratio of the pressure drop coefficient to the drag coefficient. Airflow resistance is reduced with mesh fibers that have a smoother cylindrical shape (Rivera, 2011), such as is seen in the nonwoven materials.

2.4.7 Recommendations For Testing

Evaluating materials for fog collection can be difficult, due to varying fog conditions and the influence of site conditions on performance. We make some recommendations for experimental design based on our experience that will allow for improved fog collection testing. First, testing outdoors in addition to testing in a laboratory tunnel is essential to understand the impacts of wind direction, wind speed, fog droplet size and other climatic conditions on the performance of the new fog collection prototype. Second, when testing in the field evaluating fog collection prototypes will be best done with side by side testing (in which one of the units is an SFC) in an area with minimal spatial differences in terrain. If multiple collectors are tested side by side, the fog

collectors should be spaced far enough apart to allow for wind-flow around the collectors. Minimum recommended spacing between wind turbines is three rotor diameters (World Wind Energy Association www.wwindea.org/technology Accessed July 18, 2014); we recommend three times the width of a fog collector as the minimum spacing between fog collector prototypes. If fog collection prototypes are tested at multiple locations in the same site, it is best to evaluate the same type of prototypes concurrently at the multiple locations. Third, the length of field testing must allow time for sufficient variability in fog conditions, and in particular to account for days in which there is no fog; we evaluated meshes for two weeks. Finally, there are steps that can be taken to improve ease of testing. Fog collection measurement can be automated with a precipitation gage if at a secure site; this would additionally allow for more detailed comparison with weather conditions. And given the nature of field experiments, it is best to ensure replacements of fog collector materials are readily available in case any are broken over the course of testing.

2.5   Conclusions

In summary, nonwoven, three-dimensional TRM collected more fog water than 35% Raschel mesh. Enkamat® 7010 and 7220, materials that are easily installed and available worldwide, increased collection yields by 50% to 200%. A full size fog collection system (large fog collector) is 40 m^2 (R.S. Schemenauer et al., 2005). With average fog collection yields of 3 to 10 L m^{-2} day^{-1} (R.S. Schemenauer, 2012), a large fog collector can collect 120 to 400 L day^{-1}. Considering a collection rate of 5 L m^{-2} day, standard large fog collector volumes would be 200 L day^{-1}, with Enkamat® collecting

www.manaraa.com

300 L day^{-1} to 600 L day^{-1}. Considering a rate of water use of residents in informal settlements at 60 L day^{-1}, use of Enkamat® materials increases the number who can be served by a large fog water collector from 3.3 to between 5 and 10 people. Another advantage of this system is its potential to increase yields on days of light fog and thus turn a site with marginal fog resources into a viable fog collection site. The improvements in fog collection are of even greater value in communities that have no water resource infrastructure, or communities where water supply does not provide sufficient surplus for local agriculture and maintenance of green space.

We note that the permeability of TRM changes with varying wind directions. Thus improvements in performance over the current standard are tied to how well the fog collector is sited. Any new collection material should be tested in the field in addition to the lab in order to assess impacts of wind direction variation, wind speeds, and fog droplet size distribution and to validate laboratory results under field conditions. Further potential for research includes continued investigation of fog-collection materials composed of cylindrical fibers and testing the TRMs in full scale fog collectors. A full scale installation may raise additional issues such as the ability of the material to maintain shape over time and necessity for further reinforcement. At the current scale, Enkamat® 7010 and 7220 TRMs are a low-cost, readily available material that can increase fog collection in the field.

2.6 Acknowledgements

2.7 Glossary

Modis = Moderate Resolution Imaging Spectroradiometer

SFC = Standard Fog Collector

TRM = Turf-Reinforcement Mat

Chapter 3 Physical and Mental Health Assessment of Informal Urban Dwellers in Lima Peru

3.1 Abstract

Background: Physical and mental health issues are pervasive in informal settlements in Lima, Peru. While surveys have measured demographics and chronic disease prevalence, gaps exist in knowledge about social capital, mental health and familial stressors in the informal settlements of Lima, Peru.

Methods: Demographic and physical health indicators were measured as well as validated scales for stress indicators, empathy towards children and partners, threatening life experiences, social capital in the community, and quality of life.

Results: We found high body mass index levels, little evidence of non-communicable diseases, and that older participants had higher levels of partner empathy. Quality of life scores indicated good QOL. Low levels of threatening experiences were observed. Social capital scores were low compared to other low-income countries, yet comparable to analysis in Peru.

Conclusions: We found a relatively healthy population, which voiced concerns in social capital. More research is needed on how to improve social capital in urban informal settlements.

3.2 Introduction

A third of the 8.8 million residents of Lima Peru live in informal settlements that lack adequate infrastructure (running water, sewer system, electricity) and basic services (health services, police and fire departments public parks etc.) (Riofrío, 2003). This urban poverty prevails despite Peru's rapid economic growth, its high rates of poverty reduction and expansion of basic and health services (World Bank, 2011). Peru.is considered an upper middle-income country with a mean annual income of $5,600 (INEI, 2012). However, this economic growth has not translated into the population of the urban informal settlements.

Little is known about these residents and what physical and mental health challenges they face. The National Quality of Life Surveys summarize information across all residents of Lima: the population is relatively young - 53.7% of the urban population is less than 30 years old; the average age of first marriage is 22.4 years and age of having the first child is 22.8 years (INEI, 2012); the majority of women are married or live with a partner (57.0%); most urban households have an average of 3.8 residents, which may include children, a partner, or relatives (INEI, 2012); male residents of Lima have completed a median of 10.3 years of education, and female residents a median of 10.2 years (INEI, 2012). However, it cannot be assumed that the demographics and health risk factors of residents in informal settlements are the same compared to the rest of the urban populations. Furthermore, the rapid influx of incoming residents to informal settlements creates another category of unknown data as these recent arrivals face additional challenges and stressors as they adjust to life in their new

51

environment. Since existing data from informal neighborhoods cannot be differentiated from the data of more affluent communities, the physical and mental health needs of informal communities may very well be masked (Riofrío, 2003).

More recently, two particular areas of research highlighted a number of health concerns in informal settlements in Peru: non-communicable diseases, mental health, and status of social relations of residents. The importance of looking at non-communicable diseases is becoming increasingly evident as the leading causes of death in Peru include lower respiratory infections, ischemic heart disease, stroke, cirrhosis, chronic kidney disease and diabetes (IHME, 2013). Studies in informal settlements in Peru have illustrated high rates of obesity (Vega et al., 2006), yet low rates of diabetes (Heitzinger et al., 2014) and hypertension (Davies et al., 2008; Heitzinger et al., 2014). The alcohol and drug use in South America continues to grow (Kirsch, 1995), with more than a million Peruvians dependent on alcohol and half a million Peruvians dependent on tobacco (INEI, 2003). The top four risk factors for disease in Peru are related to dietary risks such as high sugar and salt consumption, high blood pressure, high body mass index, and excessive alcohol consumption (IHME, 2013). However, collection of data on these risks has been inconsistent across informal settlements. Understanding the profile of these risks in a young settlement would provide a stronger basis for eventually developing informed health intervention strategies geared toward this unique and rapidly changing population.

Similarly, the importance of measuring mental health and the status of social relations is growing (Darkey & Kariuki, 2013; Loret de Mola et al., 2012). Previous

studies have documented the impact of depression on many urban adults in developing countries, with the poor suffering the highest rates of depression (National Academy of Sciences, 2003). More recently, the Institute for Health Metrics Evaluation (IHME, 2013) found that major depressive disorder is the second highest cause of disability-adjusted life years in Peru. Yet again, little is known about mental health and social supports or stressors in the informal, and poverty-ridden, informal settlements of Peru, and further work is needed to assess the mental health characteristics of new arrivals (Loret de Mola et al., 2012).

Finally, researchers and clinicians are increasingly recognizing the validity of what has been called the "biopsychosocial model," (Drossman, 1998) which recognizes the inter-connectedness among social, psychological and physical events. Thus, it is important that researchers not only focus on specific individual constructs such as demographics or mental health in any community being studied, but that they examine how these factors might be related, and associated with phenomena such as physical health risk factors. Very few data exist examining these relationships, particularly in informal settlements where, arguably given a multitude of potential stressors, this kind of knowledge is most needed.

To address these gaps, demographic, physical health and mental health characteristics in a recently established (2007) informal settlement in northern Lima were assessed.

Research aims:

1. To describe the health status of these community members, including social capital, stress, empathy, threatening life experiences, BMI, blood pressure, and fasting blood glucose levels and quality of life.

2. To identify correlations between demographic factors and the mental and physical health indicators in the community.

3.3 Methods

3.3.1 Study Design and Procedures

This study reports on the baseline data for a repeated measures longitudinal study. That study will assess how household and socioeconomic variables influence the implementation and cultivation of gardens, and how these gardens affect physical and mental health as measured through quantitative surveys, simple physiological metrics and qualitative methods. Additional data will be collected to obtain a more in-depth look at meaningful changes in the lives of participants, as measured through participatory impact assessment exercises. The home gardens in this study are one of the projected end uses for water collected from fog nets. Here we report the baseline data of (N=43) residents.

The overall study began in September 2013 and will end in September of 2014. The study obtained institutional review board approval from the University of Washington (IRB #44864C) and Universidad Nacional Mayor de San Marcos. Written

54

consent from all participants was obtained by meeting them at their homes to explain

the details of the study and review the Spanish-language informed consent forms.

3.3.2 Participants

Participants were recruited through announcements broadcasted by a town

leader and posters placed throughout the neighborhood. An initial introductory meeting

was held on July 21, 2013 to explain the goals, requirements and eligibility criteria of the

study.

Inclusion criteria for this study were that participants had to:

1) live in the Eliseo Collazos (EC) neighborhood,

2) be 18 years or older,

3) be able to attend all workshops,

4) be able to consent to the health measurements.

Forty-three participants were recruited and surveyed for the baseline health and well-

being metrics.

3.3.3 Setting

EC is the newest of 19 neighborhoods in a settlement in the Cono Norte of Lima,

Peru and as such has limited official infrastructure. EC consists of about 90 families and

250 people [Figures 3.1, 3.2].

Figure 3.1. Map of Lima, Peru.
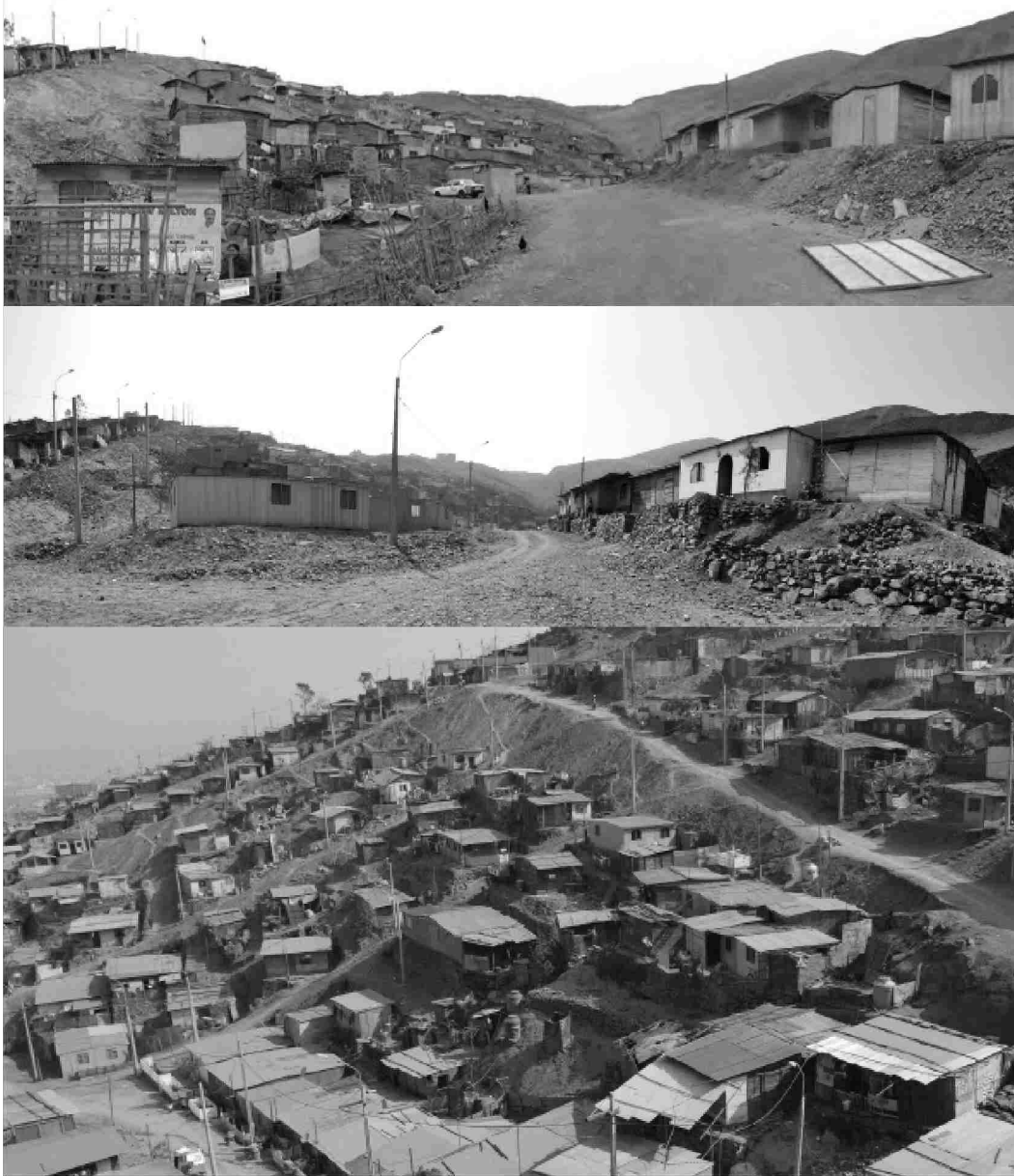
Figure 3.2. The community.

3.3.4 Measures

Physiological measures

Height, weight, blood pressure, blood glucose and waist circumference were measured. Each participant was asked to remove heavy garments and shoes to measure height and weight. Standing height was measured against the house wall. Weight was measured with a Taylor 7405 digital body weight scale. Blood pressure was measured with a Citizen CH-453 digital blood pressure monitor on the left upper arm following the guidelines of the American Heart Association. Fasting blood glucose was measured between 6 and 8 am with an Accu-Chek® Performa Nano glucometer. Waist circumference was measured with participants standing, midway between the iliac crest and lower rib margin at the end of expiration [World Health Organization Procedures (Molarius et al., 1999)]. Body mass index (BMI) was calculated by dividing weight in kilograms by height in meters squared; we used standard cut-points for the classifications of underweight (<18.5 kg/m^2), normal weight ($18.5 – 24.9$ kg/m^2), overweight ($25.0 – 29.9$ kg/m^2), and obese (>29.9 kg/m^2) (NIH, 1998).

Demographic and Mental Health Indicators

Demographic measures were obtained by questionnaire. If the participant preferred, the questionnaire was read to them. Questionnaires assessing mental health focused on stress indicators, empathy towards children and partners, threatening life experiences, social capital in the community, and quality of life. The questionnaire

booklet was reviewed by two native Peruvians to confirm that the intent of the questions was understandable to the participants.

The questionnaire consisted of the following:

1. Socio-economic demographic questionnaire variables include gender, age, languages spoken, years lived in the community, reason for moving, number of adults in the house, number of children in the house, civil status, education level, household monthly earnings, current illnesses, reasons they believed they had this illness, whether they drank alcohol, how often they drank, whether they smoked, how often they smoked, whether they did physical activity, how much time they are physically active physically active per day, including activities such as walking, lifting, carrying, playing ball, running, doing household activities, condition of their mouth and teeth, and frequency of pain in their teeth, mouth and jaws over the past year.

2. World Health Organization Quality of Life Brief Version (WHOQOL-BREF) measures quality of life through four domains: physical health, psychological health, social relationships and environment (The WHOQOL group, 1998). The scale is a shortened version of the WHOQOL-100 quality of life assessment with 26 items scored on a 5-point response scale. Higher scores indicate higher quality of life in each of the domains. The scale has high test-retest reliability and good internal consistency with $α>0.7$ in all domains performing higher in physical health, psychological and

environmental domains (Skevington, Lotfy, & O'Connell, 2004; The WHOQOL group, 1998).

3. The Perceived Stress Scale (PPS) measures the degree to which situations in one's life are considered stressful (Cohen et al., 1983). The scale has 14 items with a 5-point response scale ranging from never to very often; half of the items are reverse-scored (Remor, 2006). A higher total score indicates higher levels of perceived stress. A European Spanish version of the scale has good internal consistency (α= .81), test-retest reliability(r= .73) and demonstrated concurrent validity (Remor, 2006).

4. The List of Threatening Experiences (LTE-Q) consists of life events within the last three month including the experience of a serious illness, injury, or assault, either by the respondent or a close relative; death of a parent, spouse, or close relative; unemployment; problems with a close friend; problems with the police; or loss of a valued item. This is a short list of items that can account for a majority of long-term threatening life event categories (Brugha et al., 1985). The scale has 20 yes/no answer choices; higher total scores indicate being exposed to more stressful life events. The scale has high test-retest reliability (Kappa range=0.61 – 0.87) (Motrico et al., 2013).

5. The Social Capital Scale (SCS) measures social capital via eight sub-scales, including participation in the local community, social agency, feelings of trust and safety, neighborhood connections, friends and family connections, tolerance of diversity, value

59

of life, and workplace connections (O'Brien et al., 2004; Onyx & Bullen, 2000). The scale has 36 items on a 4-point response scale. We used a 31-item version that excluded the three workplace connection items and two work-related questions in the social agency subscale anticipating that the majority of participants in our study would be women with lower levels of employment. We also modified the response scale to include a descriptor of each point (never, sometimes, regularly, always). Higher total scores indicate more social capital. The scale has good internal consistency (α=.84) and acceptable validity (Onyx & Bullen, 2000).

6. The Parent/Partner Empathy Scale (PPES) measures parent empathy towards their children and towards their spouse or partner and provides an overall score, a parent empathy subscale and a partner empathy subscale (Feshbach & Caskey, 1985). The scale has 40 items with a 5-point Likert-type response scale. If respondents did not have a spouse or any children, they skipped the questions related to those topics. The scale has good internal consistency (α=.86). The version we utilized was back-translated into Spanish with Spanish-English bilingual psychologists (Perez-Albeniz & De Paul, 2004).

3.3.5 Statistical Analysis

Quality control included checking questionnaires for completeness, internal consistency, and spot-checking 12% of the surveys after entry. Composite variables were calculated. Statistical analyses were conducted using SPSS 19. Bivariate

analysis included cross tabulations (Pearson's chi-square test (χ^2) for 2 by 2 and 2 by 3 tables including nominal and ordinal data), independent two sample t-test (two tailed) (t) for subsets of the population as divided by a nominal variable, and Pearson's r (r) between scale data to identify the association between participants grouped by three demographic variables and social relation, physiologic and mental health metrics. Normality was assessed with the Shapiro-Wilk test. An *a priori* significance level of alpha = 0.05 was set to determine significance for all statistical tests. Some metrics were computed separately for participants under thirty years old and participants age thirty and older.

3.4. Results

3.4.1 Socio-economic Demographics

Out of the initial 43 participants, 32 fulfilled the requirements to receive a garden after the baseline survey and measurements; after 6 months 29 participants remained in the study. There were no substantial demographic differences between participants who initiated the survey and those who remain in the study either for initiation or at the 6 month interval. Results below are for the 43 baseline participants.

The mean age was 33.2 years old and the study sample was predominantly female. Most of the participants were partnered (72.1%), but only 7.0% were married, with the remainder of partnered participants' cohabitating. Households had an average of 4.1 residents, with an average of 2.1 adults and 2.0 children. Other adult residents included a partner or parents.

Only one participant had not acquired any education; almost half (46.5%) had attained a level of secondary education (7th through 11th grade) and 20.9% had studied at an institution of higher education. All four male participants had education beyond 11th grade, while only 5 of 39 women had attained that level. More than 80% of the households earned less than $270 per month, and a third earned less than $140 per month. Participants over 30 were more likely to have 9 or fewer years of education as opposed to at least 10^{th} grade than younger participants ($\chi^2 = 8.292$, *p<0.01*). Participants with 9 or fewer years of education were more strongly represented in the category of lower earnings (39.1% earning $0-$140 a month, vs. 20% of higher educated in the same category).

The average duration that participants had lived in EC was 6.3 years; this was positively correlated with age (r = 0.432, *p<0.01*). Two-thirds (69.8%) of the participants moved to the area to acquire land or have more space to live. Other reasons to move included finding work or better economic opportunities (16.3%), education opportunities for themselves or their children (14.0%), friends or family in the area (14.0%), or because of previous financial or family problems (9.3%). Participants sometimes provided multiple reasons for moving to EC so the total percentage exceeds 100%. Participants were born in provinces throughout Peru, yet immediately prior to living in EC, 74.4% had moved from elsewhere in Lima [Figure 3.3]. The majority of participants spoke only Spanish (81.4%), while the remainder spoke Quechua in addition to Spanish (18.6%); all but one of the participants who spoke Quechua was born in a province in the Andean highlands.
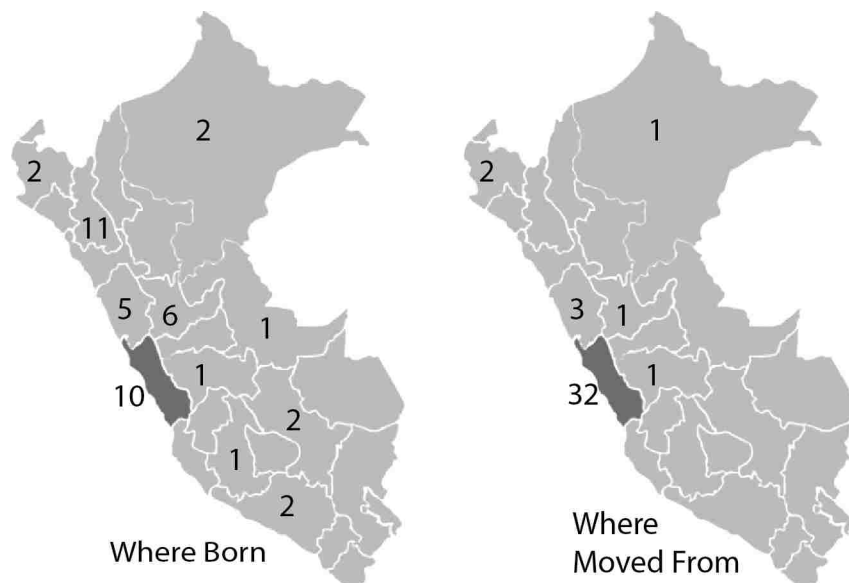
Figure 3.3. Migration demographics. Where participants were born, and where they moved from (numbers of participants by province shown).

Table 3.1. Demographic measures.

Demographics	Total
	N
Total (N,%))	43
Gender (N,%)	
Male	4 (9.3)
Female	39 (90.7)
Age (m,sd)	33.2 (9.5)
Language (N,%)	
Spanish	35 (81.4)
Spanish, Quechua	8 (18.6)
Years lived in Zapallal (m,sd)	6.3 (2.8)
Total in House (m,sd)	4.1 (1.6)
# Adults in House (m,sd)	2.1 (0.9)
# Children in House (m,sd)	2.0 (1.3)
Civil Status (N,%)	
Partnered (married or living together)	31 (72.1)
Single (single or separated)	12 (27.9%)
Education Level (N,%)	
None	1 (2.3)
Primary (1-6 years)	13 (30.3)
Secondary (7-11 years)	20 (46.5)
Higher (institute, university, technical school)	9 (20.9)
Monthly earnings[1] (N,%)	
$0-$140	13 (30.2)
$140 - $270	22(51.2)
$270 - $545	8 (18.6)

N: number

[1] 2.75 Soles is $1 USD exchange rate

Table 3.2. Physical health metrics.

Illness and Health behaviors	Total
	N
Currently sick (N,%)	19 (44.2)
Drinks alcohol[1] (N,%)	11 (25.6)
Smokes[2] (N,%)	2 (4.7)
Does physical activity (N,%)	41 (95.3)
How much per day (N,%)	
0-30 min	10 (23.3)
1-2 hours	14 (32.6)
2 - 3 hours	4 (9.3)
3 hours or more	15 (34.9)
Dental Condition (N,%)	
Bad	8 (18.6)
Normal	28 (65.1)
Good or very good	7 (16.3)
Dental pain, past year (N,%)	
Little (never, a little)	15 (34.9)
Frequent (sometimes, frequently, always)	28 (65.1)
Physiologic Averages	
Height (cm) (m,sd)	150.8 (7.0)
Weight (kg)[3] (m,sd)	58.1 (12.9)
BMI[3] (m,sd)	25.5 (4.3)
Waist measure (cm)[3] (m,sd)	87.3 (11.7)
Blood sugar (m,sd)	87.4 (9.6)
Blood pressure (mmHg) (m,sd)	114.5 / 71.8

N: number

[1]Once a month or other, [2]Once a month, [3]3 pregnant women excluded.

3.4.2 Physical Health Metrics

As noted in Table 3.2, nineteen (44.2%) of the participants experienced an illness at the time of the interview. Self-reported illnesses consisted of gastritis (5), headaches (4), ovarian cysts (4), liver problems (2) heart problems (2) cough or flu (2) kidney problems (1), high cholesterol (1) arthritis (1) and asthma (1). Half as many older participants (3) reported gastritis and headaches compared to younger participants (6). Numbers add up to > 43 due to reporting of more than one current illness by some participants.

While eleven participants (25.6%) reported drinking, the reported frequency was less than once a week. Only 2 participants smoked, and they smoked less than once a month. Almost all of the participants were physically active, with a third reporting three or more hours per day.

A total of 65% self-reported their dental conditions as normal, while 65.1% of participants also claimed to have occasional to persistent dental pain. Participants older than 30 were more likely to report their dental condition as 'bad' (χ^2 = 9.264, $p <0.01$); similarly, higher numbers of the older participants report constant dental pain.

Obesity can be used as one measure of risk for non-communicable diseases. The average height of the population was 150.8 cm (for women 149.5 cm), and weight 58.1kg (for women kg 57.1 kg), leading to an average BMI of 25.5 kg m^{-2} (same for women). Average waist circumference was 87.3 cm (for women 87.2 cm). Older participants had higher BMIs than the younger participants (26.9 kg m^{-2} vs. 24.0 kg m^{-2}) (t = -2.326, $p <0.05$), and larger waist circumferences (92.8 cm vs. 81.3 cm) (t = -3.521,

66

p<0.001). Accordingly, only 28.6% of the older participants had a normal BMI (< 25.0) (NIH, 1998), while 57.9% of the younger participants fell within the normal range of BMI. The other participants were overweight or obese. Participants that had lived in EC longer than five years had higher BMIs (27.2 kg m^{-2} vs 23.5 kg m^{-2}) (t=-2.935, *p<0.01*), which resulted in them being classified as overweight or obese (χ^2 =11.839, *p<0.01*).

Blood sugar and blood pressure can further indicate risk of lifestyle diseases. Average blood sugar was 87.4 mg dL^{-1}; only 4 participants were above diabetic thresholds (100 mg dL^{-1} or above). Average blood pressure was 114.5/71.8 mmHg; while diastolic blood pressure is higher for the older participants (75.3 mmHg vs. 67.9 mmHg) (t = 2.923, *p <0.01*), only two participants displayed systolic blood pressure over 130 mmHg.

Table 3.3. Mental health metrics

Survey	Total
	N
Parent Partner Empathy Scale (m,sd)	64.7 (8.3)
Partner Empathy (m,sd)	59.1 (11.1)
Parent Empathy (m,sd)	70.9 (9.7)
WHO Quality of Life (m,sd)	56.6 (9.6)
Physical domain (m,sd)	59.1 (12.0)
Psychological domain (m,sd)	64.6 (12.7)
Social domain (m,sd)	57.2 (16.5)
Environmental domain (m,sd)	48.4 (9.34)
Perceived Stress Scale (m,sd)	43.1 (11.9)
List of Threatening Experiences 20-item[1] (m,sd)	2.3 (2.1)
Social Capitol Scale (m,sd)	46.7 (10.5)
Feelings of Trust and Safety (m,sd)	55.1 (14.9)
Formal Participation in the Community (m,sd)	23.3 (18.7)
Tolerance of Diversity (m,sd)	66.2 (22.5)
Neighborhood Connections (m,sd)	42.2 (31.5)
Value of Life (m,sd)	63.7 (14.6)
Friends and Family Connections (m,sd)	39.2 (23.3)
Proactivity in a Social Context (m,sd)	34.1 (28.6)

Survey results standardized 0 – 100, except LTEQ 20 item. N: number
[1]On a scale of 1-20, all other items are scaled from 0 – 100.

3.4.3 Mental Health

The WHOQOL BREF internal consistency for our sample was low with physical domain $\alpha = 0.44$, psychological domain $\alpha = 0.51$, social domain $\alpha = 0.43$, environmental domain $\alpha = 0.36$, however excellent for all domains combined $\alpha = 0.80$. The Perceived Stress Scale had internal consistency within our sample of $\alpha = 0.67$. The Social Capital Scale consistency within our sample had an $\alpha = 0.76$. The Parent Partner Empathy Scale consistency within our sample had an $\alpha = 0.70$, with parental empathy $\alpha = 0.52$, and partner empathy $\alpha = 0.62$. These are all much lower than the values reported in the literature for internal consistency.

As noted in table 3.3, average parent partner empathy scores were 64.7 (on a 100-point scale), with lower partner empathy (mean of 59.1) than parent empathy (mean of 70.9). Participants under 30 reported higher total empathy scores than participants over 30 (67.7 vs. 61.3) (t=2.145, $p < 0.05$) with significantly higher levels of empathy towards their children compared to older participants based on the parent empathy subscale (75.6 vs. 67.2) (t=2.894, $p<0.01$).

Average quality of life scores were 56.6 (on a 100 point scale), with the highest scores in the psychological domain (64.6) and the lowest scores in the environmental domain (48.4). Participants with more than 9 years of education of education scored higher on the WHO Quality of Life scale (59.9 vs. 53.8) (t=-2.156, $p<0.05$); while all domains showed higher scores for more educated participants, only the environment domain was significantly different (52.7 vs. 44.7) (t=0.003, $p<0.01$).

Perceived stress scores averaged 43.1 (on a 100 point scale). Overall, low levels of threatening experiences were reported (average of 2.3 on the 20-item scale) [Table 3.3], but older participants experienced more threatening experiences (2.9 vs. 1.7 on the 20-item scale) (t=-2.066, *p<0.05*). Participants with higher levels of education had also experienced significantly fewer threatening life experiences (3.2 vs. 1.4) (t=3.264, *p<0.01*).

Social capital scores averaged 46.7 (on a 100 point scale), with the highest scores in the domains of tolerance of diversity (66.2) and value of life (63.7) and the formal participation in the community (23.3). Migration to EC for work and economic opportunity was associated with higher quality of life scores (t = -2.370, *p<0.05*).

The scales, as expected, were correlated. Parent Partner empathy scores were positively correlated with quality of life scores (r = 0.534, *p<0.001*), including the psychological (r = 0.667, *p<0.01*) and social domain (r = 0.671, *p<0.001*). Consequently, Partner empathy scores were positively correlated with quality of life scores (r =0.637, *p<0.001*), including the physical domain (r=0.426, *p<0.05*), psychological domain (r=0.629, *p<0.001*), social domain (r=0.610, *p<0.001*), and environmental domain (r=0.506, *p<.01*). Parent Partner empathy scores were negatively correlated with Perceived Stress (r = -0.300, *p<0.05*). Perceived stress scores were negatively correlated with Quality of Life (r = -0.437, *p<.01*), including the physical domain (r = -0.431, *p<0.01*), psychological domain (r = -0.331, *p<0.05*) and environmental domain (r = -0.407, *p<.01*). Perceived stress scores were negatively

correlated with Social Capital (r = -0.471, *p<.001*). Social capital is positively correlated

with Quality of Life (r = 0.345, *p<.05*).

3.5 Discussion

Our small sample provides an insight into the mental, physical health and quality

of life indicators in an informal settlement in Lima, Peru, and how these factors might be

inter-related. It thus presents a baseline for understanding demographics and stressors

in a young and developing part of an informal settlement. We found that some stressors

to physical health, mental health and social well-being were associated with age, level

of education and drivers of migration to EC.

Demographics: While total rates of cohabitation and marriage in the large community of

Lomas de Zapallal are comparable to the settlement, the number of residents in the

household is below average for the region (4.1 vs 5.4 residents) (Heitzinger et al.,

2014). An unexpected finding was that while the average household income in the

community was low, the attainment of secondary or technical/university education was

higher than seen in the national average (Heitzinger et al., 2014). We found differences

in education level dependent on age. In recent years, enrollment rates in education

have been improving, increasing the likelihood that younger participants would have

completed more years of education, although quality of schools is uneven (Sanchez,

2008). While a variety of reasons were stated for moving to the community, the

predominantly stated reason was to acquire land.

Physical Health Metrics: Almost half of the participants indicated that they were currently sick, with an illness profile that aligns with the predominant causes of death and disability in Peru. Gastritis and headaches seen within this population sample may be indicative of stress or depression which is, as stated previously, the second highest cause of disability-adjusted life years in Peru (IHME, 2013). In interpreting these data, it is also important to note that physical symptoms in South America are commonly reported as opposed to psychosocial complaints (Muñoz et al., 2005).

Our results show high overall rates of obesity that increase with age and tenure in the community, which reflects the numbers of metropolitan Lima residents that are overweight or obese: 45.3% of young adults (age 20-29) and 69.9% of 30-59 year olds (Alvarez-Dongo et al., 2012). In Peru, with changing dietary habits and lifestyles, increases in obesity are particularly found in urban areas and among women (Vega et al., 2006); the association seen could reflect dietary changes and changing activity levels.

Despite high BMIs, we found almost no evidence of diabetes and hypertension in our population based on fasting blood sugar and blood pressure. Studies indicate rates of diabetes between 6-8% in Latin America, with higher rates observed in lower income populations (Barceló & Rajpathak, 2001). In northern Lima, Peru, diabetes rates have been observed to be 3.7% (Vega et al., 2006) with rates across low socioeconomic status residents of Peruvian cities as high as 33% of women and 30.7% of men (Goldstein et al., 2005). Only four participants had blood pressure within hypertensive ranges; indeed low rates of hypertension have been observed in informal settlements in

72

Lima (Davies et al., 2008; Heitzinger et al., 2014). It is possible that the high rates of physical activity – with 35% of participants reporting three or more hours daily – accounts for the low rates of these non-communicable diseases.

Prior studies have indicated a growing concern with alcohol and drug use in low-income Latin American countries (Kirsch, 1995). In Peru, a 2003 survey indicated 75% of participants had drunk alcohol within the past year and 40% had smoked (INEI, 2003). Nonetheless, only a quarter of the participants in our study reported drinking and 5% reported smoking, both of these infrequently. However, with a predominantly female sample this is consistent with studies in Peru that report low levels of drinking or alcohol use disorders among women (Gálvez-Buccollini et al., 2008; Heitzinger et al., 2014), and low socioeconomic status groups (Vega et al., 2006).

Mental Health: Mental health and social relations are an increasingly recognized important component to any evaluation of conditions in informal settlements internationally (Camfield, 2012). As noted, few studies have been conducted to date on mental stressors and social capital in the informal settlements in Peru. Overall, scores were mid-range on most scales, with notably higher partner empathy scores and low amounts of threatening experiences.

Parent partner empathy scores emphasize relationships within the nuclear family. We note that strong relationships are observed in parents towards their children within our population group and higher levels of familial relations are correlated with higher quality of life and lower perceived stress.

73

Quality of life is a construct designed to capture a comprehensive picture of general well-being. Our scores are comparable to those observed in informal settlements in other parts of the world (for example, Bangladesh and India) (Mudey et al., 2011; Tsutsumi et al., 2006). While there is indication that quality of life scales may not fully capture the factors that participants consider relevant in developing countries (Skevington, 2009), these scales can be combined with participant interviews to further clarify elements that would contribute to improved quality of life, such as improved services and economic empowerment in African urban settlements (Darkey & Kariuki, 2013), or household gardens as indicated by participants in our study.

Study participants reported slightly below average levels of perceived stress (Cohen et al., 1983) and few major threatening experiences. Lower levels of stress are associated with improved health outcomes in low income populations (Watson et al., 2008); this may contribute to the physical health outcomes observed in the population.

Social capital is a construct that has been found to be beneficial to measure engagement in civil society, and is a useful construct to evaluate integration of new residents into the informal settlement. Overall social capital scores were moderate; consistent with other research in Peru, as compared to other low-income countries such as Vietnam, India and Ethiopia (De Silva & Harpham, 2007). Lower overall social capital scores could also be due to the high proportion of girls in the society – female young adults in Peru have shown lower trust in members of immediate society than boys (Dercon & Singh, 2014). Participants with longer duration of residence had higher rates of social capital, particularly with greater levels of participation in community.

Communal work is often needed in establishing the settlements; while newer settlers are moving into areas that are already established (Riofrío, 2003). It is possible that these residents of longer tenure established ties as early settlers. However, this relationship is dependent on how recent migration to the community occurred. A study of migrants in Lima found no difference in social capital between urban residents of an informal settlement born in Lima and those who had migrated to the same settlement at some point in their lives – 90% of whom had migrated more than 20 years ago (Loret de Mola et al., 2012).

Limitations: Our findings are based on a small sample within a single community and may not be generalizable to other groups. There may be sample bias, as the group was selected for ability to participate in a garden implementation study, that required attending multiple workshops and garden construction. Scale consistency was low for the WHOQOL-BREF domains, and subdomains of the parent-partner empathy scale. This may be due either the smaller sample size, or how well concepts measured in the survey resonated with the community. Translations of instruments developed in the Western hemisphere may have poorer psychometric properties in other cultures (Ware & Sherbourne, 1992). Finally, while the WHOQOL-BREF was developed to create a cross-cultural quality of life measure (Skevington et al., 2004), it still may not fully represent the dimensions of quality of life in developing countries (Camfield, 2012; Skevington, 2009).

Nevertheless, the findings in this report provide new information on the health and well-being of residents in a relatively new settlement in Lima, and this work can serve as a foundation and referent point for future studies in EC and in other similar communities. Additionally, relational findings such as that quality of life scores were positively correlated with parent partner empathy and social capital scores, and negatively correlated with perceived stress, can aid in assessing stressors to participant's life, as well as guiding efforts in future evaluations and interventions.

3.6. Conclusions

This study provides a demographic, health and well-being profile of an informal urban community in the Lima, Peru area. It lays the groundwork for future work that can assess the impact of household gardens on health and well-being in informal settlements; additional measures will be repeated at 6 months and one year. Generalizability in both assessing profiles of informal urban communities and the impact of gardens can be acquired by scaling the project up to a larger sample size and with multiple communities. Our pilot study provides both an initial assessment that can be explored further in future studies, and a procedural template for these studies. Ultimately, this work can provide a comprehensive understanding of informal settlement conditions, with the ultimate goal of improving health conditions in these communities.

3.7 Acknowledgements

Chapter 4 Predicting Duration of Fog Cover in Lima, Peru

4.1 Abstract

Fog can be used as a water resource in the otherwise arid, coastal Peru. This resource can be characterized as climate conditions in Peru are heavily influenced by the state of the tropical Pacific through El Niño. This paper informs the use of the fog resource in coastal Peru, with a focus on Lima, by investigating whether there are significant correlations between the frequency of cloud cover or the mean seasonal duration of the fog season with sea surface temperature. The analysis was performed using coastal station observations of stratus and stratocumulus clouds (low clouds that would be observed as fog in the coastal mountains) and cloud fraction determined by satellite over a 30 year time period. We found the mean annual duration of stratus and stratocumulus cloud cover to exist between May and November, with variation in the length of the cloud season along coastal Peru. Stratocumulus cloud cover is in general positively correlated with the El Niño 3.4 index, yet negatively correlated with El Niño indices during the peak fog season; also negatively correlated with SST along coastal Peru. Stratus cloud cover is negatively correlated with the El Niño 3.4 and El Niño 1+2 index. There is potential to predict fog water availability in coastal Peru due to the predictability of El Niño   In addition, this suggests that reductions in Peruvian cloud cover may be observed with warming sea temperatures.

4.2 Introduction

Coastal Peru, in particular the rapidly growing capital city Lima, is currently experiencing a high level of water stress (Smakhtin, Revenga, & Döll, 2004). The climate is extremely arid, despite high relative humidity (80-90%), the Lima receives less than 10 mm of rain a year (Molina, 1999; Riofrío, 2003). The severity of this situation will be exacerbated by both the demands of a growing population and reductions in glacial sources to the rivers that serve the city (Painter, 2007).

However, despite the low rainfall, atmospheric water resources are available in the area. The combination of cool waters from the Humboldt Current that flows along the Chilean and Peruvian coastlines produces a temperate marine climate with temperatures in the capital Lima between 14°C and 20°C in the winter and 18°C and 30°C in the summer (Molina, 1999; Riofrío, 2003). These conditions, combined with the stabilizing influence of the South Pacific anticyclone, trap moisture near the surface to produce a low layer of clouds from roughly May to November (Heileman et al., 2009; Mantua & Hare, 2002). Coastal Peru consists of a narrow coastal plain on the Pacific Ocean that meets the steep rise of the Western Cordillera of the Andes Mountains. As the clouds intercept the steep hillsides surrounding Lima, they form a thick fog.

Stratus and stratocumulus clouds will factor differently into fog inputs at elevation. Stratus clouds are dense clouds are formed at low elevations, usually between the surface and 600 m, but up to 1200 m (Meteorological Office UK, 2006); these clouds can appear as incoming fog in the coastal hills (Pedgey, 1967). Stratocumulus clouds include small-scale convective mixing resulting in a patch appearance that is capped by

79

a strong inversion; these clouds may spread out under an inversion to form a layer of fog (Meteorological Office UK, 2006). These clouds tend to form at a higher elevation than stratus, between 300 m and 1400 m, but up to 2000 m (Meteorological Office UK, 2006). In addition to cloud elevation, while both status and stratocumulus are low cloud layers capped by a temperature inversion, the dynamics of stratocumulus clouds are driven by shallow convective instability as opposed to a strong temperature stratification found in stratus clouds (Wood, 2012). This instability can result in periodic drizzle and development of a more open cloud structure as the cloud mass moves inland from the moisture source supporting its development (Stevens et al., 2005; Wood, 2012). Thus the importance of the cloud type to producing fog in the coastal hills depends on the elevation and distance inland to the location of interest.

Fog provides a critical water resource to the region. It supports native ecosystems along the Peruvian coastline that have adapted to capture water from the fog as it is blown into the hillsides (Rundel & Dillon, 1998). It also has the potential to be harvested for human use using fog collection techniques, a technology that has been used since the 1960s to acquire water for drinking, irrigation, and re-vegetation projects using large mesh nets (Klemm et al., 2012). Understanding the availability of fog throughout the year is essential if it is to be incorporated into water resource planning and considered for ecological restoration.

Fog production is temporally intermittent, yet may be predictable through its relationship to large-scale climate phenomenon such as El Niño. Initial conversations with residents in Lomas de Zapallal in Lima, Peru indicated that the duration of fog

80

cover is typically during May to October, yet can vary significantly from year to year with durations of 3 – 9 months.

Climate conditions in Peru are heavily influenced by the state of the tropical Pacific Ocean through El Niño (Glantz, 1996). El Niño is a coupled ocean-atmosphere phenomenon whereby the easterly trade winds weaken and the thermocline in the eastern Pacific declines, leading to reduced upwelling of cool water along the Peruvian coast and warmer sea surface temperatures through the equatorial Pacific Ocean (Philander, 1990). Likewise, La Niña events are periods of unusually cool waters, with Eastern Pacific precipitation. These warming temperatures can be characterized in the Niño 1+2, Niño 3, Niño 3.4 and Niño 4 regions; a standard index can be defined such that El Niño or La Niña events are identified when the 5-month running mean of the sea surface temperature (SST) index in the Niño 3.4 region (which is 5°N–5°S, 120°–170°W) exceeds the threshold value of $0.4^{\circ}C$ (for La Niña, below $-0.4^{\circ}C$) for a minimum of 6 months (Trenberth, 1997). El Niño conditions peak at the end of the calendar year, with predictability starting during the late spring and summer. Previous work using ship observations showed that fog and low cloud frequencies in the Eastern Pacific Ocean are linked to sea surface temperatures anomalies, with reduced amounts of marine stratocumulus clouds but increased cumulus clouds during warm phases of El Niño – Southern Oscillation (ENSO) (Park & Leovy, 2004). Reanalysis datasets furthermore indicated that higher June through August precipitable water content occurs during El Niño conditions as defined by the El Niño 3.4 region (Eichler & Londoño, 2013). The relationship between coastal cloud conditions (with precipitation as a proxy) and El Niño

81

1+2 is shown to be stronger than El Niño 3.4 (Lagos el al., 2008); the power of cloud condition prediction can vary by region of the ocean used in analysis.

To some extent, El Niño events can be predicted (Chen & Cane, 2008). Coupled ocean-atmosphere models have moderate skill at forecasting onset and spatial patterns of El Niño events with a six-month lead time, and up to two years lead on large El Niño events (Chen et al., 2004), although predictive power is limited for small events and during the spring (Chen & Cane, 2008; Torrence & Webster, 1998). Multi-model forecasts have increased skill at predicting SST anomalies at a coarse resolution, providing greater opportunity to develop SST forecasts (Kaiser Khan et al., 2014).

Using El Niño conditions or sea surface temperature variations to understand the prevalence and duration of fog and low cloud cover throughout the year in coastal Peru, and particularly Lima, would allow communities, water resource managers and ecologists to forecast fog duration in advance. This study sought to determine (1) the mean seasonal duration of low cloud cover in coastal Peru, (2) the correlation between amount and duration of low cloud cover and El Niño indices (El Niño 3.4 and El Niño1+2), and (3) the correlation between amount and duration of low cloud cover and sea surface temperatures in the Pacific Ocean between 30° south and 30° north. We discuss the importance of these correlations for how coastal fog can be better used as a water resource, and how future sea surface temperatures and climatic conditions could influence changes in this low cloud cover.

4.3 Data Sources

In this study, we used cloud cover data from station data throughout Peru (EECRA, Extended Edited Cloud Reports Archive) as well as satellite observations of cloud cover (ISCCP, International Satellite Cloud Climatology Project) (Eastman et al., 2011; Roslow, 1991). In addition, sea surface temperature was used to define the state of the tropical Pacific and any linkages to changes in the coastal ocean (OISST, Optimum Interpolation Sea Surface Temperature data set and NCAR El Niño SST indices) [Figure 4.1]. Analysis was conducted for the period of available data, from 1971 through 2009.
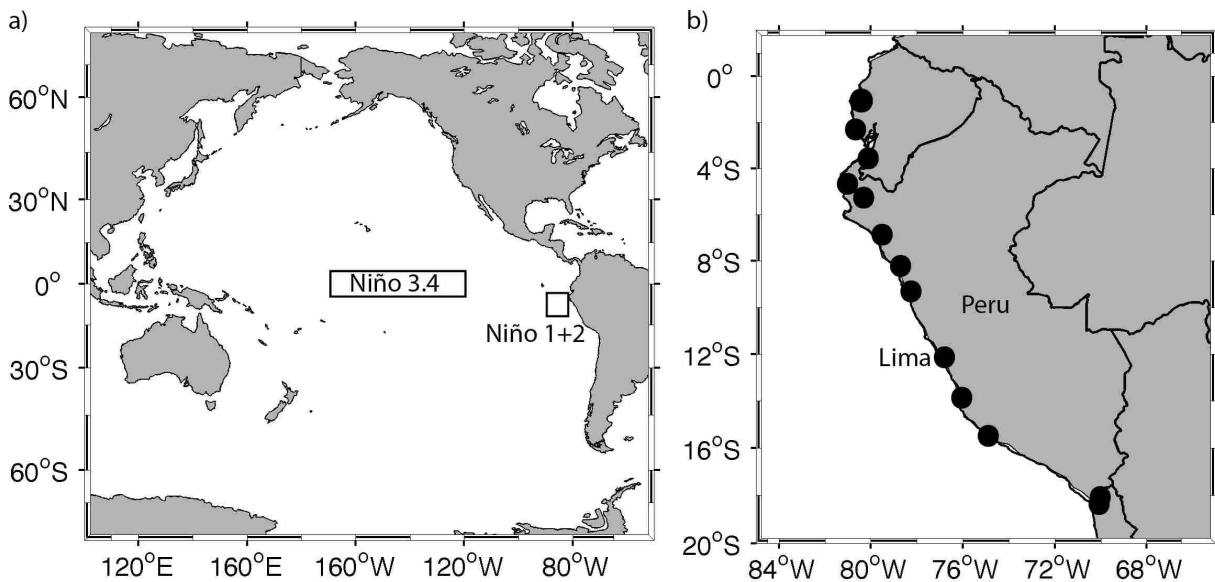
Figure 4.1. a) Pacific Ocean regional map, showing location of El Niño SST indices. b) Map of Peru, with 13 coastal EECRA stations. ISCCP data were interpolated to these points. Scale shows latitude and longitude in equidistant cylindrical projection.

Extended Edited Cloud Reports Archive (EECRA). EECRA is an archive of observations on land from surface meteorological stations and over the sea from ships which includes monthly percent cloud cover of low-elevation clouds (stratus,

83

stratocumulus and heavy fog). Heavy fog is considered to be <1/4 mile visibility, or a

cloud base at or below 400 m above ground level. Stratus, stratocumulus and fog data

were acquired from 13 coastal airport stations in Peru from 1971 through 2009. We

used average percent cloud cover observed over the month, where observed clouds

could range from no cloud coverage to full sky coverage. [NDP-026E data set

http://cdiac.ornl.gov/epubs/ndp/ndp026e/ndp026e.html Accessed December 8, 2012].

(Eastman et al., 2011)

International Satellite Cloud Climatology Project (ISCCP). ISCCP is a global gridded

(280 kilometer) dataset of infrared and visible radiance images from which cloud

parameters can be derived. Cloud parameters include average cloud fraction, cloud top

pressures, and cloud types. Each map grid cell is labeled land, ocean or coast.

Monthly data were acquired from the dataset at points collocated with the EECRA

stations from 1984 through 2009. These data were acquired by 2D linear interpolation

from the ISSCP grid onto the latitude and longitude of the EECRA stations [ISCCP

dataset http://isccp.giss.nasa.gov/ Accessed November 29, 2013]. (Roslow & Schiffer,

1991)

Equatorial Sea Surface Temperatures. 1 degree latitude by 1 degree longitude gridded

sea surface temperatures were acquired from optimum Interpolated Sea Surface

Temperature (OISST), generated using interpolated in situ and satellite measurements

from 1971 through 2009 (www.esrl.noaa.gov/psd/data/gridded/data.noaa.oisst.v2.html).

Monthly SST anomalies were acquired for El Niño region 3.4 and Niño region 1+2 SST

indices from the NOAA Climate Prediction Center from 1971 through 2009 (http://www.cpc.ncep.noaa.gov/data/indices/). These anomalies were calculated by subtracting the monthly average SST calculated from a 1981 to 2010 base period from the timeseries of SST values. El Niño region 3.4 is 5°N to 5°S, 120° to 170°W and Niño region 1+2 is 0° to 10°S, 80°W to 90°W [Figure 4.1].

Methods

For analysis, data were quality controlled and converted into time series of cloud cover and SST anomalies. These anomalies were then analyzed to determine correlations that would allow projections of cloud cover.

Data quality control and preparation

Data quality controlled procedures are described in Hahn & Warren (1999) and NCAR (2013). Low cloud and seasonal fog cover data were further quality controlled by inter-comparison of stations within the EECRA data set, to ensure that data were representative of cloud conditions, by removing time periods where jumps in cloud cover fraction were significantly greater than the average values observed.

The monthly average percent fog and low-cloud cover was determined from the EECRA archive of airport meteorological stations and the ISCCP dataset interpolated to the points collocated with the EECRA stations. Average percent fog and low-cloud cover includes all days within each month whether there is full cloud coverage, no cloud coverage, or partial cloud coverage.

We determined the anomalies from seasonal patterns by subtracting monthly average cloud and fog cover from the time series of cloud cover fractions. We determined sea surface temperature (SST) anomalies by subtracting monthly average sea surface temperatures (using the full dataset to determine monthly averages) from the timeseries SST values in the OISST grid. The Niño regions 3.4 and Niño 1+2 anomalies were calculated by NOAA as described above.

Regression analysis

The duration of fog and low cloud cover in coastal Peru was assessed using EECRA and ISCCP data. Presence of fog or low cloud cover was considered to be a month containing either greater than 50% stratocumulus cloud cover, greater than 40% stratus cloud cover or greater than 25% ISCCP cloud fraction. Thresholds were selected to match algorithmic assessments of cloud cover duration with reported values. The annual duration of cloud cover was the number of months with a consistent sequence of cloud presence above the threshold, or a sequence only interrupted by one month. Years during which there were greater than one missing data point are removed from the analysis. As the fog season develops during the southern hemisphere winter, the year is measured from April to March the following year. A time series of number of months with fog or low cloud cover per year was created for each of the EECRA stations and ISCCP grid points. These time series were averaged to determine the average duration of low cloud cover at each station. A time series of annual anomalies was created by subtracting this average duration of cloud cover from the overall time

series, where positive anomalies indicate a longer annual duration of cloud cover, and negative anomalies indicate a shorter duration of cloud cover.

We assessed the influence of El Niño conditions on cloud cover in coastal Peru with time series of cloud anomalies and SST indices. Sea surface temperatures anomalies from El Niño region 3.4 and Niño 1+2 were correlated to EECRA and ISCCP cloud cover anomalies on a month by month basis using linear regression. We multiplied the correlation by the standard deviation of the cloud cover anomalies divided by the standard deviation of the El Niño indices to convert to regression coefficients. These regression coefficients represent the percent cloud cover change per °C of SST change. We assessed whether there was a stronger seasonal correlation by conducting linear regression between El Niño index anomalies and cloud cover during the fog season with a time series that only included data from July through September (and compared with 3-month time series for earlier and later in the fog season). We converted seasonal correlation values to regression coefficients as well. We used the unlagged correlation at the 95% confidence interval, excluding results that were non-significant. To assess the influence of El Niño on annual duration of low cloud cover, we regressed the time series of annual cloud cover duration against the average July August September (JAS) SST temperatures in the El Niño region 1+2 and El Niño region 3.4. JAS temperatures reflect a time period after El Niño has begun to develop, and is also within the fog season; this time period was also used based on correlation coefficients from the prior analysis. Regression coefficients (that represent the change

in number of months of cloud cover per °C of SST change) were also calculated as noted previously for the correlation between cloud cover duration and El Niño indices.

We assessed the influence of sea surface temperatures on cloud cover in coastal Peru with time series of cloud anomalies and the anomalies of the gridded dataset of Pacific sea surface temperatures, between 30° south and 20° north. Monthly linear regression was conducted between EECRA station cloud cover anomalies and the SST grid in the Pacific Ocean (from the OISST data set) to determine the region within the Pacific Ocean where SST is most linked to cloud cover anomalies over coastal Peru. We also assessed whether there was a stronger seasonal correlation by conducing linear regression between El Niño index anomalies and the JAS period of the fog season.

4.4. Results

Data are available from 1971 – 2009 for monthly average percent cloud cover for fog, stratus and stratocumulus clouds from 13 coastal airport meteorological stations in Peru in the EECRA archive and from 1984 – 2009 for monthly average cloud fraction over a grid cell from the ISCCP [Figure 4.2]. Some data were removed in quality control, or observations were unavailable from the station.
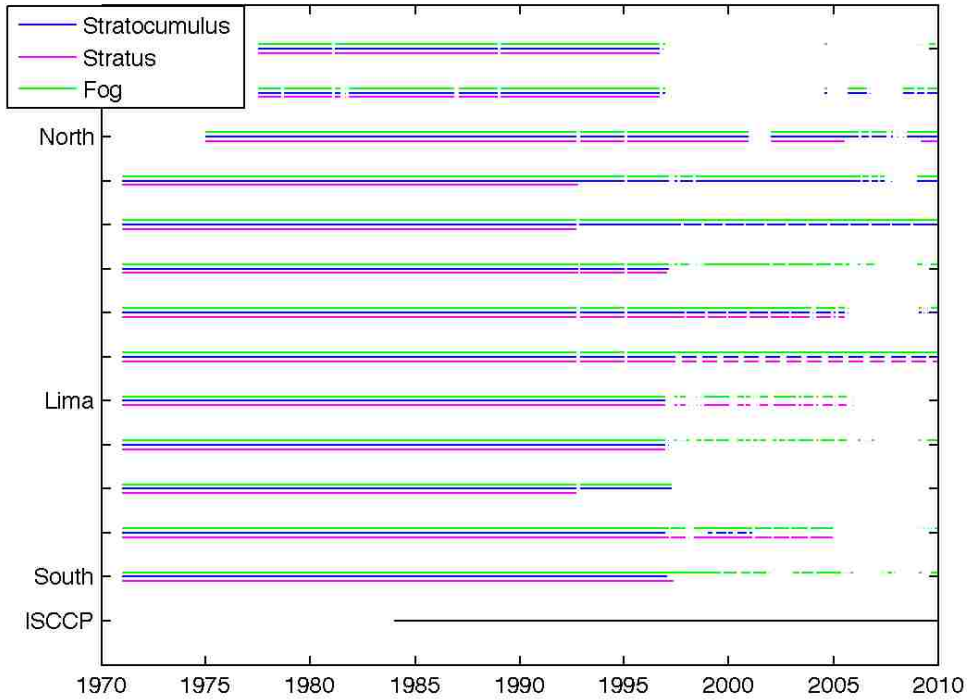
Figure 4.2. Monthly availability of seasonal fog and low-cloud cover data from 13 coastal airport meteorological stations (EECRA archive), listed north to south, and the ISCCP dataset.

The average duration of cloud cover was assessed at each of the EECRA stations and the ISCCP grid point for all cloud types using the monthly average cloud fraction over the period of record [Figure 4.3]. Many of the stations in northern coastal Peru reported low stratocumulus cloud cover amounts in January, followed by a brief increase of stratocumulus clouds in February. This pattern was not observed in southern coastal Peru.
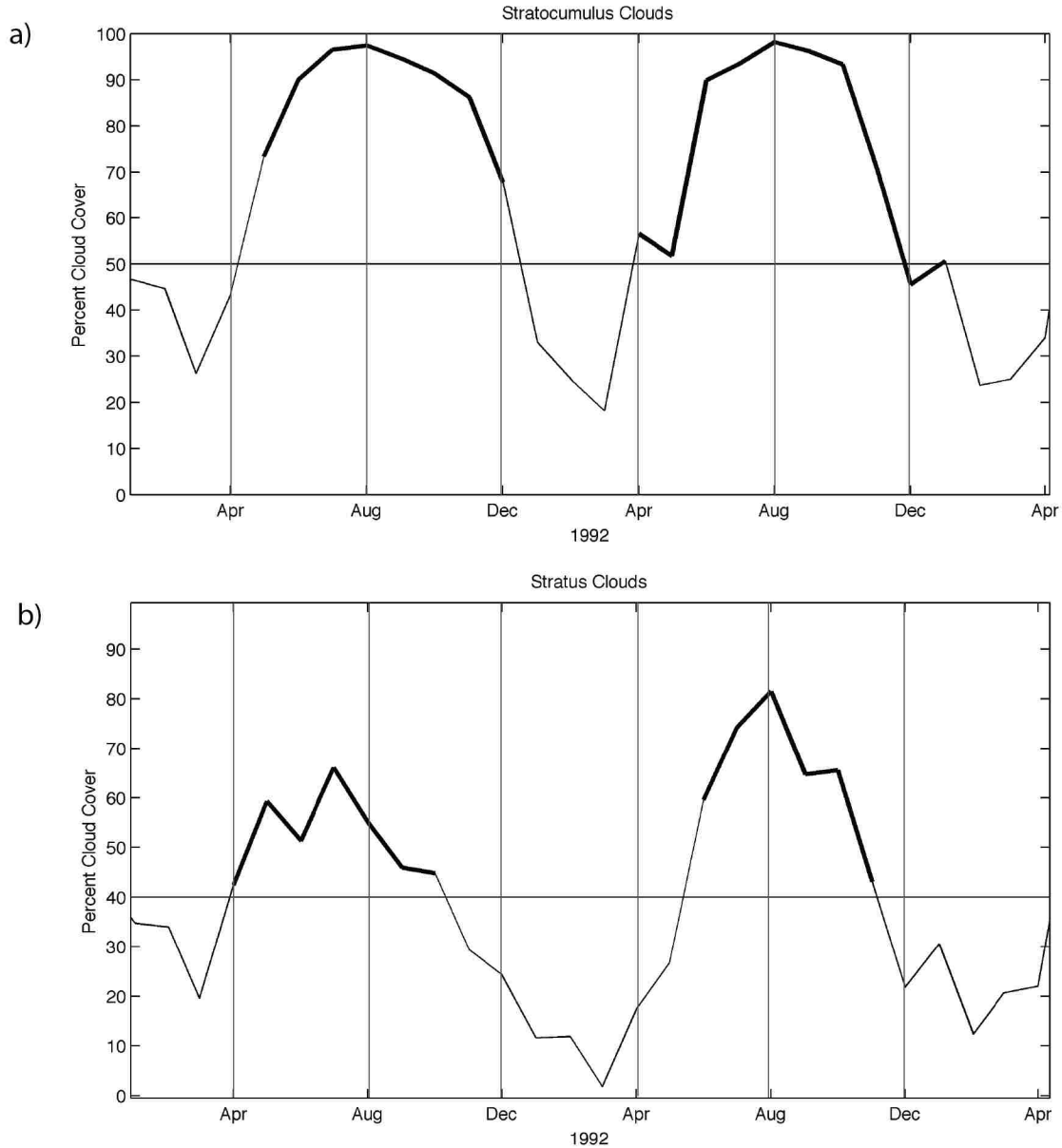
Figure 4.3. Bold lines indicate the part of the year with months of greater than the threshold cloud cover that are included in the months of cloud cover count, for (a) stratocumulus clouds (50% threshold) and (b) stratus clouds (40% threshold). Also included are months that reflect a brief dip in an overall cloud cover season.

The coastal airport stations showed a wide range of monthly average low cloud coverage over the period of record. At the Lima station, slightly lower amounts of sky coverage was observed with stratus clouds [Figure 4.4a] than stratocumulus cloud

90

cover [Figure 4.4b]. The northern stations showed significantly higher amounts of stratocumulus clouds with more consistent frequencies throughout the year [Figure 4.5b] than stratus clouds [Figure 4.5a]. Fog cover at the meteorological stations is generally a poor predictor of fog potential at higher elevations, as little fog is observed at the airport stations (which are often intentionally situated in regions of low fog). The ISSCP gridded data interpolated to EECRA station locations had higher average cloud fractions at stations north of Lima [Figure 4.4c, 4.5c].

The mean annual duration of the cloud cover season in Lima can be seen when peak quantities of cloud cover for both stratus and stratocumulus clouds were observed, between May and November [Figure 4.4a, 4.4b]. At the stations along coastal Peru, stations near Lima reported the highest average frequency of both stratus and stratocumulus cloud cover, with some stations displaying almost 100% stratocumulus cloud cover during the peak months July through September [Figure 4.4b]. Stratus cloud cover frequency ranged from average highs above 80% in September at the stations near Lima [Figure 4.4a] to lows of nearly nonexistent cover at the northern stations [Figure 4.5a]. The ISCCP data over Lima showed the highest percent cloud cover during May through November [Figure 4.4c].

Figure 4.4. Boxplots show the range of cloud cover fraction by month observed at Lima EECRA station and ISCCP gridded data interpolated to Lima station location. The median, lower quartile and upper quartile are represented. The whiskers extend to the extreme data points not considered outliers (within $+/-2.7\sigma$). a) Stratus clouds, b) stratocumulus clouds and c) ISCCP cloud fraction data.

Figure 4.5. Boxplots show the range of cloud cover fraction by month observed at northern EECRA station and ISCCP gridded data interpolated to northern station location. The median, lower quartile and upper quartile are represented. The whiskers extend to the extreme data points not considered outliers (within $+/-2.7\sigma$). a) Stratus clouds, b) stratocumulus clouds and c) ISCCP cloud fraction data.

   Duration of stratus and stratocumulus cloud cover, as evaluated by our metric, varies

along coastal Peru. Both the areas near Lima and North Peru have relatively long

durations of at least 50% stratocumulus cloud cover during the year [Figure 4.6a]. The

Lima station has a mean of 9 months of at least 50% stratocumulus cloud cover per

year, though this ranges from six to twelve months [Figure 4.7a]. The greatest overall

duration of at greater than 40% stratus cloud cover was observed near Lima, Peru [Figure 4.6b]. The Lima station has an average of 8 months of greater than 40% stratus cloud cover, with the duration ranging from three to eleven months [Figure 4.7b]. Northern Peru had very low amounts of monthly stratus cloud cover. When ISCCP gridded data were interpolated to EECRA station locations, the stations north of Lima had a median of 5-7 months of cloud cover, while generally low cloud fractions were observed south of Lima [Figure 4.6c]. While longer fog seasons could be an indication of either early low cloud cover, or the fog season extending later in the year, in Lima, we found longer fog seasons when low cloud cover started earlier in the year [Table 4.1].
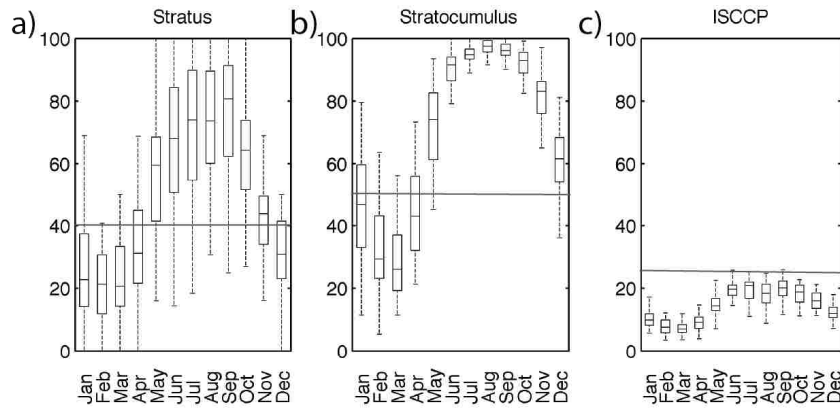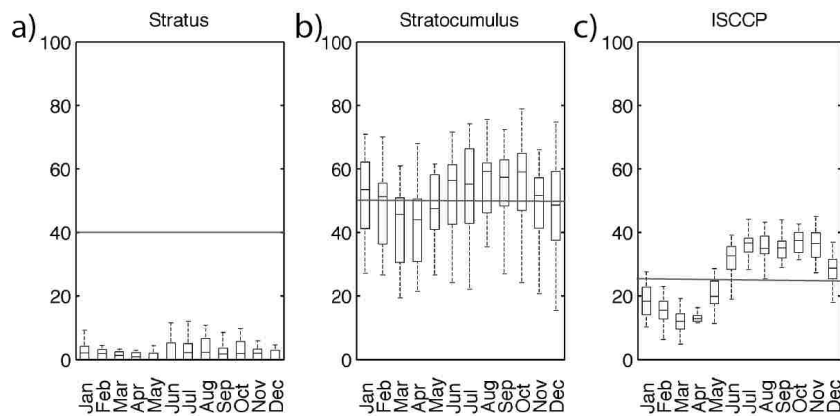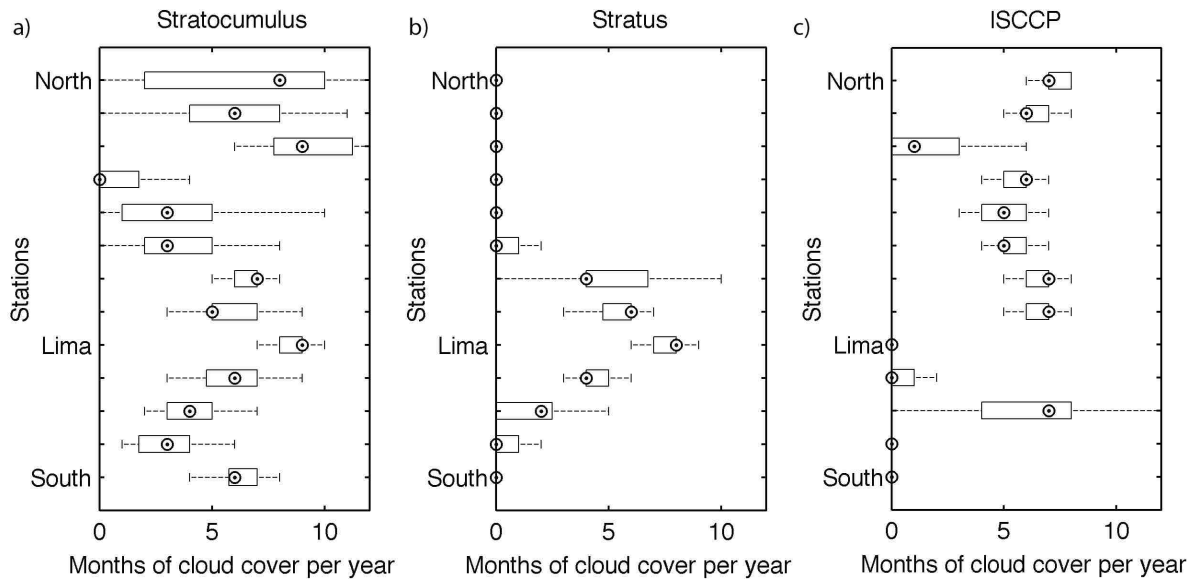

Figure 4.6. Boxplots show the range of cloud cover duration in months observed at EECRA coastal stations and ISCCP gridded data interpolated to EECRA station locations. The median, lower quartile and upper quartile are represented. The whiskers extend to the extreme data points not considered outliers. (a) Stratocumulus clouds, (b) stratus clouds and (c) ISCCP data.
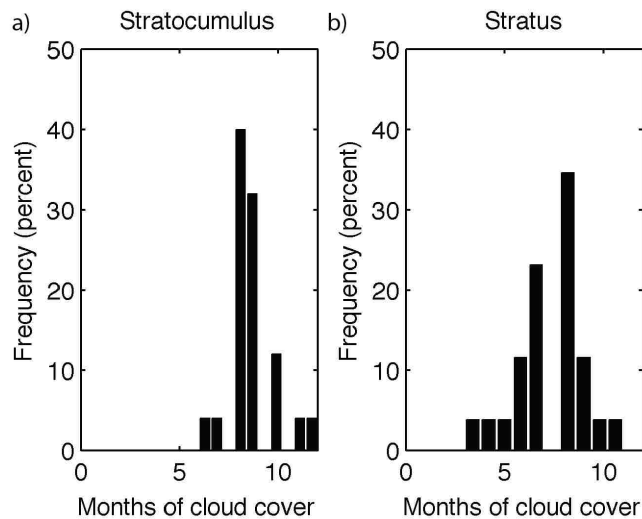
Figure 4.7. Histogram of cloud cover duration in months observed at the Lima EECRA station. (a) Stratocumulus clouds, (b) stratus clouds.

Table 4.1. Average duration (months) of stratocumulus and stratus cloud cover in Lima based on the first month of the fog season (>50% stratocumulus cloud cover or >40% stratus cloud cover)

Month	Stratocumulus Duration	Stratus Duration
April	9.6	7.7
May	8.4	7.5
June	7.0	6.0
July	-	4.0

4.4.1 Low Cloud Cover and SST Indices (El Niño region 3.4 and Niño 1+2)

A positive correlation was found between stratocumulus cloud cover and Niño 3.4 SST anomalies in coastal Peru, except in north Peru, where this correlation is negative [Figure 4.8a]. A positive correlation was also found between Niño 1+2 SST anomalies and the amount of stratocumulus cloud cover for most of the stations, however this correlation is negative in both north Peru and in Lima [Figure 4.8d]. As much as a ±8% change in stratocumulus cloud fraction can be explained by 1°C change in El Niño 3.4 or El Niño 1+2 (α = .05). This is compared to a mean stratocumulus cloud fraction of

35% to 70%. The value of the correlations were negative when regressions were run with data from time periods within the fog season, particularly correlations between cloud cover and El Niño indices early or mid fog season (June July August (JJA) or July August September (JAS)), with cloud cover change of up to 6.5% change in stratocumulus cloud fraction with a 1°C change in El Niño 3.4 or El Niño 1+2 ($\alpha = .05$) [Figure 4.8a, 4.8d].

A negative correlation is observed between Niño 3.4 SST anomalies and the amount of stratus cloud cover at the EECRA stations along coastal Peru [Figure 4.8b]; this correlation is more pronounced near Lima. Likewise, a negative correlation is observed between Niño 1+2 SST anomalies and the amount of stratus cloud cover [Figure 4.8e]; with a more pronounced negative correlation near Lima. As much as a –8.5% change in stratus cloud fraction can be explained by 1°C change in El Niño 3.4 or El Niño 1+2 ($\alpha = .05$). This is compared to a mean stratus cloud fraction of 0% to 50%. When we evaluated the regression between cloud cover and El Niño indices early and mid fog season (June July August (JJA) or July August September (JAS)) the correlations were enhanced to as much as a -10% change in stratus cloud fraction with a 1°C change in El Niño 3.4 or El Niño 1+2 ($\alpha = .05$).

A small positive correlation is observed between Niño 3.4 SST anomalies and the ISCCP fraction of cloud cover along coastal Peru [Figure 4.8c]. A negative correlation is observed between Niño 1+2 SST anomalies and the ISCCP fraction of cloud cover in north coastal Peru [Figure 4.8f]. These correlations account for +2% changes in stratocumulus cloud fraction explained by 1°C change in El Niño 3.4 ($\alpha = .05$) or –2%

95

changes in stratus cloud fraction explained by El Niño 1+2 ($\alpha = .05$), with cloud fraction that ranges from 6% to 26%.
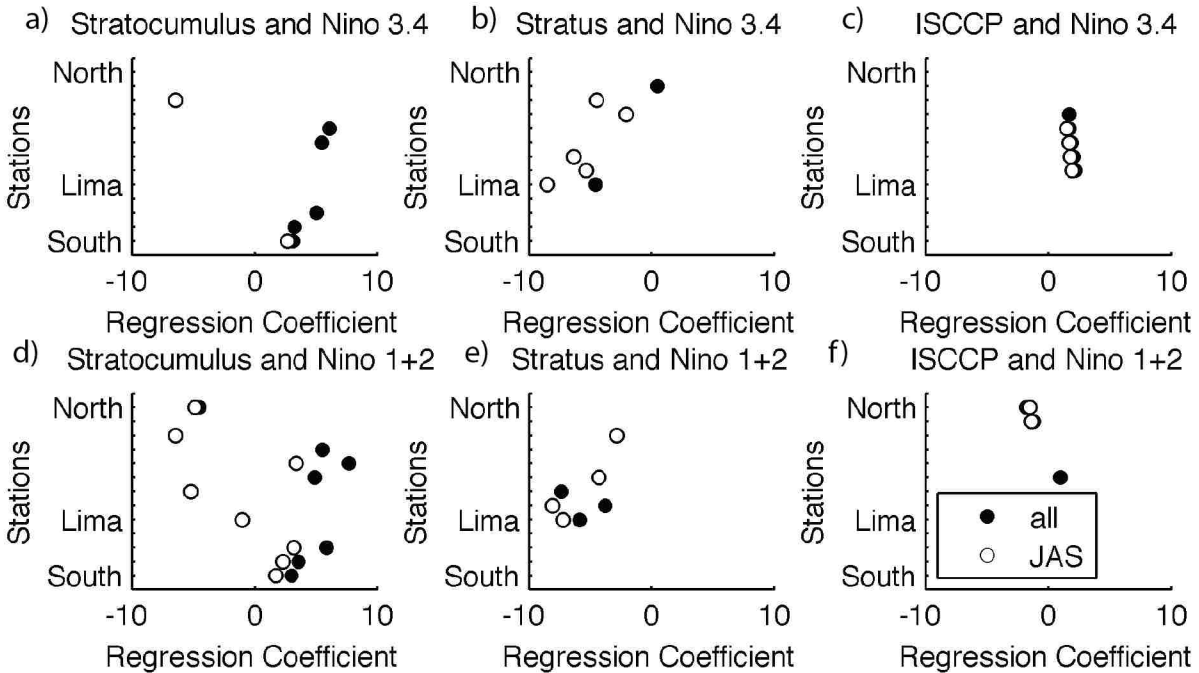
Figure 4.8. Regression coefficient ([% cloud cover $°C^{-1}$]) for (a) stratocumulus cloud cover anomalies and Niño 3.4 anomalies, (b) stratus cloud cover anomalies and Niño 3.4 anomalies, (c) ISCCP cloud fraction anomalies and Niño 3.4 anomalies, (d) stratocumulus cloud cover anomalies and Niño 1+2 anomalies, (e) stratus cloud cover anomalies and Niño 1+2 anomalies, and (f) ISCCP cloud fraction anomalies and Niño 1+2 anomalies. Shown are regression coefficients from significant ($p<0.05$) correlations for all months, and JAS. Stations are shown from north to south. Correlation values are found in Appendix A [Figure A1].

Increases in SST indices (both El Niño 3.4 and El Niño 1+2) generally correspond with one to two months per °C longer durations than average of stratocumulus cloud cover and one to two months per °C shorter durations than average of stratus cloud cover in coastal Peru [Figure 4.9]. Correlations were similar for

96

comparisons with SST in both El Niño region 3.4 and El Niño region 1+2. Correlations

with $\alpha > .05$ are not shown.
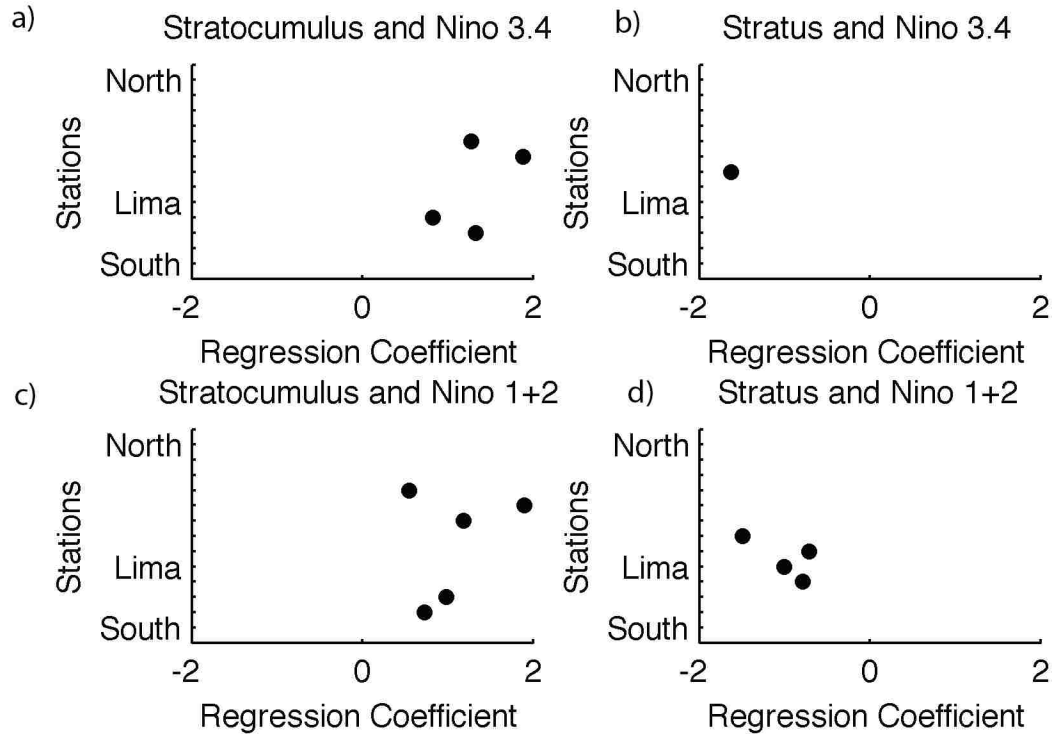
Figure 4.9. Regression coefficient ([months cloud cover] [°C]$^{-1}$) between duration
(months) of (a) stratocumulus cloud cover and JAS Niño 3.4 anomalies, (b) stratus
cloud cover and JAS Niño 3.4 anomalies, (c) stratocumulus cloud cover and JAS Niño
1+2 anomalies, and (d) stratus cloud cover and JAS Niño 1+2 anomalies. Stations are
shown from north to south. Correlation values are found in Appendix A [Figure A2].

4.4.2. Low Cloud Cover and SST

The influence of particular regions of the ocean on stratus and stratocumulus

cloud cover near Lima, Peru can be seen when the station data are compared to SST

between 30° S and 30° N, in the Pacific Ocean. There is a small and significant positive

correlation ($r = 0.22, \alpha = .05$) between SST in the El Nino region 3.4 and overall

stratocumulus cloud cover percent at the Lima station as expected from the earlier

97

results (Fig. 4.6) [Figure 4.10]. Yet when we consider the peak cloud season, there is a negative correlation ($r = 0.5 – 0.63$, $\alpha = .05$) between SST near coastal Peru and in the El Niño region 1+2 and stratocumulus cloud cover at the Lima station. This correlation is consistent with the previously discussed correlations with El Niño SST indices. The overall month by month correlations are low, with IRI<0.3. However, the overall magnitude of the correlation increases when the regression analysis is restricted seasonally; in this case the correlation in the coastal Peru and El Nino region 1+2 approaches IRI=0.6. There is a negative overall correlation between SST in El Nino region 1+2 and along coastal Peru and stratus cloud cover percent [Figure 4.10]. However, overall correlations are low, with r<0.3 ($\alpha = .05$). Likewise, the strength of this correlation increases slightly when the analysis is restricted seasonally, particularly in coastal Peru; we additionally measure a negative correlation between SST in El Nino region 3.4 and stratus cloud cover percent.

Figure 4.10. Heat map of the correlation between SST and stratocumulus and stratus cloud cover percent at the Lima EECRA station. Shown is a month by month correlation for the whole year (All), and a seasonal correlation (JAS). Scale shows latitude and longitude in equidistant cylindrical projection.

Further north in Peru, negative correlations are observed between cloud cover at the coastal EECRA stations and SST near coastal Peru and the regions of the El Niño indices, particularly El Niño 1+2 [Figure 4.11]. The magnitude of this correlation increases and gains significance in the central equatorial Pacific Ocean (roughly the El Niño 3.4 region) as the analysis is restricted seasonally [Figure 4.11]. Stratocumulus cloud cover is more strongly linked to the El Niño 3.4 region while stratus cloud cover had more significant correlations with the El Niño 1+2 region and coastal Peru. Further examples of this are seen in Appendix A [Figures A3 – A15]. While North Peru has a negative correlation between stratus and stratocumulus cloud cover and SST in the El Niño 1+2 region and El Niño 3.4 region, there is a positive correlation where the stations were located just inland with a broad coastal plain before the mountains [Appendix A, Figures A3 – A15].
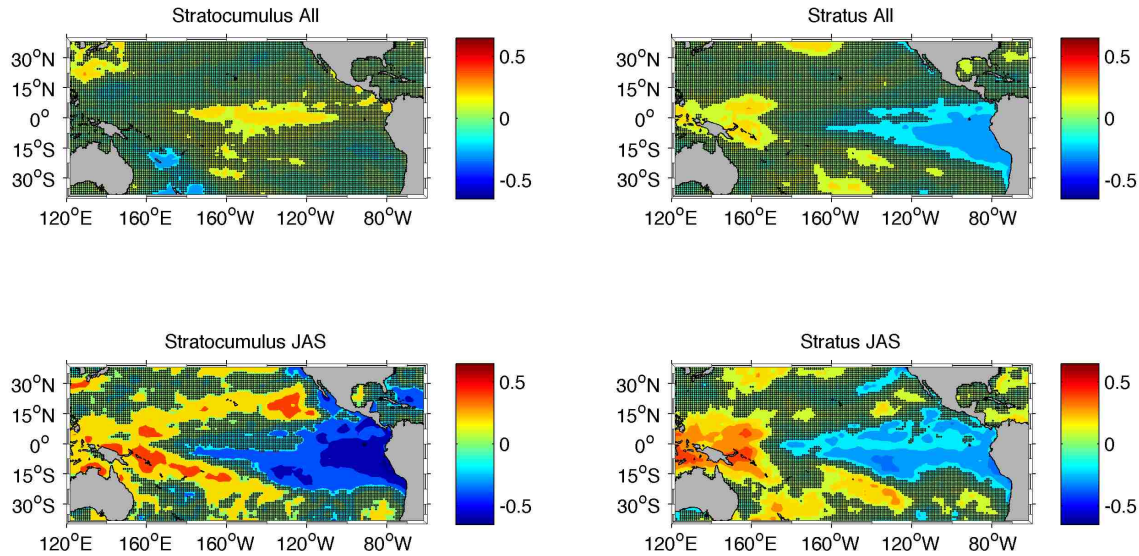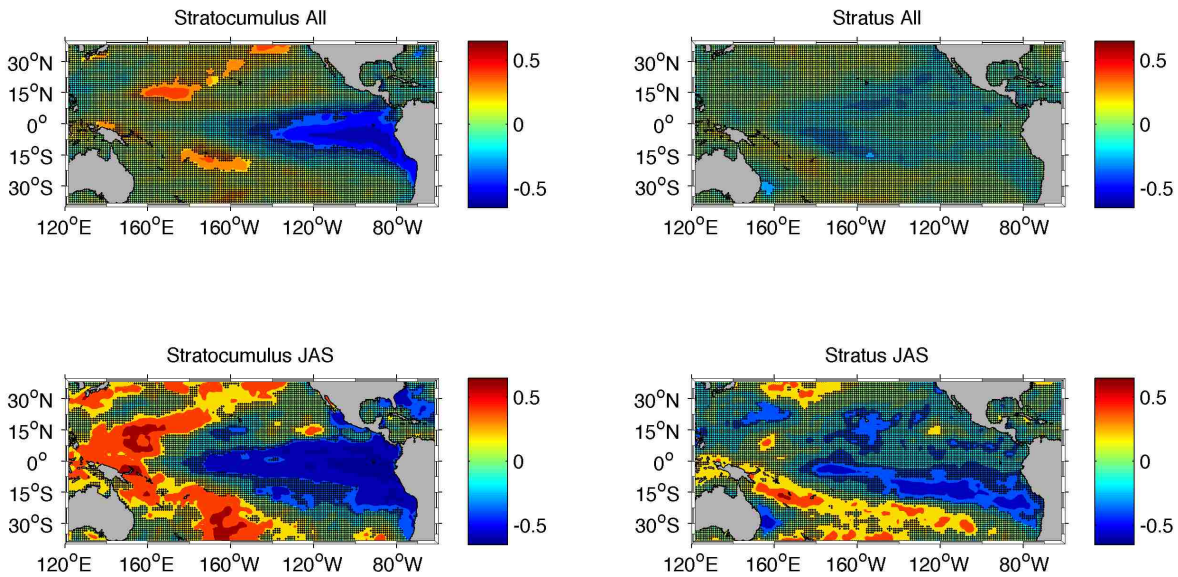
Figure 4.11. Heat map of the correlation between SST and stratocumulus and stratus cloud cover percent at the EECRA station 1 (the northern most station). Shown is a month by month correlation for the whole year (All), and a seasonal correlation (JAS). Scale shows latitude and longitude in equidistant cylindrical projection.

4.5 Discussion and Conclusion

This study examined the mean seasonal duration of fog and low cloud cover in Lima and along coastal Peru, and the correlations between the amount of fog and low cloud cover and El Niño indices, and the amount of fog and low cloud cover and sea surface temperatures over a 30 year time period. In brief, we found mean annual duration of stratus and stratocumulus cloud cover between May and November, with variation in prevalence along coastal Peru. This variation was an interquartile range of a season 3-7 months long of at least 50% stratocumulus cloud cover along coastal Peru. Very low amounts of stratus cloud cover were observed in north Peru, with the longest duration around Lima being an average of 8.7 months with at least 40% stratus cloud cover. Interpolated ISCCP cloud cover fractions generally diverged from cloud cover observations at EECRA stations. Stratocumulus cloud cover is in general weakly

positively correlated with the El Niño 3.4 index, while stratus cloud cover is negatively correlated with the El Niño 3.4 and El Niño 1+2 index. However, we see that stratocumulus cloud cover when considering only the peak fog season, or year round in some parts of coastal Peru, is negatively correlated with El Niño indices and also negatively correlated with SST along coastal Peru.

We examined seasonal marine low cloudiness and variations associated with sea surface temperatures. This analysis provided information on the impact of SST variations depending on the region of the ocean on the marine cloud variations over nearly a thirty-year period of record. While the dataset included observations from 1971 to 2009, fewer data were available after 1997.

The analysis concentrated on stratus and stratocumulus clouds. Fog observations were also recorded at the airport stations, low overall frequency of fog occurred. Given that airports are intentionally sited in low fog areas to reduce impedance to air traffic, that frequency level was expected. Furthermore, given that we may be considering water resources available from fog at sites at a higher elevation than the airport, stratus and stratocumulus cover will indicate water potential intercepting the hills at locations of interest.

The seasonal duration of cloud cover is consistent with expectations near Lima (Heileman et al., 2009). The amount of stratus clouds seen in North Peru is quite low. There is a greater distance between the coastline and steep terrain in North Peru, thus low clouds can spread out and dissipate over the flat coastal topography. This

101

dissipation reduces cloud cover before it is observed as incoming fog at elevation. ISCCP cloud cover fractions were most representative of EECRA station observations in north Peru.

While correlations between SST and cloud cover observations and satellite measurements are low, the linear regression rho values are the same magnitude as observed values in prior studies (Park & Leovy, 2004). The regression analysis shows that there is a weak relationship between sea surface temperature in ocean regions and cloud cover in Lima, Peru. Warmer ocean temperatures in region 3.4 correlate with greater amounts of stratocumulus cloud cover in Lima; resulting in extensive flooding in North and Central Peru which has been noted during El Niño periods (Diaz & Markgraf, 2000). However, during periods of cooler sea surface temperature in the region 1+2 and coastal waters, (or local la Niña conditions), reduced stratus clouds are observed, resulting in observed drought conditions (Diaz & Markgraf, 2000). In general, negative correlations were observed between low cloud cover at the coastal EECRA stations and SST near coastal Peru and the regions of the El Niño indices; the magnitude of this correlation increased as the analysis is restricted seasonally. Stronger seasonal correlations than overall month by month correlations were expected, given that low clouds are not present throughout the year. As the El Niño or La Niña conditions develop, the predictive power of SST increases.

Differences in correlations between SST and cloud cover along coastal Peru can be explained by variations in SST and coastal moisture content, with warmer SST and higher amounts of atmospheric moisture towards the equator (Xie & Seki, 1997).

102

Highest correlations between SST indices (such as Niño 3.4 or 1+2) and low cloud cover depend on the latitude of the site of interest; though coastal SST is most strongly correlated. With improved possibilities to forecast SST (Kaiser Khan et al., 2014), predictability is possible for fog cover.

Sea surface temperatures are projected to change with warming global temperatures. Sea surface temperatures are projected to warm, with stronger warming seen along the equator (Collins et al., 2010; Deser et al., 2010). There is debate on the response of El Niño/La Niña amplitude to climate change – with some models projecting an increase in intensity, others a decrease, and still others no change (Latif & Keenlyside, 2009; Stevenson, 2012; Stevenson et al., 2012). Yet recent historical analysis shows that ENSO activity has been anomalously high in the past century, indicating a likely response to climatic warming (Li et al., 2013). Warmer temperatures could drive greater quantities and duration of stratocumulus clouds, with reduction in stratus cloud cover, increasing a shift towards rainfall and reduced supply of the clouds that most directly translate into fog cover. However, this is not uniformly the case. SST increases along coastal Peru during the peak fog season could actually translate into reduced stratocumulus cloud cover, and overall drier conditions. Larger anomalies of ENSO conditions further impacts the range seen in duration and prevalence of cloud cover, increasing the difficulty of year to year consistency in water resource planning.

This study was limited by several factors. One was the quantity of coastal stations reporting cloud cover. Given that there is variation in the relationship between

103

SST and stations along the coast, a denser network of observations could improve our understanding of the influence of SST on cloud cover conditions. A further limitation is availability of data from these stations – particularly within the past two decades. Even when data are available, the stations are located at lower elevations than the regions where fog collection occurs. Thus, there was a need to extrapolate from low cloud types to the projected fog season.

Future work can both take advantage of existing datasets and install additional stations. While typically satellite imagery only gives the top of clouds, improvements in data processing and finer resolution sampling may provide potential to use for the analysis. Installing more observations to record cloud types, will improve accuracy of fog prediction. Long-running observations of fog collection yield at high elevation sites would be particularly useful for correlations. Plant growth, particularly the Lomas vegetation that depends on fog for water inputs, can be considered a proxy for measurements of high elevation fog cover (Manrique et al., 2010). Finally, future work can incorporate correlations between observed cloud cover and SST with modeled projections of change in both El Niño indices and coastal SST; this will refine projections about how the fog resource can be expected to change with climatic conditions.

Given the potential to use fog water both for human needs and ecological improvement, it is important that we have a more comprehensive understanding of the current, and future, availability of that resource. Average fog collection yields can be 3 to 10 L m^{-2} day^{-1}(R.S. Schemenauer, 2012), with standard large fog collectors at 40 m^2 a foggy day can provide a significant local water input. For the most effective fog water

collection, it is useful to be able to understand estimated prevalence early in the season. We have presented information about predicting fog and low cloud cover along coastal Peru based off the El Niño climate indices and SST, with attention to the capitol Lima.

4.6 Appendix A

Figure A1. Correlation between (a) stratocumulus cloud cover anomalies and Niño 3.4 anomalies, (b) stratus cloud cover anomalies and Niño 3.4 anomalies, (c) ISCCP cloud fraction anomalies and Niño 3.4 anomalies, (d) stratocumulus cloud cover anomalies and Niño 1+2 anomalies, (e) stratus cloud cover anomalies and Niño 1+2 anomalies, and (f) ISCCP cloud fraction anomalies and Niño 1+2 anomalies. Shown are regression coefficients from significant ($p<0.05$) correlations for all months, and JAS. Stations are shown from north to south.
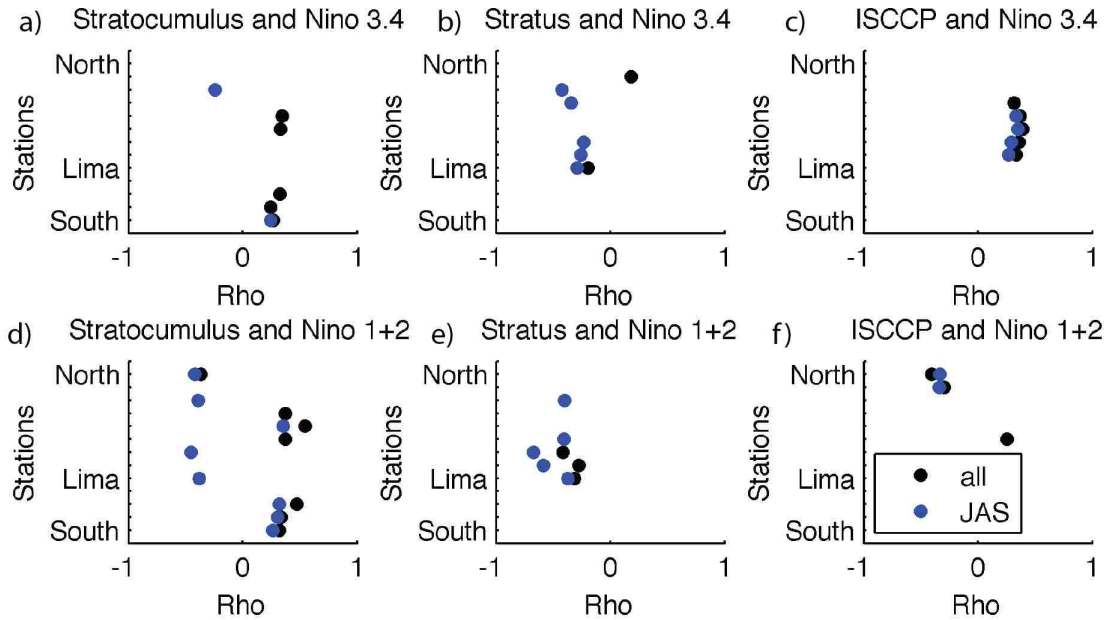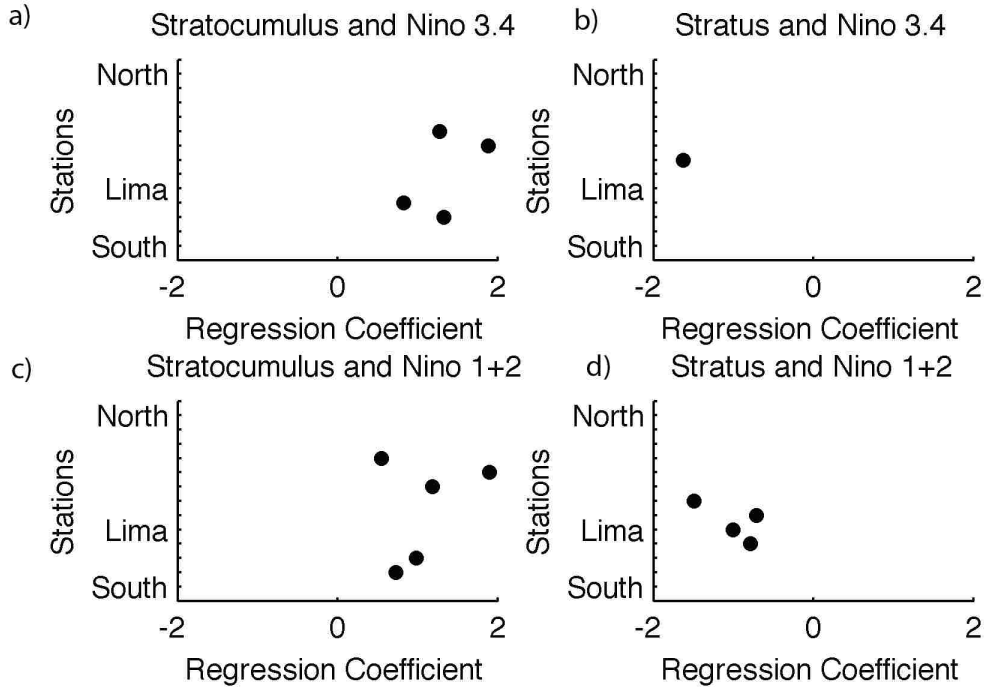
Figure A2. Correlations between duration of (a) stratocumulus cloud cover and JAS Niño 3.4 anomalies, (b) stratus cloud cover and JAS Niño 3.4 anomalies, (c) stratocumulus cloud cover and JAS Niño 1+2 anomalies, and (d) stratus cloud cover and JAS Niño 1+2 anomalies. Stations are shown from north to south.

Figure A3. Heat map of the correlation between SST and stratocumulus and stratus cloud cover percent at the EECRA station 1 (where station 1 is in the north, station 13 in the south of Peru). Shown is a month by month correlation for the whole year (All), and a seasonal correlation (JAS).

Figure A4. Heat map of the correlation between SST and stratocumulus and stratus cloud cover percent at the EECRA station 2 (where station 1 is in the north, station 13 in the south of Peru). Shown is a month by month correlation for the whole year (All), and a seasonal correlation (JAS).

Figure A5. Heat map of the correlation between SST and stratocumulus and stratus cloud cover percent at the EECRA station 3 (where station 1 is in the north, station 13 in the south of Peru). Shown is a month by month correlation for the whole year (All), and a seasonal correlation (JAS).

Figure A6. Heat map of the correlation between SST and stratocumulus and stratus cloud cover percent at the EECRA station 4 (where station 1 is in the north, station 13 in the south of Peru). Shown is a month by month correlation for the whole year (All), and a seasonal correlation (JAS).
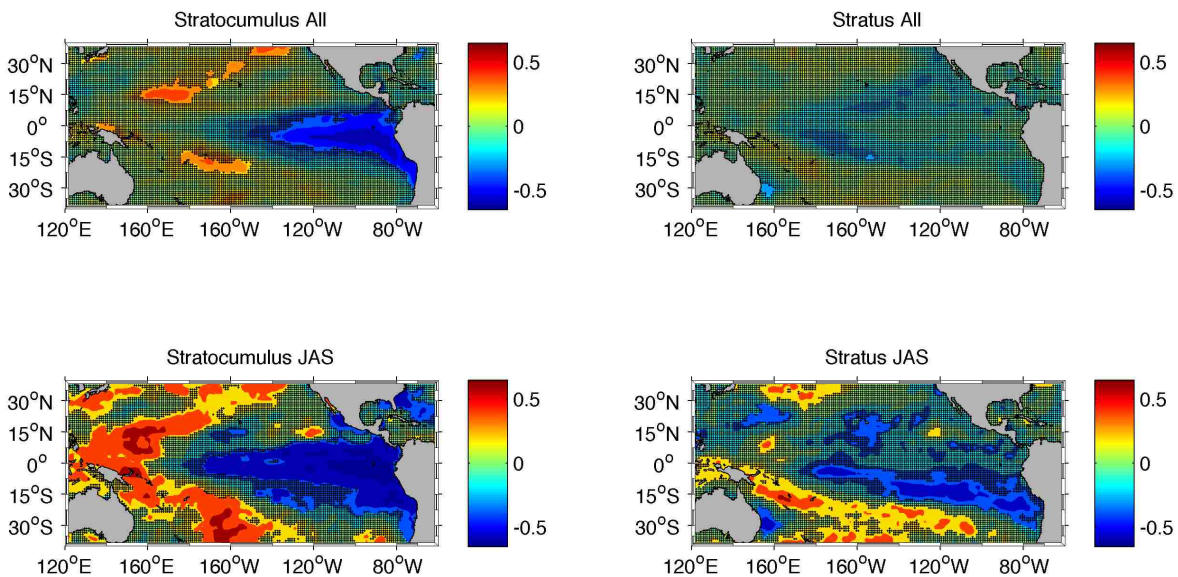

Figure A7. Heat map of the correlation between SST and stratocumulus and stratus cloud cover percent at the EECRA station 5 (where station 1 is in the north, station 13 in the south of Peru). Shown is a month by month correlation for the whole year (All), and a seasonal correlation (JAS).

109

Figure A8. Heat map of the correlation between SST and stratocumulus and stratus cloud cover percent at the EECRA station 6 (where station 1 is in the north, station 13 in the south of Peru). Shown is a month by month correlation for the whole year (All), and a seasonal correlation (JAS).
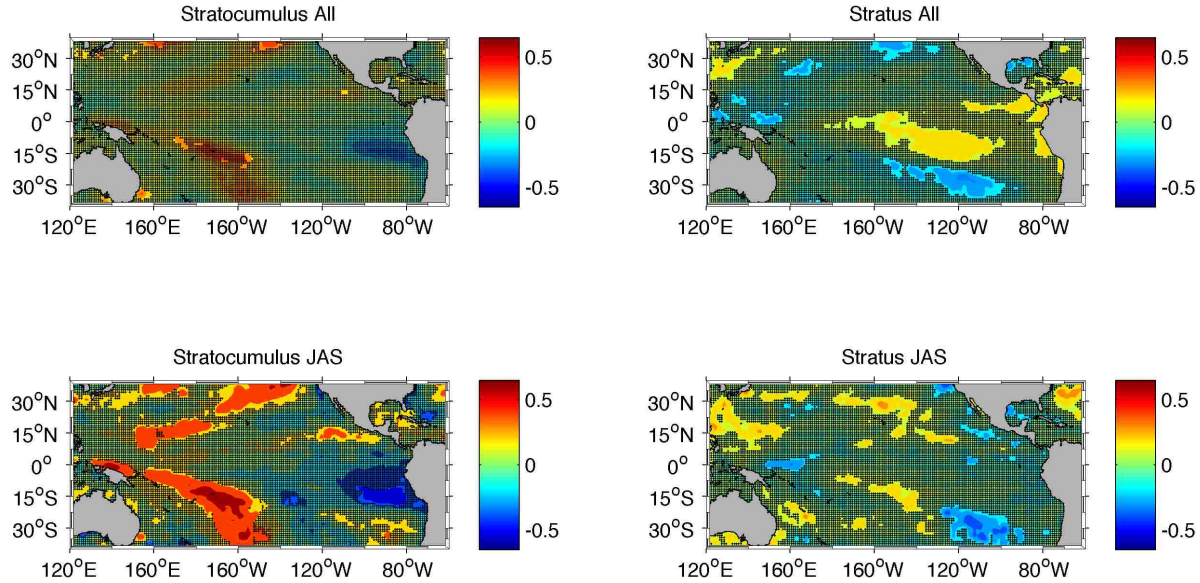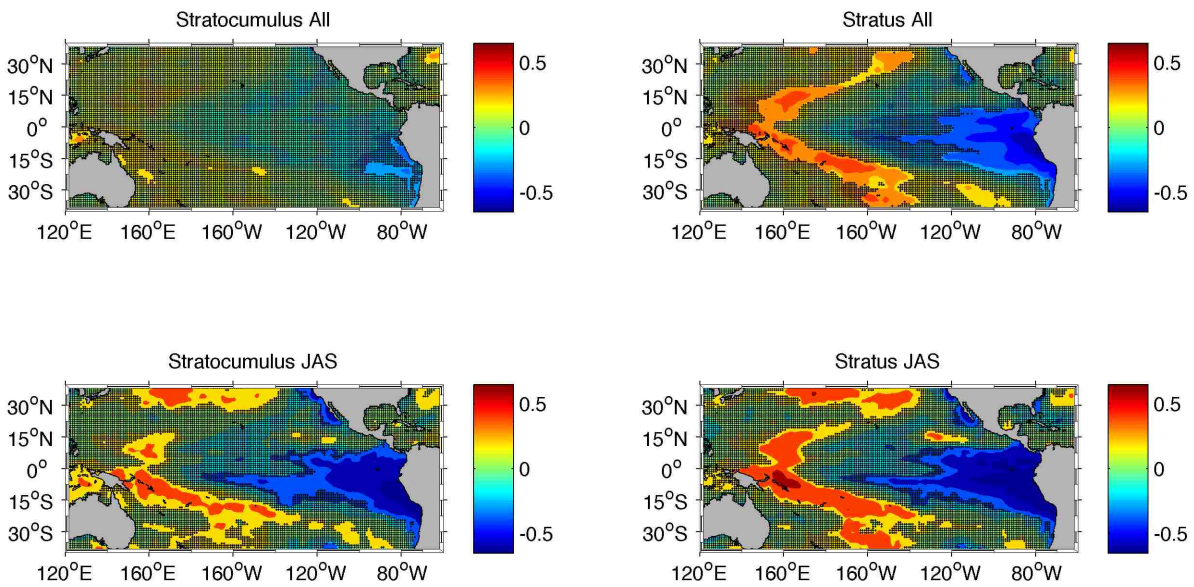

Figure A9. Heat map of the correlation between SST and stratocumulus and stratus cloud cover percent at the EECRA station 7 (where station 1 is in the north, station 13 in the south of Peru). Shown is a month by month correlation for the whole year (All), and a seasonal correlation (JAS).
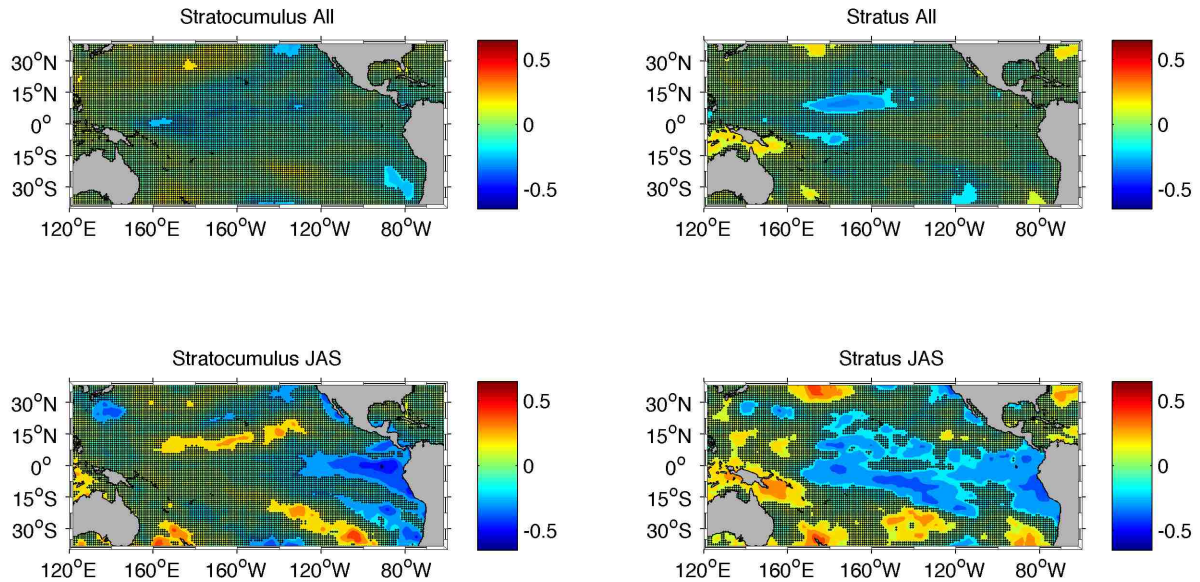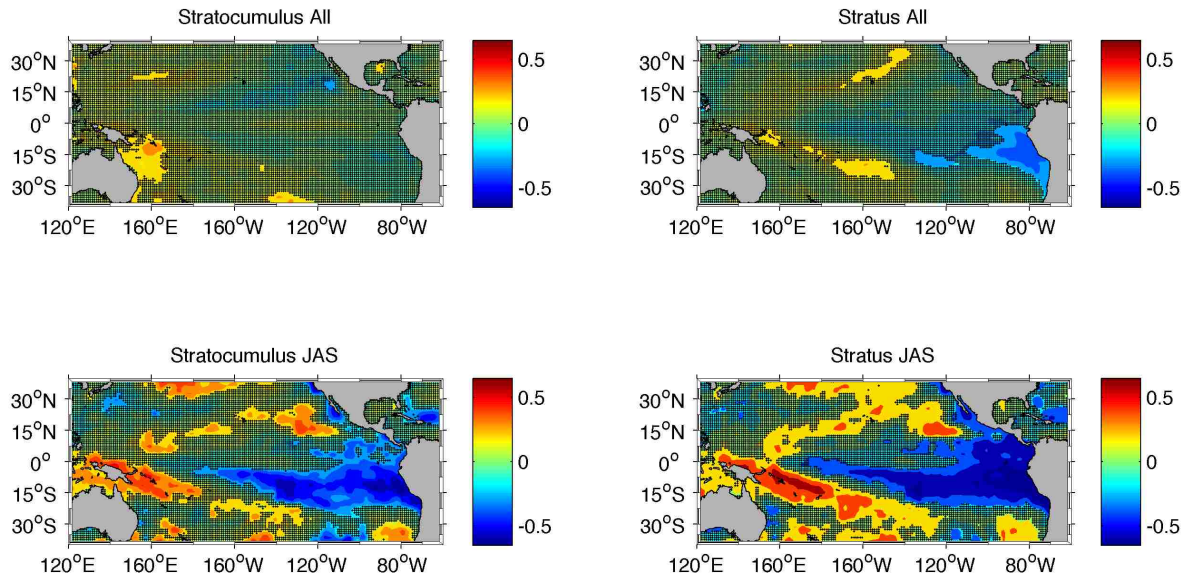
Figure A10. Heat map of the correlation between SST and stratocumulus and stratus cloud cover percent at the EECRA station 8 (where station 1 is in the north, station 13 in the south of Peru). Shown is a month by month correlation for the whole year (All), and a seasonal correlation (JAS).
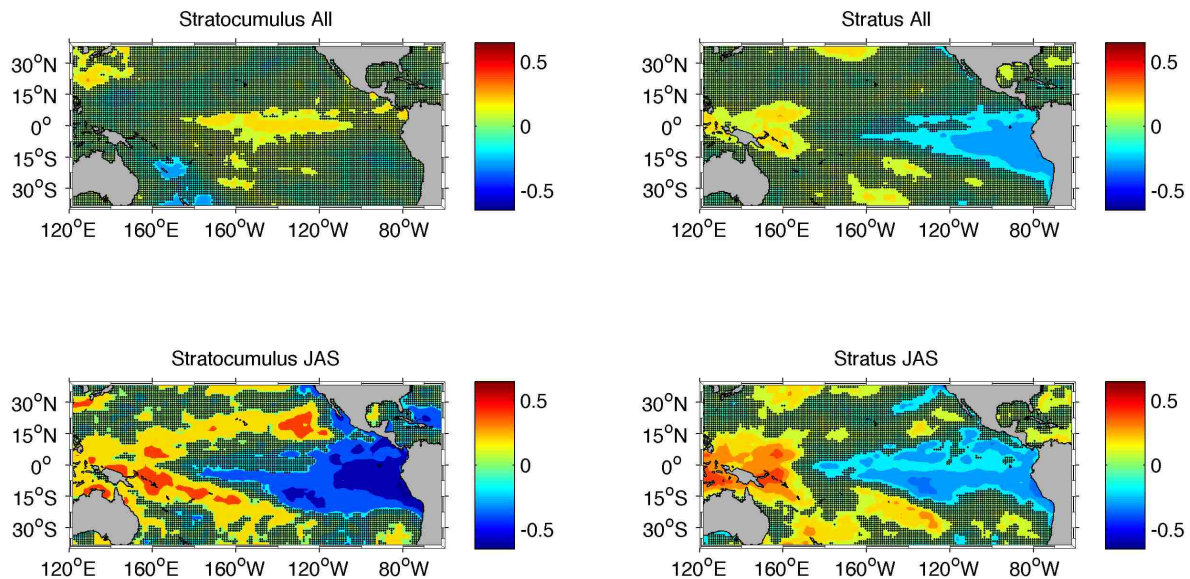
Figure A11. Lima Station. Heat map of the correlation between SST and stratocumulus and stratus cloud cover percent at the EECRA station 9 (where station 1 is in the north, station 13 in the south of Peru). Shown is a month by month correlation for the whole year (All), and a seasonal correlation (JAS).
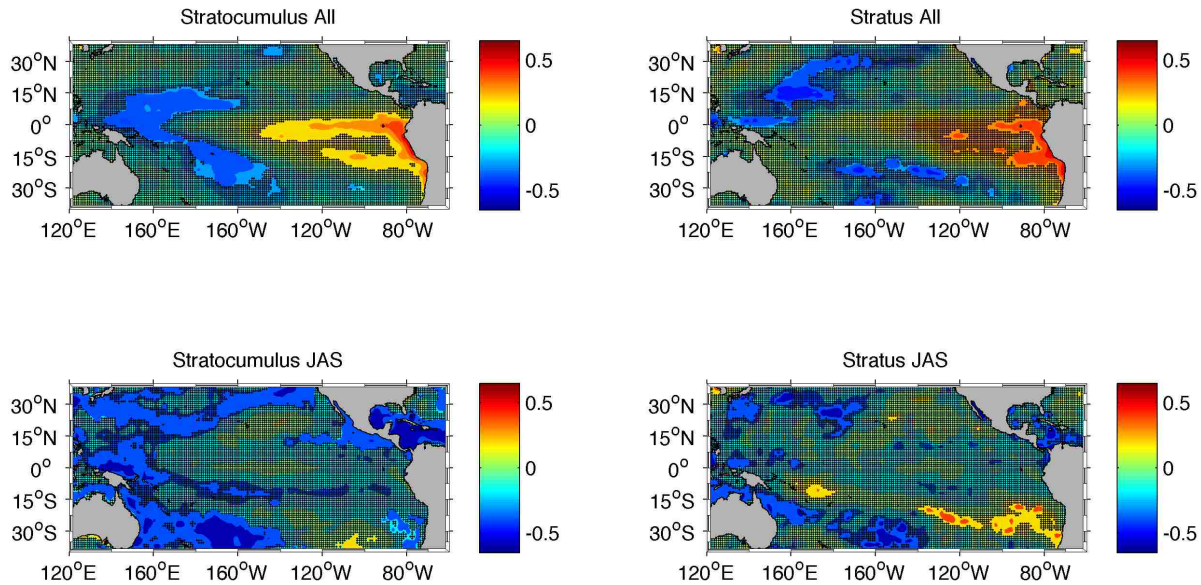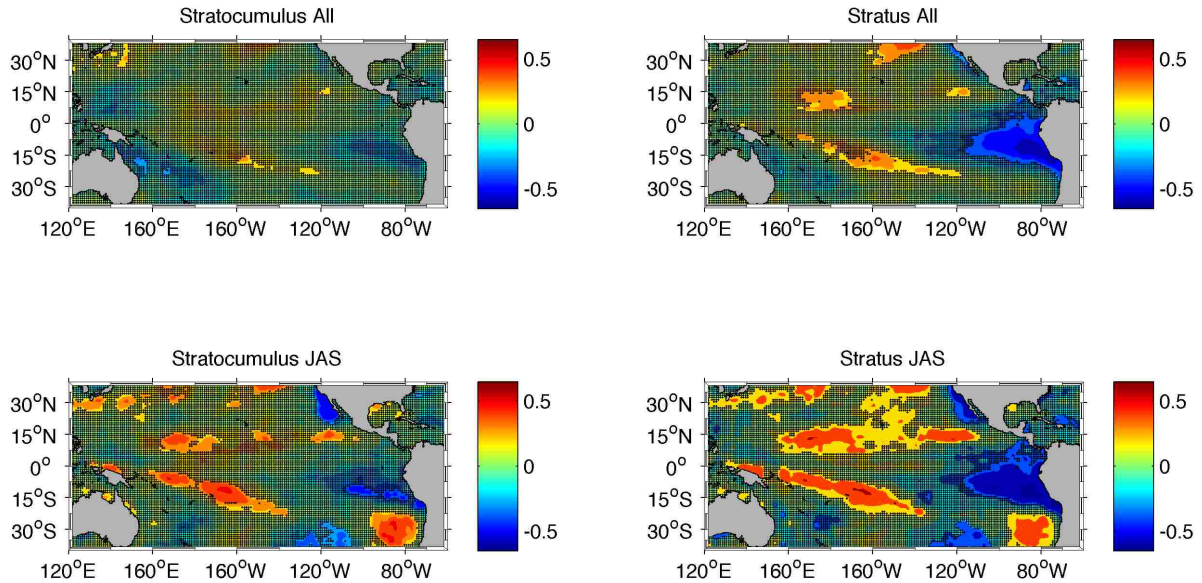
Figure A12. Heat map of the correlation between SST and stratocumulus and stratus cloud cover percent at the EECRA station 10 (where station 1 is in the north, station 13 in the south of Peru). Shown is a month by month correlation for the whole year (All), and a seasonal correlation (JAS).
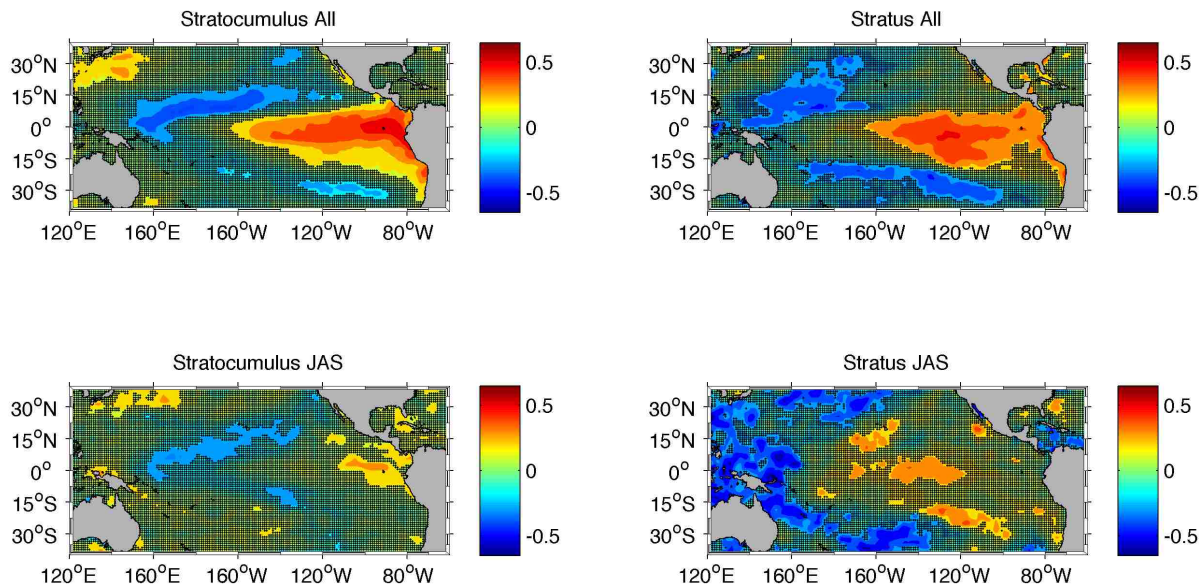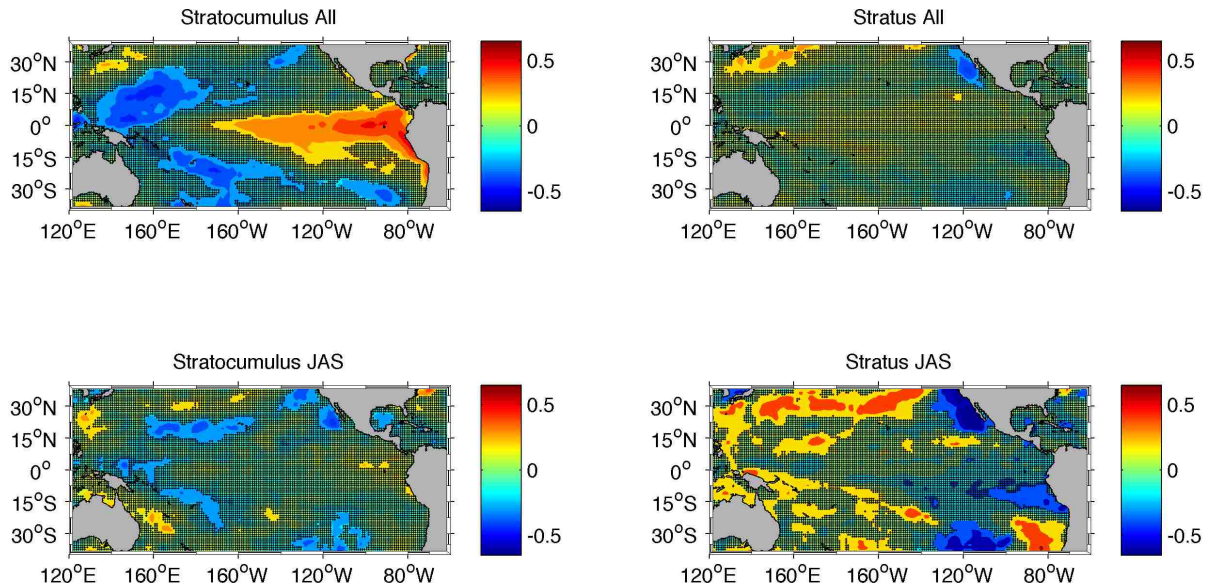

Figure A13. Heat map of the correlation between SST and stratocumulus and stratus cloud cover percent at the EECRA station 11 (where station 1 is in the north, station 13 in the south of Peru). Shown is a month by month correlation for the whole year (All), and a seasonal correlation (JAS).
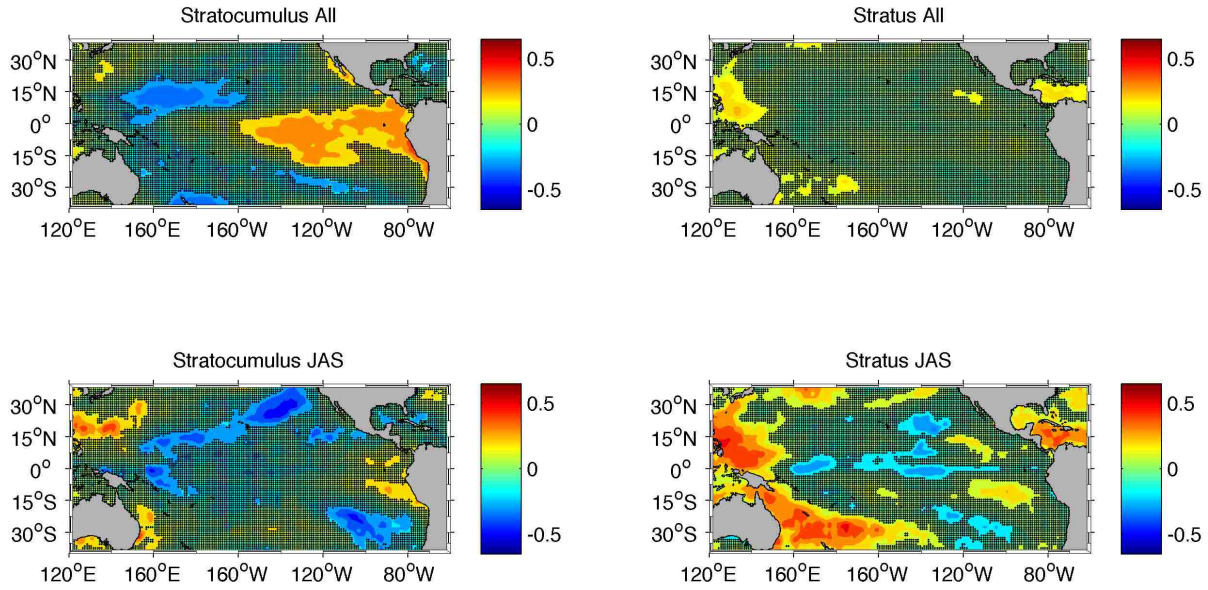
Figure A14. Heat map of the correlation between SST and stratocumulus and stratus cloud cover percent at the EECRA station 12 (where station 1 is in the north, station 13 in the south of Peru). Shown is a month by month correlation for the whole year (All), and a seasonal correlation (JAS).
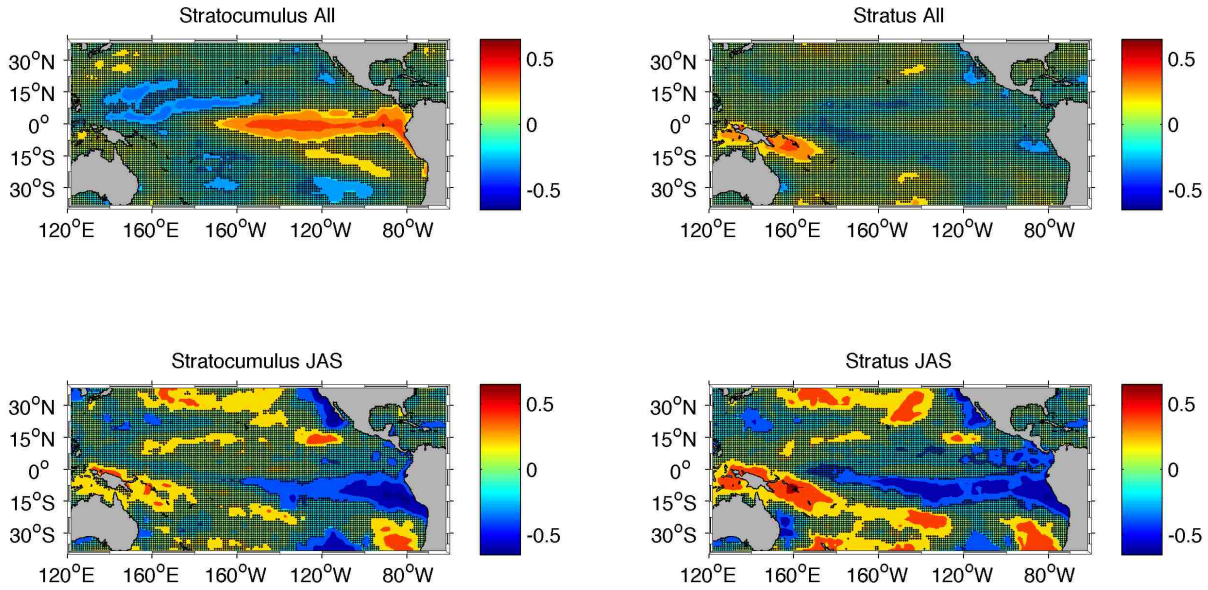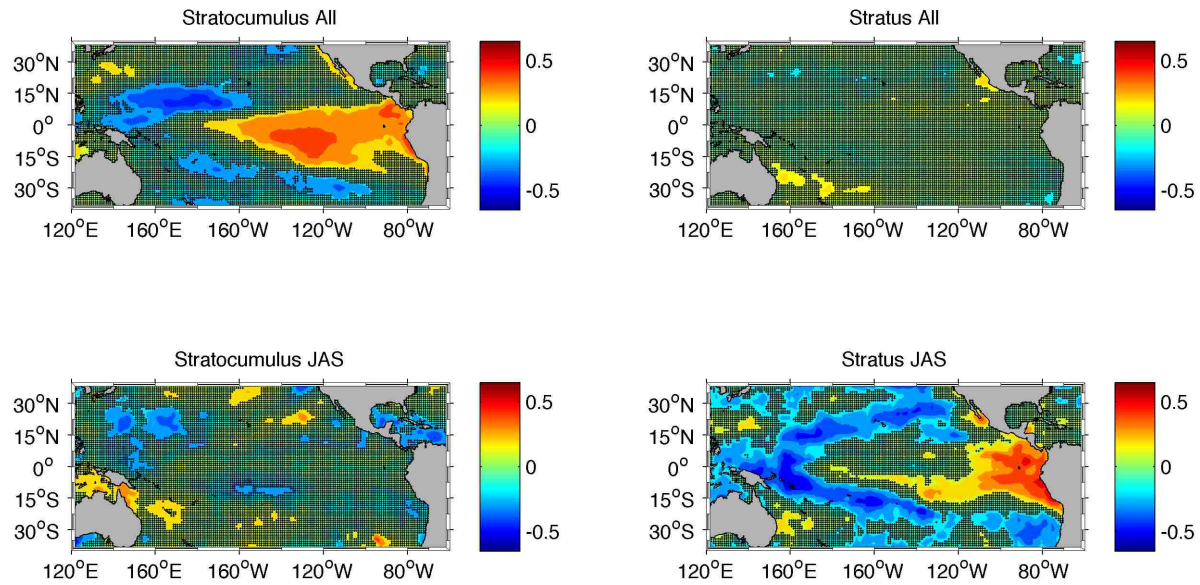

Figure A15. Heat map of the correlation between SST and stratocumulus and stratus cloud cover percent at the EECRA station 13 (where station 1 is in the north, station 13 in the south of Peru). Shown is a month by month correlation for the whole year (All), and a seasonal correlation (JAS).

Chapter 5 Discussion

5.1 Importance and Overall Approach

Water is an essential resource, but many regions have limited and/or declining water availability. The situation is exacerbated in impoverished communities where access is affected by political and economic factors in addition to technological and environmental factors. Coastal Peru is one of the many areas facing imminent water shortages due to a combination of limited, local water resources, declining glacial sources, and a rapidly growing population. In Lima, around 30% of the population lives in informal urban settlements where the bureaucratic process of developing a municipal water supply can be complex and costly. In fact, SEDEPAL, the municipal supplier acknowledges that supplying water for the projected growth of Lima is not possible with the current water reserves (Lubovich, 2007). This reduces water available for human needs, and developing green space within the arid city.

Solving the problem of inadequate water availability in informal and impoverished communities is complex, requiring a multidisciplinary approach. Such an approach should consider 1) affordable technologies that will improve the ability to acquire water resources, 2) social factors that might be impacted by, and could enhance or hinder the use of these technologies and 3) environmental factors that influence water resource availability. This dissertation addressed each of these three factors.

5.2 Review

This dissertation investigated 1) the effect of technological improvements to a method to capture water through a fog water collection system, 2) the physical health, mental well-being, and community social factors of the community members in the Lima informal settlement research site that could be related to the project's impact, development and maintenance, and 3) climatological patterns that could affect the sustainability of a fog water resource.

Chapter 2 presented an investigation of the performance of a nonwoven three-dimensional turf reinforcement mat (TRM) for use in fog water collection. Enkamat 7010 and 7220 was evaluated in both an artificial fog tunnel and at a field site in Lima, Peru. We found that off-the shelf TRM materials could increase fog collection yields by 50% to 150% over standard materials in side by side comparisons in Lima. This was greater than the increase seen in the lab, illustrating the importance of field-testing new materials. Further, the two test sites, which were situated at different aspects to the predominant wind direction, displayed different fog collection efficiencies with the new material, illustrating the importance of following best siting practices. Overall, we demonstrated that a low-cost, widely available, technologically-simple material could provide increased fog water collection yields.

Chapter 3 presented an analysis of baseline demographic, physical health, mental health and social relation factors of individuals who participated in the implementation of a community garden project and would be served by fog water collection. While the average household incomes in the community were low, the level of education attainment was relatively high - two thirds of the participants had completed

at least some secondary education, and 21% had completed higher education. There were some indications of poor physical health of the community – almost half of the participants reported a current illness, and high levels of obesity were observed (57.5% of the population was overweight or obese) – but there was little evidence of hypertension or diabetes based on blood pressure or blood sugar levels. The mental health survey did not indicate outstanding concerns for well-being in the community and quality of life scores were comparable to those in informal settlements in other countries. Lower levels of perceived stress and threatening experiences were observed, with social capital scores low compared to other low-income countries, yet comparable to other analyses in Peru. Strong parental relationships were also observed, with high parent empathy scores. Overall, the survey found some areas of strength that could contribute to successful water resource project development and maintenance over time (for example, good educational background and parental relationships).

Chapter 4 explored predictability of low cloud conditions, to understand the availability of the fog resource needed for fog collection systems. We analyzed the annual duration of low cloud cover along coastal Peru, correlations between the amount of low cloud cover and El Niño indices, and correlations between amount of low cloud cover and SST anomalies in the equatorial Pacific Ocean. We found the predominant season with low cloud cover was between May and November, although the extent of low cloud cover varied along the coast of Peru such that cloud cover conditions were more consistent throughout the year in North Peru, with a stronger seasonal variation

116

around Lima. Interpolated ISCCP cloud cover fractions generally diverged from cloud cover observations at EECRA stations. Stratocumulus cloud cover was in general positively correlated with the El Niño 3.4 index, while stratus cloud cover is negatively correlated with the El Niño 3.4 and El Niño 1+2 index. However, we see that stratocumulus cloud cover when considering only the peak fog season, or year round in some parts of coastal Peru, is negatively correlated with El Niño indices; also negatively correlated with SST along coastal Peru. With projected increases in equatorial sea surface temperatures, and warming coastal Peruvian current, we could see reductions in low cloud cover, although warmer equatorial temperatures result in the production of cumulonimbus clouds and thus enhanced precipitation (Philander, 1990). Greater intensity of ENSO conditions further alters the range seen in duration and prevalence of cloud cover, increasing the difficulty of year to year consistency in water resource planning. This finding suggests factors in assessing optimal times to attempt to utilize a fog collection methodology based off SST, and also provides relevant data to help understand not only current fog collection and climate analysis, but plan for future duration of cloud cover under conditions of warming ocean temperatures.

5.3 Future Work

These studies highlighted several areas for future work. The next steps to enable bringing this research into practice include testing of full scale fog collection using the TRM, expanded or repeat health surveys, and analysis of the impact of local topography and location on cloud cover conditions. The analysis of 3D TRM fog collection material would benefit from further study at scale, and as used within a water

117

collection system. This would clarify further structural supports needed for the mesh and feasibility of the larger panels. More widespread side by side testing could further refine the percentage yield increase expected. A larger sample size in the health analysis would provide stronger validation of the demographic and health analysis results, and also may facilitate improvement of the internal consistency of the scales. The research group will be conducting repeat measures of the health survey to understand health and well-being benefits of the garden implementation. Finally, further climate analysis should extend to evaluate factors such as latitude, site elevation and recent cloud observations related to the variance in cloud cover correlations with SST along the coast of Peru. This information could allow for greater predictability and planning of fog collection efforts.

In conclusion, this dissertation presents data in three important areas, all of which are critical for a system to work effectively to improve the availability of water resources that can be used for human consumption or agriculture: efficiency improvements to a method to acquire atmospheric water, individual and social conditions within the type of community where this system could be used, and a method for evaluating the availability of water throughout the year. It is hoped that future research will continue to address this critical need of inadequate water resources, particularly in under-served communities, and that this research will also recognize the importance of a multi-disciplinary approach to this multifaceted problem.

References

Alvarez-Dongo, D., Sanchez-Abanto, J., Gomez-Guizado, G., & Tarqui-Mamani, C. (2012). Overweight and obesity: prevalence and determining social factors of overweight in the Peruvian population (2009-2010). *Rev Peru Med Exp Salud Publica*, *29*(3), 303–313.

Barceló, A., & Rajpathak, S. (2001). Incidence and prevalence of diabetes mellitus in the Americas. *Revista Panamericana de Salud Pública*, *10*(5), 300–8.

Brugha, T., Bebbington, P., Tennant, C., & Hurry, J. (1985). The List of Threatening Experiences: a subset of 12 life event categories with considerable long-term contextual threat. *Psychological Medicine*, *15*(1), 189–94.

CA (Comprehensive Assessment of Water Management in Agriculture). (2007). *Water for food, water for life: A comprehensive assessment of water management in agriculture.* London, UK: Earthscan; and Colombo, Sri Lanka; IWMI.

Camfield, L. (2012). Quality of life in developing countries. In K. C. Land, A. C. Michalos, & M. J. Sirgy (Eds.), *Handbook of social indicators and quality of life research* (pp. 399–432).

Cereceda, P., Osses, P., Larrain, H., Farías, M., Lagos, M., Pinto, R., & Schemenauer, R. S. (2002). Advective, orographic and radiation fog in the Tarapacá region, Chile. *Atmospheric Research*, *64*, 261–271.

Chaker, M. A. (2007). Key parameters for the performance of impaction-pin nozzles used in inlet fogging of gas turbine engines. In *Proceedings of GT2005. ASME Turbo Expo 2005: Power for Land, Sea and Air* (pp. June 6–9, 2005). Reno-Tahoe, Nevada, USA.

Chen, D., & Cane, M. A. (2008). El Niño prediction and predictability. *Journal of Computational Physics*, *227*(7), 3625–3640.

Chen, D., Cane, M. A., Kaplan, A., Zebiak, S. E., & Huang, D. (2004). Predictability of El Niño over the past 148 years. *Nature*, *428*(6984), 733–6.

Chhatre, S. S., Tuteja, A., Choi, W., Revaux, A., Smith, D., Mabry, J. M., McKinley, G.H., Cohen, R. E. (2009). Thermal annealing treatment to achieve switchable and reversible oleophobicity on fabrics. *Langmuir : The ACS Journal of Surfaces and Colloids*, *25*(23), 13625–32.

Cohen, S., Kamark, T., & Mermelstein, R. (1983). A global measure of perceived stress. *Journal of Health and Social Behavior*, *24*(4), 385–396.

Collins, M., An, S., Cai, W., Ganachaud, A., Guilyardi, E., Jin, F., Jochum, M., Lengaigne, M., Power, S., Timmermann, A., Vecchi, G., Wittenberg, A. (2010). The impact of global warming on the tropical Pacific Ocean and El Niño. *Nature Geoscience*, *3*(6), 391–397.

Cueto, S., Escobal, J., Penny, M., & Ames, P. (2011). *Tracking Disparities : Who Gets Left Behind? Initial findings from PERU. Round 3 Survey Report.* (p. 126).

Darkey, D., & Kariuki, A. (2013). A study on quality of life in Mathare, Nairobi, Kenya. *J Hum Ecol*, *41*(3), 207–219.

Davies, A. R., Miranda, J. J., Gilman, R. H., & Smeeth, L. (2008). Hypertension among adults in a deprived urban area of Peru - undiagnosed and uncontrolled? *BMC Research Notes*, *1*(2), Published online 2008 February 26.

De Silva, M. J., & Harpham, T. (2007). Maternal social capital and child nutritional status in four developing countries. *Health & Place*, *13*(2), 341–55.

Dercon, S., & Singh, A. (2014). From Nutrition to Aspirations and Self-Efficacy : Gender Bias over Time among Children in Four Countries. *World Development*, *45*, 31–50.

Deser, C., Phillips, A. S., & Alexander, M. A. (2010). Twentieth century tropical sea surface temperature trends revisited. *Geophysical Research Letters*, *37*(10).

Diaz, H. F., & Markgraf, V. (2000). *El Nino and the Southern Oscillation: Multiscale Variability and Global and Regional Impacts* (p. 496). Cambridge University Press.

Drossman, D. A. (1998). Presidential address: gastrointestinal illness and the biopsychosocial model. *Psychosomatic Medicine*, *60*, 258–267.

Eastman, R., Warren, S. G., & Hahn, C. J. (2011). Variations in cloud cover and cloud types over the ocean from surface observations, 1954–2008. *Journal of Climate*, *24*(22), 5914–5934.

Eichler, T. P., & Londoño, A. C. (2013). ENSO impacts on Lomas formation in south coastal Peru: implications for the Pliocene? *Advances in Meteorology*, *2013*, 7.

Escobal, J. (2012). *Multidimensional poverty and inequality of opportunity in Peru: taking advantage of the longitudinal dimension of Young Lives. Working paper No. 79* (p. 60).

Feshbach, N. D., & Caskey, N. (1985). *A new scale for measuring parent empathy and partner empathy: Factorial structure, correlates and clinical discrimination.*

Gálvez-Buccollini, J. A., Paz-Soldan, V., Herrera, P., DeLea, S., Gilman, R. H., & Anthony, J. C. (2008). Links between sex-related expectations about alcohol, heavy episodic drinking and sexual risk among young men in a shantytown in Lima, Peru. *International Family Planning Perspectives*, *34*(1), 15–20.

Glantz, M. H. (1996). *Currents of Change: El Niño's Impact on Climate and Society* (p. 194 pp.). Cambridge University Press.

Goldstein, J., Jacoby, E., del Aguila, R., & Lopez, A. (2005). Poverty is a predictor of non-communicable disease among adults in Peruvian cities. *Preventive Medicine*, *41*, 800–806.

Hahn, C. J., & Warren, S. G. (1999). *Extended edited synoptic cloud reports from ships and land stations over the globe, 1952 - 1996.* (p. 76).

Harpham, T. (2009). Urban health in developing countries: what do we know and where do we go? *Health & Place*, *15*, 107–16.

Heerden, J. V., Olivier, J., & Schalkwyk, L. V. (2010). Fog Water Systems in South Africa : An Update. In *5th International Conference on Fog, Fog Collection and Dew. Münster, Germany, 25–30 July 2010.*

Heileman, S., Guevara, R., Chavez, F., Bertrand, A., & Soldi, H. (2009). XVII-56 Humboldt Current: LME #13. *NOAA*.

Heitzinger, K., Montano, S. M., Hawes, S. E., Alarcón, J. O., & Zunt, J. R. (2014). A community-based cluster randomized survey of noncommunicable disease and risk factors in a peri-urban shantytown in Lima, Peru. *BMC International Health and Human Rights*, *14*, 19.

Institute for Health Metrics. (2013). *Global Burden of Disease: Peru* (Vol. 2010, p. Accessed March 14, 2014.).

Instituto Nacional de Estadística e Informática (INEI). (2003). *Encuesta Nacional de Prevención y Consumo de Drogas 2002.* (p. 135).

Instituto Nacional de Estadística e Informática (INEI). (2012). *Encuesta Demográfica y de Salud Familiar 2012* (p. 438).

Kaiser Khan, M. Z., Mehrotra, R., Sharma, A., & Sankarasubramanian, A. (2014). Global sea surface temperature forecasts using an improved multimodel approach. *Journal of Climate*, *27*(10), 3505–3515.

Kirsch, H. (1995). *Drug lessons & education programs in developing countries* (p. 331).

Klemm, O., Schemenauer, R. S., Lummerich, A., Cereceda, P., Marzol, V., Corell, D., Heerden, J., Reinhard, D., Gherezghiher, T., Olivier, J., Osses, P., Sarsour, J., Frost, E., Estrela, M.J., Valiente, J.A., Fessehaye, G. M. (2012). Fog as a fresh-water resource: overview and perspectives. *Ambio*, *41*(3), 221–34.

Lagos, P., Silva, Y., Nickl, E., & Mosquera, K. (2008). El Nino – related precipitation variability in Peru. *Advances in Geosciences*, *14*, 231–237.

Latif, M., & Keenlyside, N. S. (2009). El Nino/Southern Oscillation response to global warming. *Proceedings of the National Academy of Sciences of the United States of America, 106*(49), 20578–20583.

Li, J., Xie, S. P., Cook, E. R., Morales, M. S., Christie, D. A., Johnson, N. C., Chen, F., D'Arrigo, R., Fowler, A.M., Gou, X., Fang, K. (2013). El Niño modulations over the past seven centuries. *Nature Climate Change*, *3*(9), 822–826.

Loret de Mola, C., Stanojevic, S., Ruiz, P., Gilman, R. H., Smeeth, L., & Miranda, J. J. (2012). The effect of rural-to-urban migration on social capital and common mental disorders: PERU MIGRANT study. *Social Psychiatry and Psychiatric Epidemiology*, *47*(6), 967–73.

Lubovich, K. (2007). *FESS Issue Brief. The coming crisis: water insecurity in Peru.*

Lummerich, A., & Tiedemann, K. J. (2011). Fog water harvesting on the verge of economic competitiveness. *Erdkunde*, *65*(3), 305–306.

Manrique, R., Ferrari, C., & Pezzi, G. (2010). The influence of El Niño Southern Oscillation (ENSO) on fog oases along the Peruvian and Chilean coastal deserts. In *5th International Conference on Fog, Fog Collection and Dew. Münster, Germany, 25–30 July 2010.* (p. 4).

Mantua, N. J., & Hare, S. R. (2002). The Pacific Decadal Oscillation. *Journal of Oceanography*, *58*(1991), 35–44.

Meteorological Office UK. (2006). *Cloud Types for Observers. The Geographical Journal* (Vol. 129, p. 45).

Molarius, A., Seidell, J. C., Sans, S., Tuomilehto, J., Kuulasmaa, K., & Project, W. M. (1999). Waist and hip circumferences, and waist-hip ratio in 19 populations of the WHO MONICA Project. *International Journal of Obesity*, *23*(2), 116–125.

Molina, J. (1999). Lima , un clima de desierto litoral. *Anales de Geografía de La Universidad Complutense*, *19*, 25–45.

Motrico, E., Moreno-Küstner, B., Luna, J., Torres-González, F., King, M., Nazareth, I., Montón-Franco, C., Gómez-Barragan, M., Sanchez-Celaya, M., Diaz-Barreiros, M., Vicens, C., Moreno-Pe, P., Bellón, J. (2013). Psychometric properties of the List of Threatening Experiences—LTE and its association with psychosocial factors and mental disorders according to different scoring. *Journal of Affective Disorders*, *150*(3), 931–940.

Mudey, A., Ambekar, S., Goyal, R. C., Agarekar, S., & Wagh, V. V. (2011). Assessment of quality of life among rural and urban elderly population of Wardha District, Maharashtra, India. *Ethno Med*, *5*(2), 89–93.

Multisectoral Technical Commission. (2004). *National Strategy for Freshwater Resources Management in Peru.*

Muñoz, R. A., McBride, M. E., Brnabic, A., López, C. J., Hetem, L., Secin, R., & Dueñas, H. J. (2005). Major depressive disorder in Latin America: the relationship between depression severity, painful somatic symptoms, and quality of life. *Journal of Affective Disorders*, *86*(1), 93–8.

National Academy of Sciences. (2003). *Cities transformed: demographic change and its implications for the developing world*. New York: National Academies Press.

National Center for Atmospheric Research Staff (Eds). "The Climate Data Guide: Nino SST Indices." (2013).

NIH. (1998). *The Evidence Report. NIH publication. No. 98-4083.* (p. 228 pp.).

O'Brien, M. S., Burdsal, C. A., & Molgaard, C. A. (2004). Further development of an Australian-based measure of social capital in a US sample. *Social Science & Medicine*, *59*(6), 1207–1217.

Onyx, J., & Bullen, P. (2000). Measuring social capital in five communities. *The Journal of Applied Behavioral Science*, *36*(1), 2000.

Painter, J. (2007). Deglaciation in the Andean Region, UNDP Human Development Report 2007/2008, Fighting Climate Change: Human Solidarity in a Divided World. *UN Development Programme. New York*, 1–13.

Park, S., & Leovy, C. B. (2004). Marine Low-Cloud Anomalies Associated with ENSO. *Journal of Climate*, *17*, 3448–3469.

Pedgey, D. (1967). Weather in the mountains. *Weather*, *22*, 266–275.

Perez-Albeniz, A., & De Paul, J. (2004). Gender differences in empathy in parents at high- and low-risk of child physical abuse. *Child Abuse & Neglect*, *28*, 289–300.

Philander, S. (1990). *El Niño, La Niña and the Southern Oscillation.* (p. 289 pp.). San Diego, CA: Academic Press.

Proyecto Regional Manejo Integrado del Gran Ecosistema de la Corriente de Humboldt. (2002). *Integrated overview of the oceanography and environmental variability of the Humboldt Current system. Chile.*

Remor, E. (2006). Psychometric properties of a European Spanish version of the Perceived Stress Scale (PSS). *The Spanish Journal of Psychology*, *9*(1), 86–93.

Riofrío, G. (2003). Urban Slums Reports:The Case of Lima, Peru. *UN-Habitat Global Report on Human Settlements.*, *London. Pa*, 195–228.

Rivera, J. (2011). Aerodynamic collection efficiency of fog water collectors. *Atmospheric Research*, *102*(3), 335–342.

Roslow, W. B., & Schiffer, R. A. (1991). ISCCP cloud data products. *Bulletin of the American Meteorological Society*, *72*(1), 2–20.

Rundel, P. W., & Dillon, M. O. (1998). Ecological patterns in the Bromeliaceae of the Lomas formations of Coastal Chile and Peru. *Plant Systems and Evolution*, *212*(3-4), 261–278.

Sanchez, A. (2008). *Childhood Poverty in Peru: An Annotated Literature Review. Young Lives Technical Note No. 8* (p. 37).

Sarsour, J., Stegmaier, T., Linke, M., & Planck, H. (2010). Bionic development of textile materials for harvesting water from fog. In *5th International Conference on Fog, Fog Collection and Dew. Münster, Germany, 25–30 July 2010.*

Schemenauer, R. S. (2012). Fog-water collection in arid coastal locations, *20*(7), 303–308.

Schemenauer, R. S., & Cereceda, P. (1994). A proposed standard fog collector for use in high-elevation regions. *Journal of Applied Meteorology*, *33*(11), 1313–1322.

Schemenauer, R. S., & Cereceda, P. (1994). Fog collection's role in water planning for developing countries. *Natural Resources Forum*, *18*(2), 91–100.

Schemenauer, R. S., Cereceda, P., & Osses, P. (2005). *Fog Water Collection Manual* (p. 94).

Schemenauer, R. S., & Joe, P. I. (1989). The collection efficiency of a massive fog collector. *Atmospheric Research*, *24*(1-4), 53–69.

124

Sclar, E. D., Garau, P., & Carolini, G. (2007). The 21st century health challenge of slums and cities. *Lancet*, *365*(9462), 901–903.

Sheuya, S. A. (2008). Improving the health and lives of people living in slums. *Annals of the New York Academy of Sciences*, *1136*, 298–306.

Skevington, S. M. (2009). Conceptualising Dimensions of Quality of Life in Poverty. *Journal of Community & Applied Social Psychology*, *19*, 33–50.

Skevington, S. M., Lotfy, M., & O'Connell, K. A. (2004). The World Health Organization's WHOQOL-BREF quality of life assessment: Psychometric properties and results of the international field trial. A Report from the WHOQOL Group. *Quality of Life Research*, *13*(2), 299–310.

Smakhtin, V., Revenga, C., & Döll, P. (2004). A pilot global assessment of environmental water requirements and scarcity. *Water International*, *29*(3), 307–317.

Stevens, B., Vali, G., Comstock, K., Wood, R., Van Zanten, M. C., Austin, P. H., Bretherton, C.S., Lenschow, D. H. (2005). Pockets of open cells and drizzle in marine stratocumulus. *Bulletin of the American Meteorological Society*, *86*, 51–57.

Stevenson, S., Fox-Kemper, B., Jochum, M., Neale, R., Deser, C., & Meehl, G. (2012). Will There Be a Significant Change to El Niño in the Twenty-First Century? *Journal of Climate*, *25*(6), 2129–2145.

Stevenson, S. L. (2012). Significant changes to ENSO strength and impacts in the twenty-first century: Results from CMIP5. *Geophysical Research Letters*, *39*(17), 5.

The WHOQOL group. (1998). Development of the World Health Organization WHOQOL-BREF Quality of Life Assessment. *Psychological Medicine*, *28*, 551–558.

The World Bank. (2011). *Peru : Country Program Evaluation for the World Bank Group , 2003-2009* (p. 135).

The World Factbook 2013-14. (2013). Washington, DC.

Torrence, C., & Webster, P. J. (1998). The annual cycle of persistence in the El Nino/Southern Oscillation. *Q. J. R. Meteorological Society*, *124*, 1985–2004.

Trenberth, K. E. (1997). The Definition of El Niño. *Bulletin of the American Meteorological Society*, *78*(12), 2771–2777.

Tsutsumi, A., Izutsu, T., Kato, S., Islam, A., Yamada, H. S., Kato, H., & Wakai, S. (2006). Reliability and validity of the Bangla version of WHOQOL-BREF in an adult

population in Dhaka, Bangladesh. *Psychiatry and Clinical Neurosciences*, *60*(4), 493–8.

UN Habitat Global Report on Human Settlements. (2003). *The Challenge of Slums—Global Report on Human Settlements 2003.*

UN Water. (2005). Water for Life 2005-2015. Accessed March 18. *http://www.un.org/waterforlifedecade/scarcity.shtml.*

UN-Water. (2007). *Coping with water scarcity. Challenge of the twenty-first century.* (p. 29).

United Nations (Centre for Human Settlements). Cities in a globalizing world: global report on human settlements (2001).

United Nations (Population Division). (2003). *World urbanization prospects: the 2003 revision.*

United Nations Development Programme (UNDP). (2006). *Human development report 2006. Beyond scarcity: power, poverty and the global water crisis.* New York.

Valiente, J. A., Estrela, M. J., Corell, D., Fuentes, D., Valdecantos, A., & Baeza, M. J. (2011). Fog water collection and reforestation at a mountain location in a western Mediterranean basin region: air-mass origins and synoptic analysis. *Erdkunde*, *65*(3), 277–290.

Vega, L. S., Agusti, R., Ramirez, J. P., & Tornasol. (2006). Factores de riesgo de las enfermedades cardiovasculares en el Peru. *Revista Peruana de Cardiologia*, *XXXII*(2), 82–128.

Vlahov, D., Freudenberg, N., Proietti, F., Ompad, D., Quinn, A., Nandi, V., & Galea, S. (2007). Urban as a determinant of health. *Journal of Urban Health : Bulletin of the New York Academy of Medicine*, *84*(1), 16–26.

Ware, J. E., & Sherbourne, C. D. (1992). The MOS 36-item short-form health survey (SF-36). I. Conceptual framework and item selection. *Medical Care*, *30*, 473–483.

Watson, J. M., Logan, H. L., & Tomar, S. L. (2008). The influence of active coping and perceived stress on health disparities in a multi-ethnic low income sample. *BMC Public Health*, *8*(41), 9.

Wood, R. (2012). Stratocumulus Clouds. *Monthly Weather Review*, *140*(8), 2373–2423.

Xie, S. P., & Seki, M. (1997). Causes of equatorial asymmetry in sea surface temperature over the eastern Pacific. *Geophysical Research Letters*, *24*(21), 2581–2584.